Title
Signals in a synaptic vesicle membrane protein, VAMP, affecting its membrane traffic in transfected PC12 cells

Author
Grote, Eric,

Publication Date
1994

Peer reviewed|Thesis/dissertation

Signals in a synaptic vesicle membrane protein, VAMP,
affecting its membrane transport in transfected PC12 cells

by

Eric Grote

DISSERTATION

Submitted in partial satisfaction of the requirements for the degree of

DOCTOR OF PHILOSOPHY

in

Cell Biology

in the

GRADUATE DIVISION

of the

UNIVERSITY OF CALIFORNIA

San Francisco

Date **University Librarian**

Degree Conferred: SEP 4 1994

Signals in a synaptic vesicle membrane protein, VAMP, affecting its membrane transport in tranfected PC12 cells

Eric Grote

Abstract

PC12 cells express synaptic vesicle proteins and target them to synaptic vesicle-like vesicles (SVLVs) which can be separated from larger organelles on sedimentation gradients. If PC12 cells are stimulated to secrete after preloading SVLVs with horseradish peroxidase, the amount of horseradish peroxidase remaining in SVLVs declines indicating that SVLVs are a regulated secretory vesicle.

The targeting and membrane traffic of an epitope-tagged synaptic vesicle membrane protein, VAMP-TAg, has been studied in transfected PC12 cells. VAMP-TAg is targeted to both SVLVs and endosomes. By following the transport of radioactive antibody bound to VAMP-TAg at the cell surface, evidence has been obtained that VAMP-TAg is targeted to SVLVs through an endosomal intermediate. Targeting of VAMP-TAg to SVLVs is saturable by overexpression. VAMP-TAg competes with endogenously expressed VAMP-2, but not with synaptophysin, for targeting to SVLVs. Therefore, VAMP and synaptophysin do not share a common signal for SVLV targeting.

Mutations were constructed in VAMP-TAg to identify signals required for endocytosis and SVLV targeting. Mutations within the predicted amphipathic helix surrounding methionine 46 inhibited both endocytosis and SVLV targeting suggesting that an interaction with the same protein may be required for both processes. However, some mutations within this helix

inhibited SVLV targeting more effectively than endocytosis suggesting that SVLV targeting requires a more stringent interaction.

Endocytosis of VAMP-TAg was normal if the entire region surrounding methionine 46 was deleted. In addition, the methionine 46 mutation did not inhibit endocytosis in CHO cells which lack SVLVs. These data indicate that the methionine 46 signal promotes endocytosis by a different mechanism than endocytosis signals which interact with clathrin coated pits. The methionine 46 signal could promote availability of VAMP-TAg for endocytosis by releasing it from a PC12-specific inhibitory complex.

A deletion within the second predicted helix of the conserved domain of VAMP-TAg resulted in increased sorting to SVLVs. As a result, the SVLVs were saturated with the mutant VAMP-TAg leading to exclusion of endogenous VAMP-2. This deletion did not block SVLV recycling suggesting that it is functional in the SVLV exocytosis/endocytosis cycle.

Table of contents

List of Tables

List of Figures

Introduction

Synaptic vesicles store neurotransmitters within the presynaptic nerve terminal for rapid, stimulatable release into the synaptic cleft. After exocytosis, synaptic vesicles recycle within the nerve terminal in as little as one minute by endocytosis of synaptic vesicle membranes and uptake of neurotransmitter (Betz and Bewick 1992, Holtzman et al., 1971) . Many synaptic vesicle proteins have been identified, cloned, and sequenced (Sudhof and Jahn 1991) . Some of these, such as VAMP (synaptobrevin) and synaptophysin are unique to synaptic vesicles, while others such as synaptotagmin and SV2 are also found in neurosecretory granules (Kelly 1991). Since they have a diameter of only 50 nm, synaptic vesicles must form by a single budding event and have space for only 80 polypeptides of an average molecular mass of 50 kDa (Jahn and Sudhof 1993) . Thus, in order to insure that each synaptic vesicle contains enough copies of each essential protein a high degree of sorting fidelity is required for synaptic vesicle biogenesis.

Based on current knowledge of synaptic vesicle membrane protein traffic, the critical events for sorting proteins to synaptic vesicles are likely to occur in coated pits and in axonal endosomes. Synaptic vesicle membrane proteins are synthesized in the cell body and transit through the endoplasmic reticulum and the Golgi stacks. Although a fraction of some synaptic vesicle proteins exit the trans-Golgi network in regulated secretory granules, the rest leave in constitutive secretory vesicles (Regnier-Vigouroux et al., 1991) or

immature synaptic vesicles (Kiene and Stadler 1987) and are transported down the axon along microtubules. At synapses, vesicle membrane proteins ultimately enter the synaptic vesicle recycling pathway. Recycling of synaptic vesicles has been observed by electron microscopy of neuromuscular junctions quick-frozen shortly after stimulation. Competing interpretations have proposed that recycling occurs either by a direct reversal of exocytosis by pinching off from the plasma membrane at the site of fusion in the active zone (Torri-Tarelli et al., 1987) or by endocytosis through coated pits after diffusing away from the active zone (Heuser 1989). The first model may be related to the transient opening of fusion pores which has been observed by electrophysiological recording of secretory granule fusion (Alvarez de Toledo et al., 1993) . Only the second model, however, allows for mixing of synaptic vesicle proteins with resident proteins of the plasma membrane after fusion. Synaptic vesicle proteins are then segregated into coated pits for endocytosis. A second sorting step to segregate synaptic vesicle proteins from receptors and other proteins not excluded from coated pits might occur in a possible endosomal intermediate in the recycling pathway. It seems likely that the direct and indirect recycling pathways coexist. The direct pathway would be used primarily at mature synapses and the indirect pathway would be utilized for the biogenesis of synaptic vesicles from newly synthesized proteins and scavenging of proteins from synaptic vesicles that have failed to recycle directly (Valtorta et al., 1990).

PC12 cells are a model system for the study of synaptic vesicle membrane protein traffic. Although they do not form synapses, undifferentiated PC12 cells contain synaptic vesicle-like vesicles (SVLVs, also known as synaptic-like microvesicles, SLMVs) which share many features

with authentic synaptic vesicles (Cameron et al., 1991, Clift-O'Grady et al., 1990, Linstedt and Kelly 1991, Wiedenmann et al., 1988). SVLVs can be generated by recycling from the plasma membrane. (Clift-O'Grady, et al. 1990) The possible role of endosomes in the recycling of SVLVs is highlighted by the extensive colocalization observed between synaptophysin and internalized transferrin (Cameron, et al. 1991, Johnston et al., 1989). The transferrin receptor, which cycles constitutively between endosomes and the plasma membrane (Harding et al., 1983, Hopkins and Trowbridge 1983), is excluded from SVLVs implying that at least two signals are required for targeting to synaptic vesicles, a primary signal for endocytosis via coated pits and a secondary signal for sorting into synaptic vesicles (Cameron, et al. 1991, Clift-O'Grady, et al. 1990, Linstedt and Kelly 1991) . In cultured hippocampal neurons, the transferrin receptor is also excluded from axons, suggesting that additional signals may be involved in targeting proteins to synaptic vesicles in differentiated neurons (Cameron, et al. 1991).

To look for sorting domains within a synaptic vesicle protein we chose to study VAMP (also known as synaptobrevin), an 18 kDa membrane protein of synaptic vesicles (Baumert et al., 1989, Trimble et al., 1988) . There are two VAMP isoforms which have been cloned from a variety of species. The VAMP-2 isoform is expressed in PC12 cells (Elferink et al., 1989). In addition, homologous or antigenically related proteins involved in both regulated and constitutive membrane traffic have been identified (Braun et al., 1994, Cain et al., 1992, McMahon et al., 1993, Protopopov et al., 1993, Sudhof et al., 1989, Trimble 1993) . VAMP-2 is implicated in synaptic vesicle fusion since it is the unique target on synaptic vesicles for the tetanus neurotoxin (Schiavo et al., 1992) . In addition VAMP-2 is found in a complex with two plasma membrane

proteins, syntaxin and SNAP-25 (Sollner et al., 1993a). This complex serves as a binding site for the NSF and α-SNAP proteins which are required for fusion of transport vesicles (Sollner et al., 1993b) . It has been proposed that an interaction between VAMP-2 and syntaxin, a presynaptic plasma membrane protein, provides the specificity for synaptic vesicle fusion (Sollner, et al. 1993b). This important interaction must take place after synaptic vesicles have docked at release sites because both docked and undocked vesicles accumulate in nerve terminals poisoned with tetanus toxin (Hunt et al., 1994).

VAMP is located on the cytoplasmic face of synaptic vesicles and is anchored in the membrane by its hydrophobic C-terminus (Trimble 1993). The cytoplasmic domain of VAMP-2 consists of variable and conserved regions, based on comparisons between species and between the VAMP isoforms (Sudhof, et al. 1989) . The conserved region is predicted to contain two amphipathic α-helicies (Dascher et al., 1991) . Helix-1, from amino acids 39 to 53, is unusually hydrophobic and may interact with lipids during the process of membrane fusion (Jahn and Sudhof 1994). Helix-2, from amino acids 60 to 88, is of sufficient length to be predicted to interact with a similar amphipathic helix on another protein in a coiled-coil structure (Lupas et al., 1991).

The goal of the experiments presented in this dissertation is to understand how synaptic vesicles are formed. This work was carried out in PC12 cells, so the first experiments were designed to extend the analogy between the functions of SVLVs and synaptic vesicles by demonstrating that SVLVs are capable of regulated exocytosis. Next, a system was designed in which the transport to SVLVs of VAMP, a model synaptic vesicle protein, could be followed in transfected PC12 cells. Mutagenesis was used to identify signals

in VAMP required for endocytosis and SVLV targeting. A surprising result was that a predicted fusion peptide in VAMP is also required for targeting. This result highlights the close interrelationship between the targeting of synaptic vesicle proteins to vesicles and their funtions in the synaptic vesicle exocytosis/endocytosis cycle.

Chapter One

Regulated exocytosis and recycling of synaptic vesicle like vesicles in PC12 cells

Abstract

If PC12 cells are incubated with the fluid phase tracer horseradish peroxidase (HRP), a fraction of the internalized HRP can be recovered in small vesicles which sediment at 80 S in glycerol gradients. Synaptic vesicle-like vesicles (SVLVs), identified by synaptophysin immunoreactivity, co-sediment with HRP in the 80 S peak. Internalized ^{125}I-transferrin does not co-sediment with SVLVs, indicating that the internalized HRP is not contained within transport vesicles of the endosomal recycling pathway, and that transferrin is sorted away from HRP before entry into the 80 S vesicles. Two complementary techniques were utilized to demonstrate that the HRP sedimenting at 80 S is contained within SVLVs. If SVLVs are depleted from a cytoplasmic supernatant of HRP loaded PC12 cells by binding to beads coated with anti-synaptophysin antibodies, there is no remaining 80 S peak of HRP. In addition, if the density of HRP containing vesicles from a cytoplasmic supernatant of HRP loaded PC12 cells is increased by reaction with H_2O_2 and 3,3'-diaminobenzadine, a fraction of synaptophysin immunoreactivity from the 80 S peak of SVLVs sediments more rapidly through the gradient. HRP traffic into and out of the 80 S peak has been used as a marker of SVLV dynamics. Depletion of HRP from preloaded SVLVs can be stimulated by incubating PC12 cells in chase media containing carbachol/55 mM potassium

or α-lactrotoxin. This result is consistent with the proposal that HRP is being released from SVLVs by regulated exocytosis. In addition, uptake of HRP into SVLVs can also be stimulated by carbachol/55 mM potassium implying that regeneration of SVLVs by endocytosis is also regulated.

Introduction

PC12 cells secrete catacholamines from dense core granules in response to stimulation with agonists of nicotinic acetylcholine receptors. If the function of SVLVs is related to that of synaptic vesicles they should also undergo regulated exocytosis. Uptake of horseradish peroxidase has been used to demonstrate that the synaptic vesicles of the frog neuromuscular junction recycle by endocytosis after stimulation (Holtzman, et al. 1971). This technique has been extended to observe HRP uptake into small vesicles identified by physical properties rather than by morphological proximity to synapses (Clift-O'Grady, et al. 1990). We have used HRP as a bulk phase marker in PC12 cells to determine if regulated exocytosis also occurs from SVLVs.

Results

Validation of HRP as a marker for SVLVs

If PC12 cells are loaded with HRP prior to homogenization, a peak of peroxidase activity co-sediments with SVLVs on glycerol gradients (Clift-O'Grady, et al. 1990) . Because HRP internalization is non-specific, this peak could represent HRP in any small vesicle derived by endocytosis or a fragment created from a larger endosomal vesicle during homogenization. Evidence

against these possibilities came from the absence of a peak of internalized ^{125}I-transferrin migrating at 80 S (Clift-O'Grady, et al. 1990). To quantify this effect, PC12 cells were incubated with media containing both HRP and transferrin and the targeting of each to the 80 S peak was compared (Figure 1-1). 57% of the sedimentable HRP in a cytoplasmic supernatant sedimented with SVLVs in fractions 8 to 11 compared with only 8% of the ^{125}I-transferrin. Therefore, the HRP which co-sediments with SVLVs is not contained within vesicles of the transferrin recycling pathway including uncoated primary endocytotic vesicles, sorting endosomes, recycling endosomes, or fragmented plasma membrane.

Transferrin was not completely excluded from the fractions co-sedimenting with SVLVs. This would occur if sorting of the transferrin receptor out of SVLVs is inefficient. An alternative possibility is that the transferrin sedimenting at 80 S is not receptor bound. A competition experiment was carried out to determine the fraction of ^{125}I-transferrin internalization which was non-specific. In the presence of a five fold excess of unlabeled transferrin internalization was reduced by 74%. Therefore, 89% (74% x 6/5) of the internalization was specific and 11% was non-specific. Based on the result with HRP, 57% of the non-specific transferrin (6% of the total transferrin) would be expected to fractionate with SVLVs. Thus, bulk phase endocytosis of a fraction of the ^{125}I-transferrin can account for the small amount of transferrin which co-sediments with SVLVs.

An immunodepletion experiment was carried out to determine whether the peak of HRP is contained within SVLVs (Figure 1-2). Synaptophysin containing organelles from a sample of small organelles derived from PC12

Figure 1-1. Transport of HRP and transferrin to SVLVs. SVLVs were prepared from PC12 cells after incubation in media containing both HRP and ^{125}I-transferrin. Only HRP was recovered in the 80 S peak.

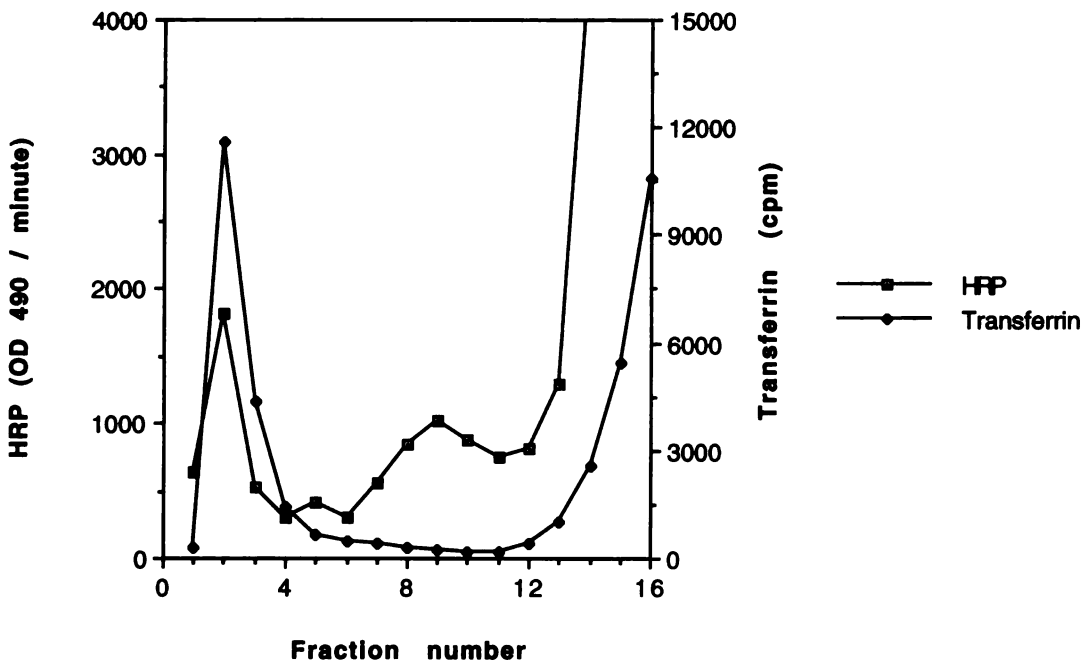
4000
3000
2000
1000
0
HRP (OD 490 / minute)
15000
12000
9000
6000
3000
0
Transferrin (cpm)
0
4
8
12
16
Fraction number
HRP
Transferrin

Figure 1-2. Immunodepletion of SVLVs containing HRP. Small organelles from PC12 cells loaded with HRP were immunodepleted by adsorption to magnetic beads coated with anti-synaptophysin or control antibodies. (A) HRP activity was depleted by anti-synaptophysin beads but not by control beads. (B) Synaptophysin immunoreactivity was depleted by anti-synaptophysin beads but not by control beads.

A

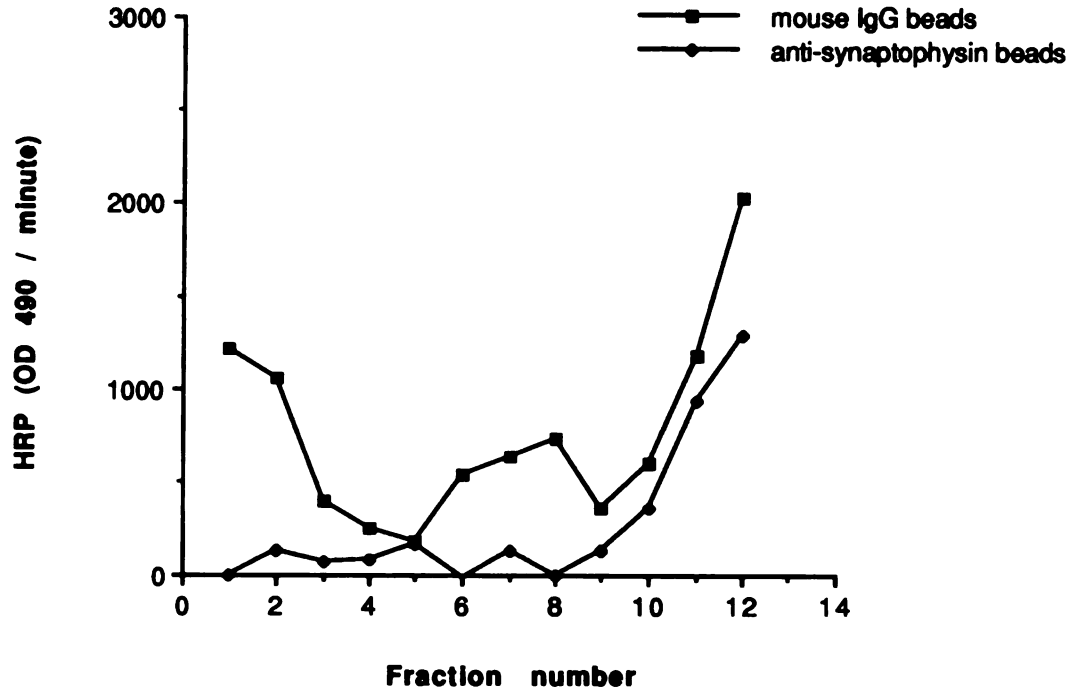
mouse IgG beads
anti-synaptophysin beads
HRP (OD 490 / minute)
3000
2000
1000
0
0
2
4
6
8
10
12
14
Fraction number

B

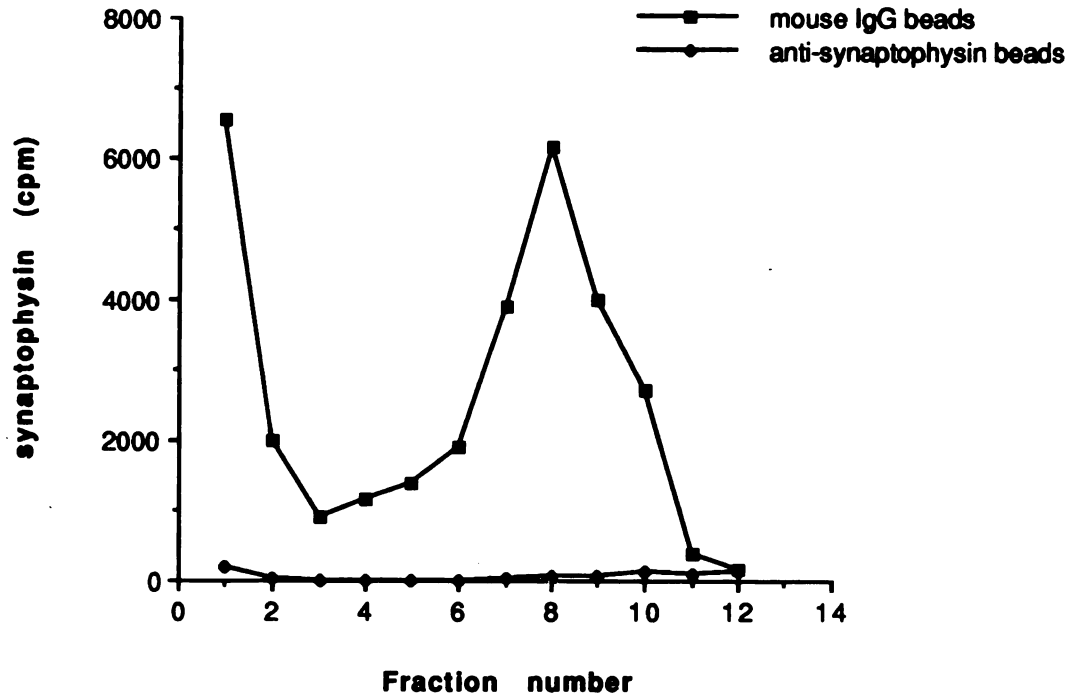
mouse IgG beads
anti-synaptophysin beads
synaptophysin (cpm)
8000
6000
4000
2000
0
0
2
4
6
8
10
12
14
Fraction number

cells loaded with HRP were immunodepleted by incubation with anti-synaptophysin antibody coated magnetic beads. When the immunodepleted sample was sedimented into a glycerol gradient, the peak of HRP migrating at 80 S was no longer present. Therefore, the HRP was contained in organelles which have synaptophysin as a membrane protein. HRP was also depleted from fractions at the bottom of the tube. These organelles are likely to be endosomes which also contain both HRP and synaptophysin. Neither peak was depleted from control samples which were incubated with magnetic beads coated with mouse immunoglobulins.

A density shift protocol was also used to demonstrate that SVLVs contain HRP. HRP catalyses the formation of free radicals from H_2O_2 which interact with 3,3'-diaminobenzadine (DAB) and crosslink it into dense aggregates (Courtoy et al., 1984). When organelles from PC12 cells loaded with HRP were incubated with DAB and H_2O_2, a fraction of the SVLVs sedimented more rapidly and accumulated at the bottom of the gradient above a sucrose cushion. This result implies that the SVLVs which shifted to the bottom of the gradient contained HRP (Figure 1-3, A).

A potential pitfall in DAB density shift experiments is that vesicles which do not contain HRP can be crosslinked into a rapidly sedimenting aggregate if DAB is activated by soluble HRP. The low capacity of SVLVs for HRP and the release of HRP from larger vesicles fragmented during homogenization (see Figure 1-1) favor non-specific aggregation. To avoid this problem, much of the free HRP was removed by pelleting and resuspending the organelles prior to adding DAB. A trace amount of HRP-free, ^{35}S labeled SVLVs were included in the reaction to test for non-specific aggregation. There was no decrease in the fraction of ^{35}S cpm recovered in the SVLV peak

Figure 1-3. DAB mediated density shift of SVLVs containing HRP. Small organelles from PC12 cells loaded with HRP were incubated with DAB in the presence or absence of H_2O_2. (A) Partial shift of synaptophysin immunoreactivity from HRP labeled cells. (B) HRP free ^{35}S-SVLVs did not shift.

A

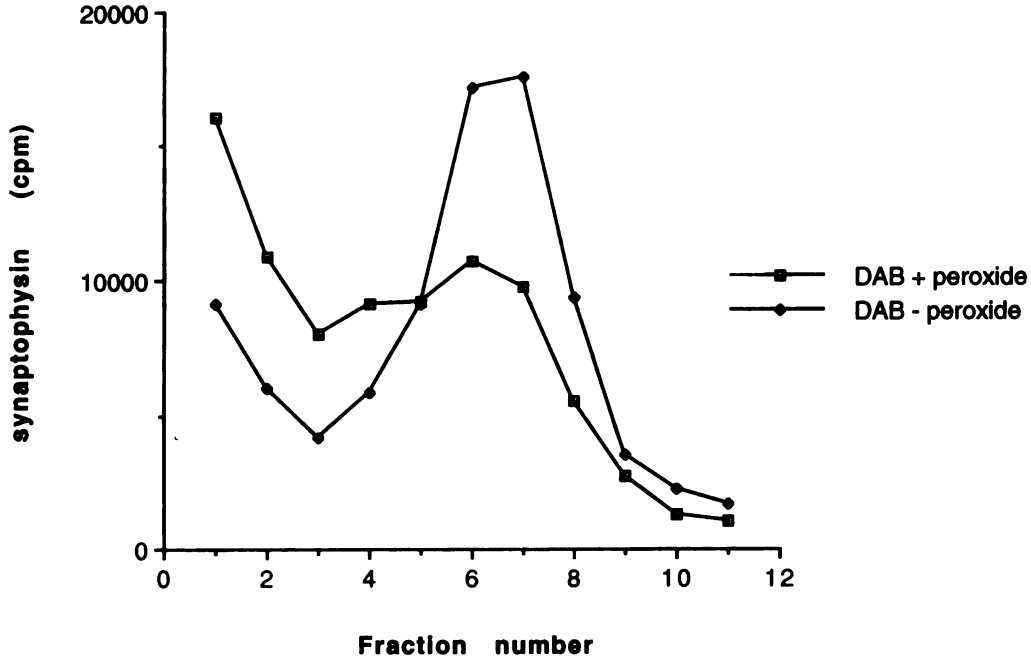
20000
10000
0
synaptophysin (cpm)
0
2
4
6
8
10
12
Fraction number
DAB + peroxide
DAB - peroxide

B

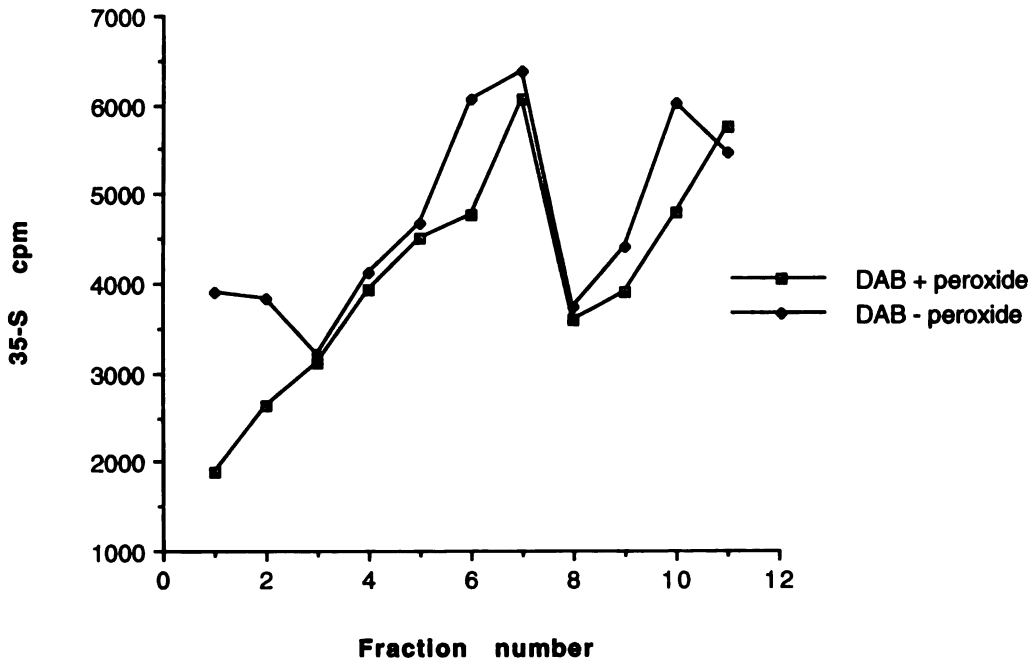
7000
6000
5000
4000
3000
2000
1000
35-S cpm
0
2
4
6
8
10
12
Fraction number
DAB + peroxide
DAB - peroxide

when H_2O_2 was included in the reaction. Therefore, the SVLVs which shifted to the bottom of the glycerol gradient contained HRP (Figure 1-3, B).

Compared with a parallel control lacking H_2O_2, 27% of the SVLVs shifted from the 80 S position to the bottom of the gradient. The SVLVs which remained in the 80 S peak did not contain sufficient HRP to catalyze crosslinking of DAB. Some of these vesicles did not load with HRP during the 1 hour preincubation. Other SVLVs remaining in the 80 S peak may have contained subthreshold amounts of HRP. These vesicles did not shift because the extent of the reaction was minimized to avoid non-specific aggregation. If the reaction time was increased, all of the SVLVs shifted, but so did a fraction of the HRP free ^{35}S cpm trace vesicles.

Regulation of SVLV membrane traffic

Once it was established that HRP sedimenting at 80 S is contained within SVLVs, the HRP peak was used as an indicator for the formation and loss of SVLVs. Conditions which stimulate release from dense core secretory granules were examined to determine if release of HRP from SVLVs is also regulated. PC12 cells preloaded with HRP were chased in media containing carbachol and high potassium. At chase times from 5 to 30 minutes, the amount of HRP remaining in SVLVs decreased compared with a parallel control chased without stimulation (Figure 1-4). In addition, the amount of HRP remaining in SVLVs could also be depleted by incubation in α-latrotoxin, a component of black widow spider venom which induces secretion from synaptic vesicles and from the dense core granules of PC12 cells (Meldolesi et al., 1983, Pashkov et al., 1993). After a 5 minute incubation with 2 nm α-latrotoxin, the amount of HRP remaining in SVLVs was depleted by 36%. The stimulatable depletion of

Figure 1-4. Stimulated loss of HRP labeled SVLVs. PC12 cells were incubated for 1 hour in HRP to load SVLVs then chased for various times in the presence (closed symbols) or absence (open symbols) of 5 mM carbachol and 55 mM KCl. HRP remaining in the SVLV fractions was compared with a control stored at 4°C during the chase period. Data from six independent experiments are presented.

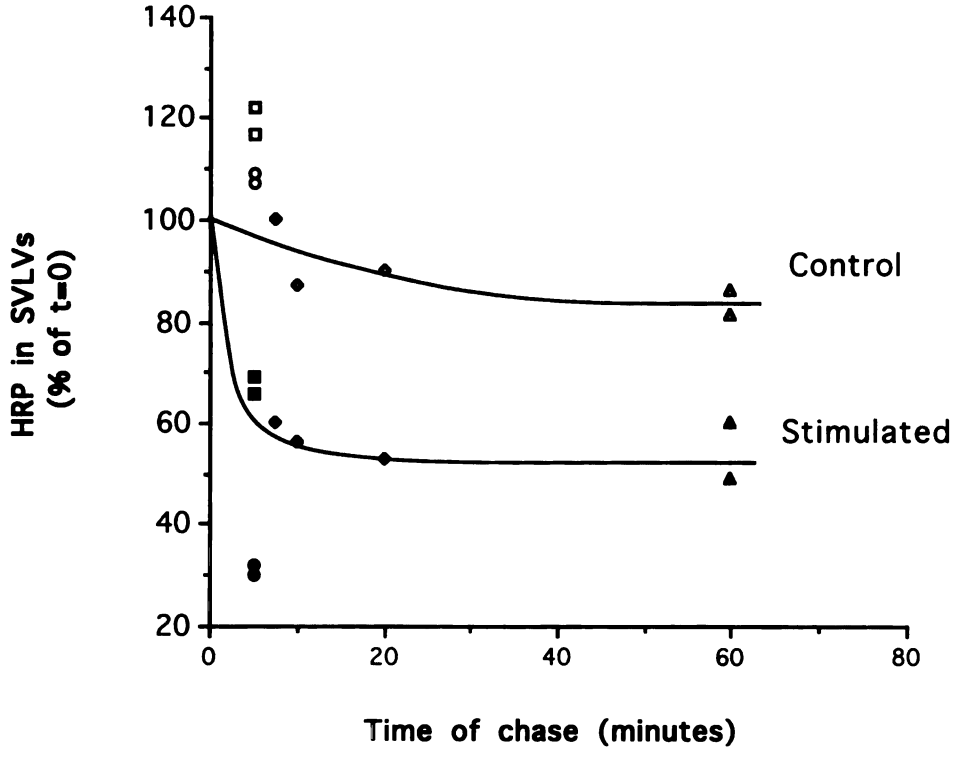
140
120
100
80
60
40
20
0
20
40
60
80
HRP in SVLVs
(% of t=0)
Control
Stimulated
Time of chase (minutes)

HRP from SVLVs results suggests that HRP is released from SVLVs by regulated exocytosis.

As a secondary indicator of regulated release, the rate of HRP loading into recycling SVLVs was measured in the presence or absence of stimulation with carbachol/KCl. In nerve terminals, the rate of synaptic vesicle recycling increases after stimulated exocytosis to replenish the pool of synaptic vesicles available for release. PC12 cells were incubated for 30 minutes in media containing HRP in the presence or absence of carbachol and high potassium. The amount of HRP recovered in SVLVs increased by 50% with stimulation (Figure 1-5). Therefore, the rate of formation of SVLVs is increases after stimulation to replenish the pool of SVLVs depleted by exocytosis.

Figure 1-5. Stimulated uptake of HRP to SVLVs. PC12 cells were incubated for 30 minutes in HRP with or without stimulation by 5 mM carbachol and 55 mM KCl. HRP activity was measured in fractions from a glycerol gradient.

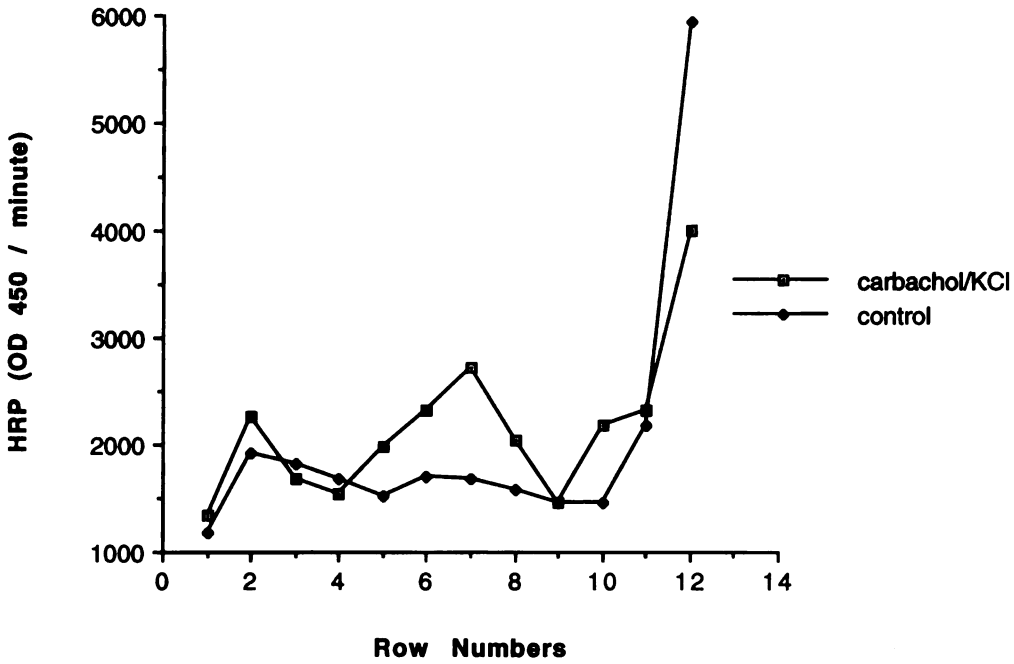
6000
5000
4000
3000
2000
1000
HRP (OD 450 / minute)
0
2
4
6
8
10
12
14
Row Numbers
carbachol/KCl
control

Discussion

The internalization of HRP, but not transferrin, from the media into SVLVs suggested that SVLVs form by a specialized endocytosis pathway. To validate the utility of using HRP as a marker for SVLVs generated by endocytosis, we have proven that the peak of HRP comigrating with synaptic vesicle markers is HRP contained within SVLVs. This proof involved two steps: (1) demonstrating that the HRP was in an organelle containing the synaptic vesicle membrane protein synaptophysin by showing that depletion of organelles containing synaptophysin lead to a loss of the HRP peak; and (2) demonstrating that shifting the density of HRP containing organelles by incubation in DAB/H_2O_2 lead to a loss of SVLVs containing HRP from the 80 S peak.

It is not possible to measure directly the amount of HRP released into the media by exocytosis from SVLVs because the amount of HRP contained within SVLVs is small and HRP is also released into the media from recycling endosomes and by dissociation from the cell surface. Therefore, the decline in the amount of HRP remaining in SVLVs was measured as an indicator of the amount of exocytosis. If SVLVs fuse with the plasma membrane and release their contents, the amount of HRP remaining in SVLVs should decline. During the chase, new SVLVs forming by endocytosis will not contain HRP, so the HRP/synaptophysin ratio in the SVLV population will decline. The rate of unloading was reproducibly stimulated by incubation in media containing carbachol/KCl. The average yield of SVLVs was not reduced by incubation in carbachol/KCl (data not shown) suggesting that the stimulated fusion of SVLVs must be matched by a corresponding increase in the rate of SVLV generation

by endocytosis. Supporting this prediction, the rate of loading SVLVs with HRP also increase when PC12 cells were incubated in carbachol/KCl.

At the molecular level, regulated exocytosis requires an interaction of specialized components of the secretory vesicle and plasma membrane. SVLVs contain all the known membrane proteins of synaptic vesicles strongly suggesting that they should be able to undergo regulated release (Cameron, et al. 1991, Clift-O'Grady, et al. 1990). Similarly, the plasma membrane of PC12 cells must contain all proteins involved in the regulated exocytosis of large dense-cored secretory granules, a process related, but not identical, to exocytosis of synaptic vesicles. In addition two proteins of the presynaptic plasma membrane thought to be required for docking of synaptic vesicles prior to fusion, syntaxin and SNAP-25, are expressed in PC12 cells (Grote et al., 1994, Osen-Sand et al., 1993).

A critical feature distinguishing neuroendocrine cells from neurons is the absence of morphologically identifiable synaptic contacts. Another distinction is that fusion and recycling of synaptic vesicles is regulated much more tightly than cycling of SVLVs in PC12 cells. Recycling synaptic vesicles can be labeled with the lipophilic dye FM1-43 after stimulation of neurotransmitter release. No dye loading of synaptic vesicles is observed in the absence of stimulation (Betz and Bewick 1992). The regulated recycling of SVLVs is more similar to the recycling of vesicles in hippocampal neurons developing in culture (Matteoli et al., 1992). Perhaps the cytoskeletal interactions that cluster synaptic vesicles near release sites allow for a tighter regulation of exocytosis.

The function of SVLVs is currently unknown. SVLVs in the insulin secreting ß-cells of pancreatic islets contain the neurotransmitter GABA.

Regulated exocytosis of GABA might modulate islet function by interacting with GABA(B) receptors on adjacent ß-cells or GABA(A) receptors on glucagon secreting α-cells (Thomas-Reetz and De Camilli 1994).

SVLVs are especially abundant in cultured PC12 cells increasing their utility as a system for the study of synaptic vesicle biogenesis. In addition, PC12 cells will express foreign proteins both after transient transfection and as stable cell lines after selection. The ability to measure regulate exocytosis from SVLVs in PC12 cells may be useful in the analysis of mutated synaptic vesicle proteins.

It may also be possible to use acetylcholine secretion as a marker for regulated exocytosis from SVLVs. It is well established that PC12 cells can secrete both catecholamines and acetylcholine and that these neurotransmitters are stored in distinct vesicles (Schubert and Klier 1977) . PC12 cells differentiated with nerve growth factor have an increased capacity for regulated acetylcholine secretion. Small quantities of acetylcholine, but not catecholamines, have been found in SVLVs from undifferentiated PC12 cells identified by size selection on a controlled pore glass column (Bauerfeind et al., 1993). However, acetylcholine might also be secreted from larger storage organelles and it has also been reported that catecholamines are contained in SVLVs (Annaert et al., 1993, Bauerfeind, et al. 1993). Therefore, measuring HRP depletion from 80 S vesicles is the best technique to insure that release is occurring from SVLVs.

Methods:

Preparation of cytoplasmic supernatants: PC12 cells were fed with DME-H21 supplemented with 10% horse serum, 5% fetal calf serum, 1000 U/ml penicillin and 1000 mcg/ml streptomycin and grown in 15 cm dishes in a 37°C, humidified 10% CO_2 incubator. After HRP loading, cells were washed in buffer A (150 mM NaCl, 1 mM EGTA, 0.1 mM $MgCl_2$, 10 mM Hepes, pH 7.4) at 4°C, collected from the dishes, pelleted, and resuspended in of 500 µl buffer A. To homogenize, cells were passed 9 times through a ball bearing cell cracker with an 8 µm clearance. A postnuclear supernatant was prepared from the homogenates by a 5 minute, 1,000 x g centrifugation. The cytoplasmic supernatant containing SVLVs was prepared from the postnuclear supernatant by pelleting larger vesicles for 15 minutes at 16,000 x g.

Velocity sedimentation: Samples were diluted to 150 µl and layered over a 5 ml, 5-25% glycerol gradient in buffer A with a 400 µl, 50% sucrose cushion where indicated. The gradients were centrifuged for 1 hour at 48,000 rpm in an SW55 rotor, then collected, dropwise, in fractions from the bottom of the tube (Clift-O'Grady, et al. 1990).

HRP and synaptophysin detection: To assay for peroxidase activity, 100 µl samples were added to 700 µl substrate mix (350 µM o-dianisidine (Sigma), 0.003% H_2O_2, 0.1 % TX-100, 50 mM $NaHPO_4$, pH 5.0) and the rate of OD_{460} increase was measured (Steinman et al., 1974) . Synaptophysin immunoreactivity was measured using a well assay (Clift-O'Grady, et al. 1990).

Cointernalization of transferrin and HRP: Mouse transferrin was saturated with iron, then iodinated to 8 x 10^5 cpm/μg in iodogen (Pierce) coated tubes. PC12 cells were incubated at 37°C for 140 minutes in DME-H21 supplemented with 10 mg/ml HRP (Sigma, Type II) and 18 μg/ml ^{125}I-transferrin. A cytoplasmic supernatant was prepared and sedimented on a glycerol gradient.

DAB density shift: A cytoplasmic supernatant was prepared from PC12 cells incubated at 37°C for 60 minutes in 15 mg/ml HRP. To separate SVLVs from soluble HRP released during homogenization, a P3 was prepared by pelleting the SVLVs during a 90 minute centrifugation at 125,000 x g in an airfuge. The P3 was resuspended in buffer A by 5 passes through a 25 gauge needle. ^{35}S-SVLVs were prepared from PC12 cells incubated overnight in 1 mCi/15 ml TRANS ^{35}S-label. To separate ^{35}S-SVLVs from soluble and peripheral membrane ^{35}S-labeled proteins the cytoplasmic supernatant was twice pelleted and resuspended as above. A trace amount of the ^{35}S labeled SVLVs was added to the HRP labeled organelles, and aliquots were incubated with 2.5 mg/ml filtered 3,3'-diaminobenzadine (DAB) in the presence or absence of 0.05% H_2O_2 for 15 minutes at 25°C in the dark then loaded onto glycerol velocity gradients.

Organelle immunodepletion: A cytoplasmic supernatant was prepared from PC12 cells incubated at 37°C with 15 mg/ml HRP for 90 minutes followed by a 20 minute chase in HRP-free medium. SVLVs were pelleted during 30 minutes at 98,000 rpm in a TLA 100.3 rotor to separate them from soluble HRP, then resuspended in buffer A supplemented with 10 mg/ml bovine serum

albumin. Magnetic beads with covalently coupled sheep anti-mouse IgG1 (Dynal) were coated with SY38 (anti-synaptophysin, cytoplasmic domain, Boehringer Mannheim) monoclonal antibodies or a control mouse IgG fraction during a 4 hour incubation at 4°C. The resuspended SVLVs were incubated with beads for 3 hours at 4°C. The beads were then removed and the remaining organelles were layered on a glycerol gradient.

Exocytosis of preloaded HRP: PC12 cells were loaded with HRP during a 1 hour incubation at 37°C then stored at 4°C or chased at 37°C in HRP free media in the presence or absence of 5 mM carbachol and 55 mM KCl for various times. Alternatively, cells were stimulated by a 5 minute incubation with 2 nM α-latrotoxin (J. Mendolesi, Milano). A P3 prepared as above was sedimented through a glycerol velocity gradient without a sucrose cushion, and HRP and synaptophysin were quantified in each fraction. The activity in four peak fractions was integrated. An HRP activity / synaptophysin immunoreactivity ratio was calculated to normalize for the yield of SVLVs. For each individual experiment, the fraction of remaining HRP labeled SVLVs was calculated by dividing the HRP/synaptophysin ratio after chase by the HRP/synaptophysin ration of the 4°C control.

Chapter Two

Targeting of an epitope-tagged VAMP to synaptic vesicle-like vesicles in transfected PC12 cells

Abstract

An epitope-tagged synaptic vesicle membrane protein (VAMP-TAg) was constructed to permit analysis of targeting and membrane traffic in transfected PC12 cells. VAMP-TAg is O-glycosylated indicating passage through the secretory pathway. Mature VAMP-TAg is localized primarily in endosomes, but is also present on the cell surface and in synaptic vesicle-like vesicles (SVLVs). The fraction of VAMP-TAg present in SVLVs is less than that of endogenously expressed synaptic vesicle membrane proteins such as synaptophysin and VAMP-2. Overexpression of VAMP-TAg in some of the transfected cells may inhibit sorting to SVLVs by saturation of the targeting pathway. VAMP-TAg competes with VAMP-2, but not with synaptophysin, for targeting to SVLVs suggesting that VAMPs are sorted to SVLVs by associating with other synaptic vesicle proteins. Antibody bound to VAMP-TAg at the cell surface of transfected PC12 cells is internalized to endosomes and sorted to SVLVs. Internalized antibody appears in SVLVs only after a 6 minute lag suggesting that SVLVs form by budding of vesicles from an endosomal intermediate.

Results

Construction of VAMP-TAg

In anticipation of the possibility that mutations affecting the membrane traffic of VAMP might also destroy epitopes required for detection, an epitope tagged version of rat VAMP-2 was constructed. (Figure 2-1) The epitope tag was appended to the C-terminus of VAMP so that it would project into the lumen of SVLVs or, upon exocytosis, the outer surface of the plasma membrane. A defined 7 amino acid C-terminal epitope from the SV40 T antigen was chosen. The KT3 monoclonal antibody binds to this epitope in the SV40 T antigen at 5.2×10^6 M^{-1} affinity. It was discovered that the sequence N-terminal to the epitope can also influence binding of KT3. Insertion of a 14 amino acid spacer between the transmembrane domain and the epitope tag increased the binding of KT3 both to the surface of transfected cells and to protein on immunoblots. The spacer used was derived from the corresponding, juxtamembrane domain of the transferrin receptor, but was modified to include 3 tyrosines and 2 lysines as possible sites for experimental modification. The final epitope tagged rat VAMP-2 derivative is referred to as VAMP-TAg and was used as the parental cDNA for all the mutants described below.

Expression of VAMP-TAg in PC12 cells

To examine the membrane transport of VAMP-TAg, a transfected PC12 cell line was selected. PC12/VAMP-TAg cells express barely detectable amounts of VAMP-TAg unless expression is stimulated by incubation in butyrate, an agent which alters transcriptional regulation by preventing deacetylation of histones. The time course of VAMP-TAg expression after butyrate induction

Figure 2-1. Epitope tagging of VAMP-2. Rat VAMP-2 has a 94 amino acid cytoplasmic domain which can be subdivided into a proline/glycine rich variable region (Var) and a highly conserved alpha helical region (Conserved). It is anchored to membranes via a 21 amino acid hydrophobic domain (TM). A 21 amino acid extension consists of a spacer region derived from the juxtamembrane region of the extracellular domain of the transferrin receptor and the 7 C-terminal amino acids of the SV40 large T antigen which serve as the epitope for the monoclonal antibody KT3.

VAMP-TAg

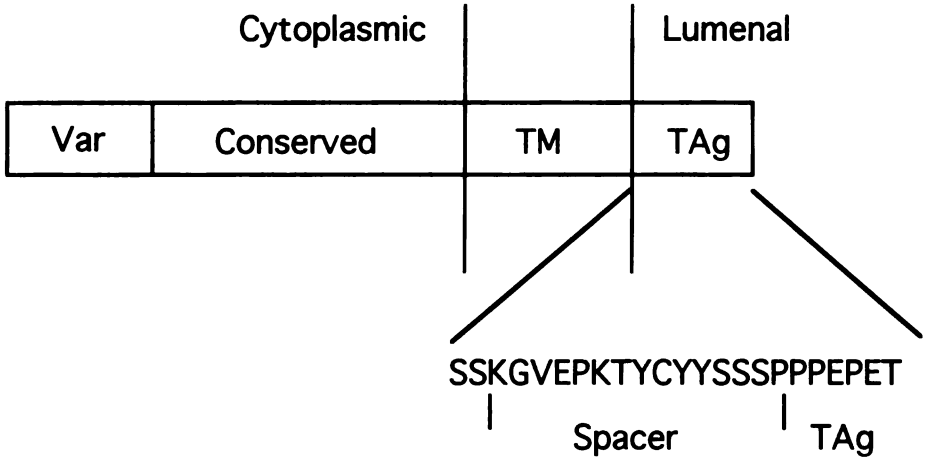
Cytoplasmic
Lumenal
Var
Conserved
TM
TAg
SSKGVEPKTYCYYSSSPPPEPET
Spacer
TAg

was measured in PC12/VAMP-TAg cells incubated in butyrate for various times prior to labeling newly synthesized proteins with ^{35}S TRANS ^{35}S-label during a 2 hour pulse. (Figure 2-2, A) VAMP-TAg was immunoprecipitated with KT3 antibodies and the immunoprecipitates were run on a polyacrylamide gel and observed by fluorography. Two VAMP-TAg bands absent from nontransfected cells were observed in each precipitate. Radioactivity in the VAMP-TAg bands was quantified by phosphorimaging. (Figure 2-2, B) VAMP-TAg biosynthesis increased after a 9 hour lag, and then declined again after 16 hours. To examine the effect of this burst of VAMP-TAg synthesis on the total amount of VAMP-TAg, extracts were prepared from PC12/VAMP-TAg cells at various times after the addition of butyrate and analyzed by electrophoresis and immunoblotting with anti-VAMP antibody. (Figure 2-2, C) When immunoblots are probed with anti-VAMP antibody, VAMP-TAg can be distinguished from endogenously expressed VAMP-2 because the epitope tag increases its molecular weight. The amount of endogenous VAMP-2 remained constant over time, but there was a large increase in the expression of VAMP-TAg. The ratio of VAMP-TAg to VAMP-2 expression was quantified by densitometry of immunoblots. At early time points, the major VAMP species detected was the endogenously expressed VAMP-2. During the burst of VAMP-TAg synthesis, the VAMP-TAg : VAMP-2 ratio increased from 0.015 to 1.5 and then reached a plateau at the end of the window of VAMP-TAg synthesis. Butyrate treated cells were used in later experiments to insure that the transfected proteins would be detected.

Two equally prominent species migrating at 24 and 26 kDa were observed in immunoprecipitates of VAMP-TAg after a 2 hour pulse label. (Figure 2-2, A) The 26 kDa species was more prominent in immunoprecipitates

Figure 2-2. Induction of VAMP-TAg expression with butyrate. (A) Rate of VAMP-TAg biosynthesis. PC12/VAMP-TAg cells were incubated in butyrate for the indicated times (hours:minutes) prior to a 2 hour labeling with ^{35}S-methionine. KT3 immunoprecipitates from clarified lysates were resolved by SDS-PAGE and detected by fluorography. (B) Radioactive VAMP-TAg in the immunoprecipitates was quantified using a phosphor-imager. (C) Accumulation of VAMP-TAg. PC12/VAMP-TAg cells were incubated in sodium butyrate for various times. Clarified lysates were resolved by SDS-PAGE, transferred to nitrocellulose, probed with anti-VAMP (10.1) antibodies and quantified by densitometry.

6:15
8:20
10:25
12:30
14:35
16:40

B

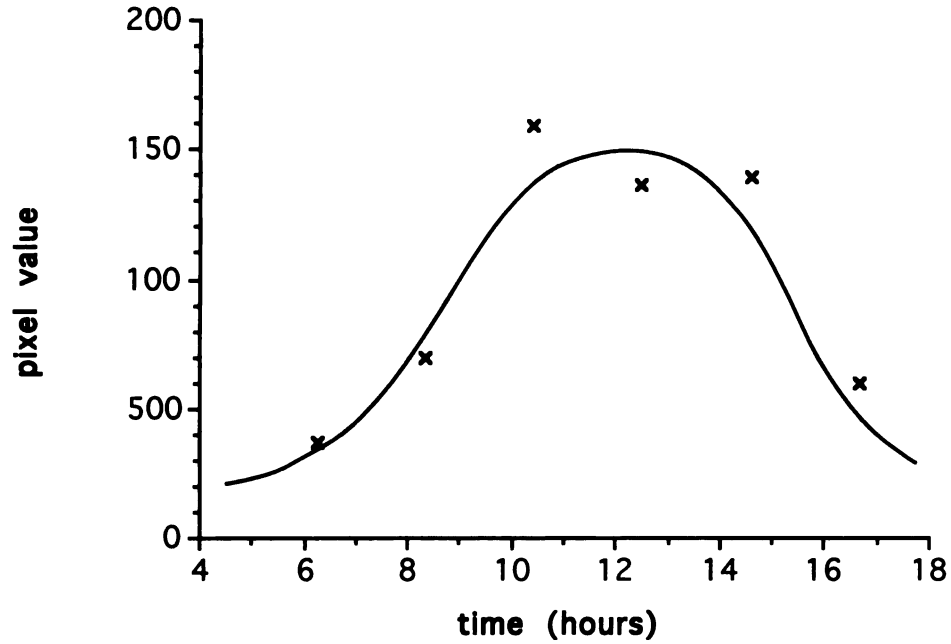
200
150
100
500
0
pixel value
4
6
8
10
12
14
16
18
time (hours)

C

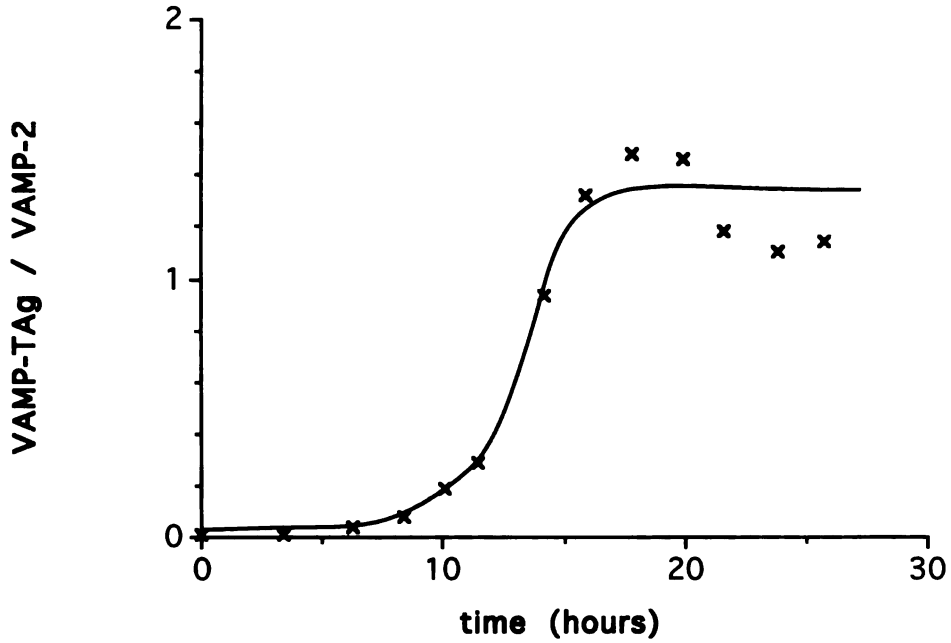
2
1
0
VAMP-TAg / VAMP-2
0
10
20
30
time (hours)

from cells labeled during a 16 hour incubation in TRANS ^{35}S-label. This observation suggested that VAMP-TAg might be post-translationally modified. To test this possibility, PC12/VAMP-TAg cells were pulsed labeled with TRANS ^{35}S-label, then chased for various times prior to immunoprecipitation. The fraction of VAMP-TAg migrating at 26 kDa increased from 19% to 81% during two hours of chase. (Figure 2-3, A) The 26 kDa species was sensitive to digestion with neuraminidase indicating that it contains sialic acid. (Figure 2-3, B) Since the epitope tag and spacer contain 7 serine or threonine residues, but lacks asparagine, it is likely that VAMP-TAg is modified by o-linked glycosylation. O-glycosylation can occur in the endoplasmic reticulum or the cis-Golgi network implying that VAMP-TAg is transported through the secretory pathway (Perez-Vilar et al., 1991) . This finding suggests that VAMP is not incorporated into synaptic vesicles directly from the cytoplasm as was suggested by Baumert *et al* (1989).

Targeting of VAMP-TAg to endosomes

As a preliminary step to determine the localization of VAMP-TAg, transfected PC12 cells were stained by indirect immunofluorescence with KT3 antibodies (Figure 2-4). When the total population of VAMP-TAg was stained in fixed cells permeabilized with saponin, a predominantly perinuclear pattern was observed with additional punctae stained throughout the cytoplasm. This staining pattern is similar to the staining patterns of synaptophysin and internalized transferrin in PC12 cells (Cameron, et al. 1991) suggesting that VAMP is primarily localized in endosomes.

To determine if VAMP-TAg cycles between endosomes and the plasma membrane, PC12/VAMP-TAg cells were incubated in KT3 antibodies for 5

Figure 2-3. Post-translational processing of VAMP-TAg. (A) Time course of VAMP-TAg maturation. PC12/VAMP-TAg cells were labeled for 10 minutes with TRANS ^{35}S-label, washed, and chased for various times with unlabeled media. Clarified cell lysate was immunoprecipitated with KT3 antibodies, resolved by SDS-PAGE and radioactivity in the 24 and 26 kDa VAMP-TAg bands was quantified using a phosphor imager. (B) Neuraminidase sensitivity. PC12/VAMP-TAg cells were labeled for 16 hours with TRANS ^{35}S-label. A clarified lysate was immunoprecipitated with KT3 antibodies and aliquots of the immunoprecipitate were incubated with or without neuraminidase, resolved by SDS-PAGE, and detected by fluorography.

A

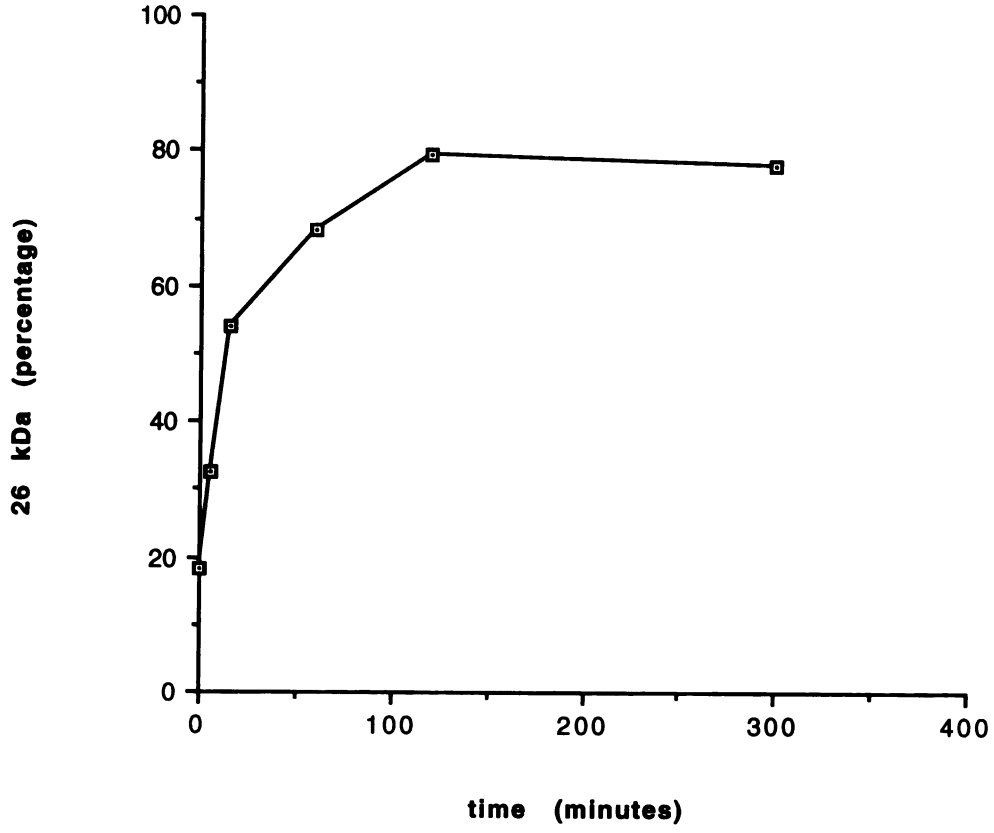
100
80
60
40
20
0
26 kDa (percentage)
0
100
200
300
400
time (minutes)

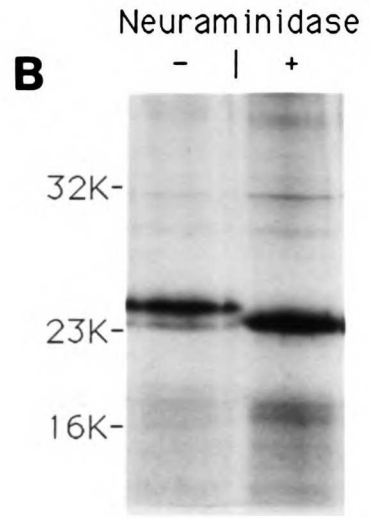
Neuraminidase
B
-
+
32K-
23K-
16K-

Figure 2-4. Detection of total and endosomal VAMP-TAg by immunofluorescence. The total population of VAMP-TAg in saponin-permeabilized PC12/VAMP-TAg cells was stained by indirect immunofluorescence with KT3 antibodies. To detect endosomal VAMP-TAg, PC12/VAMP-TAg cells were incubated with KT3 for 5 minutes at 37°C prior to fixation. The internalized antibody was detected by permeabilizing the cells and staining with FITC-coupled secondary antibodies. Process extension in the cells stained for endosomal VAMP-TAg was induced by growth on Matrigel.

Total VAMP-TAg

Endosomal VAMP-TAg

minutes at 37°C. Because the epitope tag was appended to the C-terminus of VAMP, antibody added to cells can bind to the fraction of VAMP-TAg present at the cell surface. Antibody remaining at the cell surface was removed by washing in acidic buffer prior to fixation. To visualize internalized antibody, the cells were then permeabilized and stained with FITC-coupled secondary antibodies. Because the cells used for staining endosomal VAMP-TAg were plated on extracellular matrix proteins they spread out on the slide and extended short processes allowing better visualization of cytoplasmic staining. The staining pattern of endosomal VAMP-TAg is similar to that of the total protein with a predominantly perinuclear distribution and additional staining of cytoplasmic vesicles. Endosomes containing VAMP-TAg were present throughout the cytoplasm and were present, but not concentrated, in the process. (Figure 2-4)

The fluorescent assay for VAMP-TAg endocytosis involved binding bivalent KT3 antibodies to living cells which might induce internalization by crosslinking VAMP-TAg. To determine if KT3 binding promotes VAMP-TAg endocytosis, internalization was measured by an alternate procedure. PC12/VAMP-TAg cells were incubated in NHS-SS-biotin at 4°C to label cell surface proteins with biotin. After washing in buffer containing free lysine to quench unreacted NHS-SS-biotin, the cells were warmed to 37°C for various times and then biotin was removed from proteins remaining at the cell surface by reducing the disulfide bond with glutathione. Biotinylated proteins protected from reduction by internalization were collected on streptavidin-agrose beads and identified by immunoblotting with KT3 (Figure 2-5). The amount of internalized VAMP-TAg increased with time for 10 minutes. If KT3 was bound to VAMP-TAg during the washing and internalization steps, the rate

Figure 2-5. VAMP-TAg endocytosis occurs independently of KT3. Proteins on the plasma membrane of PC12/VAMP-TAg cells were labeled at 4°C with the membrane impermeable reagent NHS-SS-Biotin. Biotin was stripped from proteins remaining at the cell surface after incubation at 37°C for the indicated times (minutes) by reduction of the disulfide bond with glutathione. A control sample was not reduced to identify the total amount of cell surface VAMP-TAg. Biotinylated proteins protected from reduction by endocytosis were collected on streptavidin-agarose, and internalized VAMP-TAg was detected by immunoblotting with KT3 antibodies.

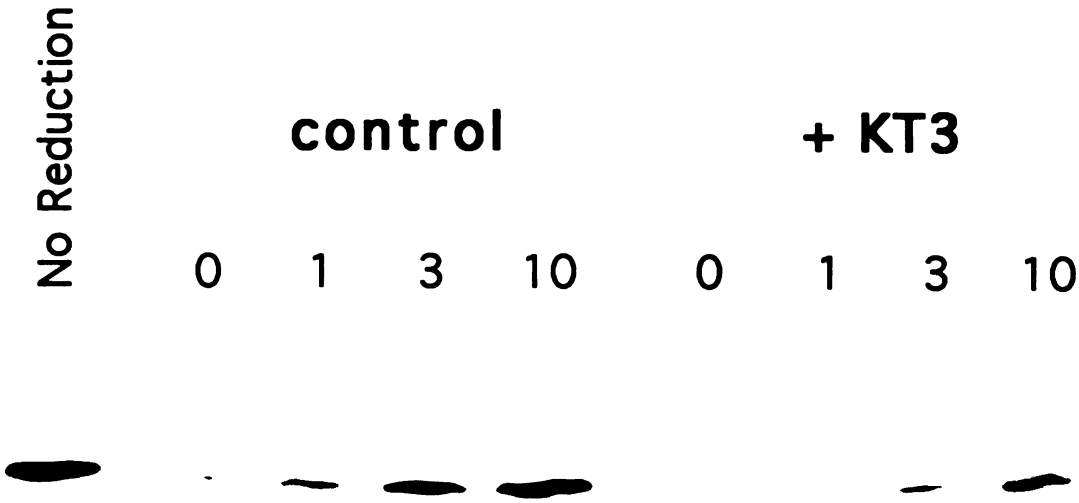
No Reduction
control
+ KT3
0
1
3
10
0
1
3
10

of VAMP-TAg internalization did not increase indicating that VAMP-TAg endocytosis is not dependent on crosslinking by KT3.

Targeting of VAMP-TAg to SVLVs

To determine if VAMP-TAg is targeted to SVLVs in addition to endosomes, PC12/VAMP-TAg cells were homogenized and a cytoplasmic supernatant was sedimented through a glycerol gradient. Trichloroacetic acid-precipitated gradient fractions were run on a polyacrylamide gel and immunoblotted with anti-VAMP and anti-synaptophysin antibodies (Figure 2-6, A). A peak of VAMP-TAg co-sedimented at 80 S with the SVLV markers synaptophysin and VAMP-2. No VAMP-TAg peak sedimenting at 80 S was found in transfected CHO cells which lack SVLVs.

A 50% sucrose cushion was layered underneath these glycerol gradients to collect rapidly sedimenting organelles such as endosomes. This made it possible to measure by densitometry the fraction of each protein in the postnuclear supernatant which was recovered in the SVLV peak (Figure 2-6, B). The fraction of VAMP-TAg sedimenting with SVLVs was less than that of synaptophysin or VAMP-2. A simple explanation for this observation is that the epitope tag partially inhibits targeting to SVLVs. Consideration of other possible explanations for the poor targeting of VAMP-TAg to SVLVs led us to characterize sorting of VAMP-TAg in transfected PC12 cells more completely providing insights into the mechanism of SVLV biogenesis.

Regnier-Vigeroux *et al* (1991) reported that synaptophysin labeled with $^{35}SO_4$ in the trans Golgi network of PC12 cells was rapidly transported to a pool which recycles between the plasma membrane and endosomes but reached SVLVs only after a 3 hour lag. Targeting to SVLVs was measured 23 hours after

Figure 2-6. Targeting of VAMP-TAg to SVLVs. (A) VAMP-TAg co-sediments with synaptic vesicle proteins in PC12 cells, but not in CHO cells. PC12/VAMP-TAg and CHO/VAMP-TAg cells were homogenized and a post nuclear supernatant from each was sedimented into a glycerol gradient underlayered with a 50% sucrose cushion. Fractions collected from the bottom of the gradient were TCA precipitated, resolved by SDS-PAGE and immunoblotted with anti-VAMP and anti-synaptophysin antibodies. (B) Quantification of the PC12/VAMP-TAg immunoblot in A by densitometry.

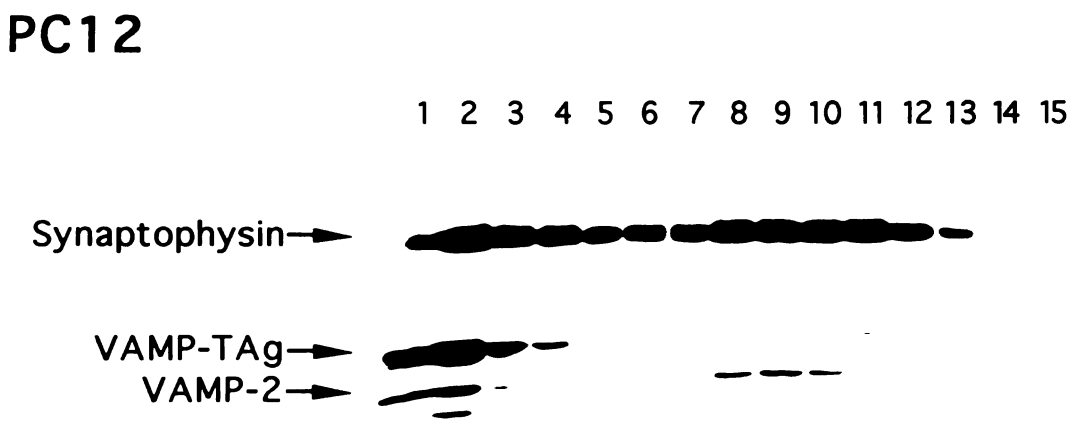
PC12
1 2 3 4 5 6 7 8 9 10 11 12 13 14 15
Synaptophysin
VAMP-TAg
VAMP-2
CHO
VAMP-TAg

B

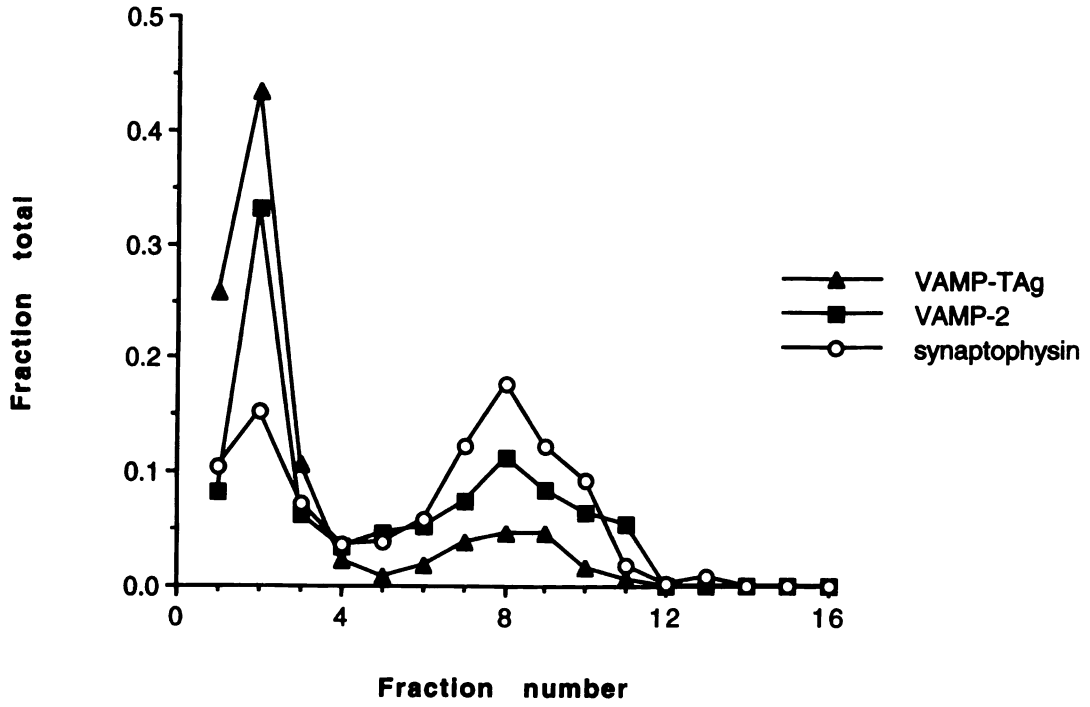
0.5
0.4
0.3
0.2
0.1
0.0
Fraction total
0
4
8
12
16
Fraction number
VAMP-TAg
VAMP-2
synaptophysin

the addition of butyrate which corresponds to 10 hours after the peak of VAMP-TAg synthesis. If the cohort of newly synthesized VAMP-TAg had not yet been completely sorted to SVLVs, the fraction recovered in SVLVs would be less than that of synaptophysin and VAMP-2 at their steady-state distribution. To determine the time required for VAMP-TAg to reach its steady-state distribution, the fraction of VAMP-TAg recovered in SVLVs was measured at various times after butyrate addition. To correct for experimental variations in the amount of heavy membranes removed in the nuclear pellet and the yield of SVLVs, the fraction of VAMP-TAg in synaptic vesicles was compared with that of VAMP-2 (Figure 2-7). The fraction of VAMP-TAg in the SVLV peak increased between 14 and 17 hours after butyrate addition as the proportion of newly synthesized VAMP-TAg declined. However, there was no further increase in VAMP-TAg targeting to SVLVs between 17 and 24 hours indicating that insufficient time for sorting newly synthesized VAMP-TAg to SVLVs is not responsible for the reduced targeting of VAMP-TAg to SVLVs compared with endogenous synaptic vesicle proteins.

Saturation of SVLVs by VAMP-TAg overexpressin

Another possible explanation for the reduced sorting of VAMP-TAg to SVLVs is that targeting to SVLVs is saturable and that overexpression of VAMP-TAg inhibits targeting. Saturation might have a particularly strong effect on VAMP-TAg sorting if the population of cells studied did not have a uniform level of VAMP-TAg expression. For example, if the mean expression level in the population of cells was similar for VAMP-TAg and VAMP-2, but only 10% of the cells expressed VAMP-TAg whereas the expression level of VAMP-2 was uniform, then sorting to SVLVs might be saturated only in VAMP-TAg

Figure 2-7. Transport of a cohort of newly synthesized VAMP-TAg to SVLVs. PC12/VAMP-TAg cells were incubated in butyrate for the indicated times prior to analysis of targeting to SVLVs as above: The fraction of VAMP-TAg recovered in SVLVs at each time point was compared with the targeting of endogenous VAMP-2. The window of VAMP-TAg synthesis induced by butyrate is indicated.

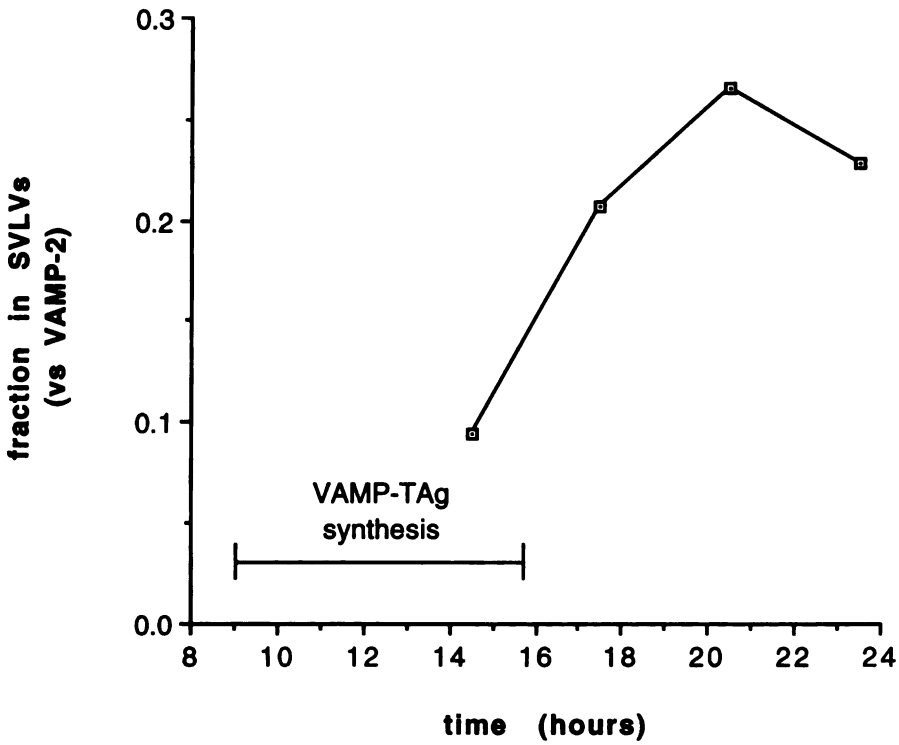
0.3
0.2
0.1
0.0
fraction in SVLVs
(vs VAMP-2)
VAMP-TAg
synthesis
8
10
12
14
16
18
20
22
24
time (hours)

expressing cells. In this case, sorting of VAMP-2 would be normal in the remaining 90% of the cells resulting in an misleadingly higher efficiency of sorting VAMP-2 to SVLVs. Since PC12/VAMP-TAg cells are clonal, an uneven expression pattern was not expected. However, the expression level did not appear uniform when observed by immunofluorescent microscopy. This effect was quantified by fluorescence activated cell sorter analysis (Figure 2-8). A broad range of VAMP-TAg expression levels was observed. Only 6% of the cells were responsible for 29% of the fluorescent signal indicating that if the SVLV sorting pathway is saturable, the uneven expression level of VAMP-TAg could contribute to the reduced fraction of VAMP-TAg in SVLVs observed.

To test for saturation, it was necessary to compare targeting to SVLVs in cell expressing different amounts of VAMP-TAg. Butyrate was used to alter VAMP-TAg expression in otherwise identical cells. Densitometry on immunoblots of gradient fractions was employed to determine the fraction of VAMP-TAg, VAMP-2 and synaptophysin from a postnuclear supernatant which was recovered in SVLVs (Table 2-1). Control experiments on cells not expressing VAMP-TAg established that butyrate itself does not affect the yield of synaptophysin in SVLVs.

Two experiments were conducted on PC12/VAMP-TAg cells which differed in their VAMP-TAg expression levels. In the first experiment the expression of VAMP-TAg was typical: After butyrate induction, there was 2.1 times as much VAMP-TAg as VAMP. Only 35% of the total VAMP in SVLVs was epitope tagged and there was no reduction in the fraction of VAMP-2 recovered in SVLVs.

By contrast, the expression level of VAMP-TAg in the second experiment was an order of magnitude higher. With high VAMP-TAg expression, the

Figure 2-8. Fluorescence activated cell sorter analysis of the range of expression levels in PC12/VAMP-TAg cells. The intensity of surface fluorescence was measured for a population of PC12/VAMP-TAg cells labeled with KT3 antibodies and a FITC coupled secondary antibody.

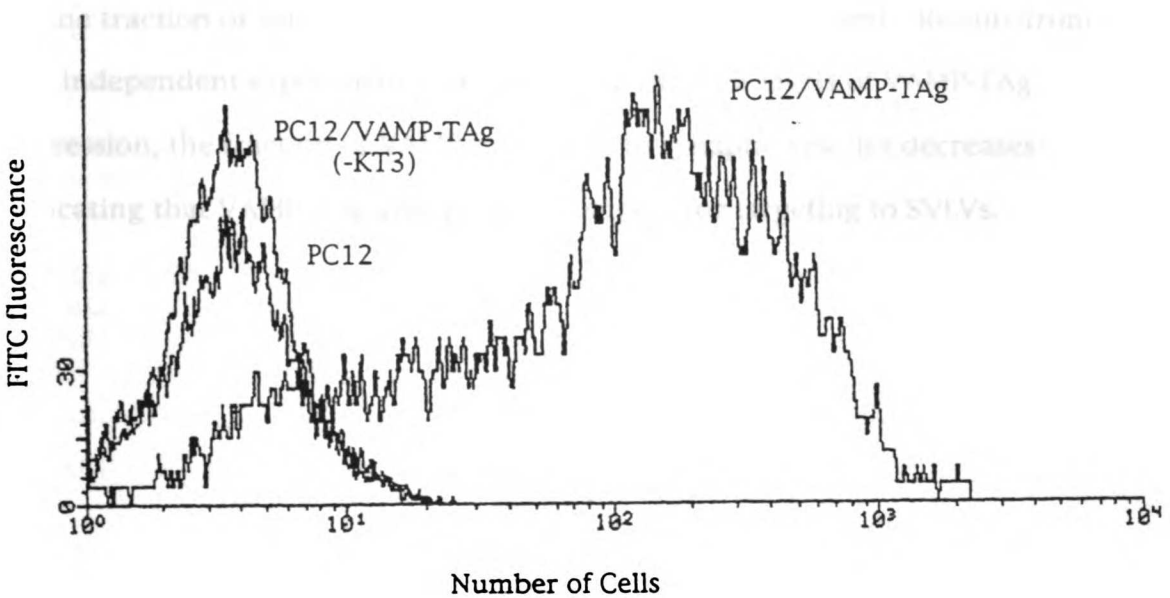
PC12/VAMP-TAg
PC12/VAMP-TAg
(-KT3)
PC12
FITC fluorescence
30
0
10⁰
10¹
10²
10³
10⁴
Number of Cells

Table 2-1. Saturable targeting of VAMP-TAg to SVLVs. PC12 VAMP-TAg cells were grown in the presence or absence of butyrate to generate variations in VAMP-TAg expression. Targeting to SVLVs was analyzed by immunoblot as in Figure 1-6 and quantified by densitometry. The fraction of each protein from a postnuclear supernatant which sediments with SVLVs is presented. To normalize for the recovery of SVLVs, the result for each protein was divided by the fraction of synaptophysin in SVLVs in the same gradient. Results from two independent experiments are presented. At high levels of VAMP-TAg expression, the fraction of VAMP-2 targeted to synaptic vesicles decreases indicating that VAMP-TAg and VAMP-2 compete for targeting to SVLVs.

	Experiment 1		Experiment 2	
	- Butyrate	+ Butyrate	- Butyrate	+ Butyrate
Total Expression Level (VAMP-TAg/VAMP-2)	<0.02	2.1	1.2	24
SVLV peak (VAMP-TAg/VAMP-2)	*	0.54	*	6.4
Fraction in SVLVs				
VAMP-TAg	*	0.10	*	0.06
VAMP-2	0.32	0.39	0.40	0.14
synaptophysin	0.50	0.57	0.60	0.46
Fraction in SVLVs (Normalized to synaptophysin)				
VAMP-TAg / synaptophysin	*	0.17	*	0.12
VAMP-2 / synaptophysin	0.65	0.68	0.68	0.30

* VAMP-TAg not detected

fraction of VAMP-2 recovered in SVLVs was reduced implying that SVLVs were saturated with VAMPs. The fraction of synaptophysin recovered in SVLVs was within the normal range suggesting that VAMP-TAg competes with VAMP-2, but not synaptophysin, for targeting to SVLVs. Even though VAMP-2 was still sorted more efficiently to SVLVs than VAMP-TAg, the expression of VAMP-TAg was so high that there was 6.4 time more VAMP-TAg than VAMP-2 in SVLVs. In total, the recovery of VAMPs (VAMP-TAg + VAMP-2) in SVLVs increased by 500% indicating that, at saturation, the capacity of SVLVs for VAMP is greater than what is observed in nontransfected PC12 cells. This result is consistent with the lower VAMP / synaptophysin ratio in the SVLVs of PC12 cells compared with rat brain synaptic vesicles. Therefore, the level of VAMP-TAg expression in a cell must be high before the fraction targeted to SVLV is reduced by saturation. However, given the variation in expression levels within the clonal population of PC12/VAMP-TAg cells and the greater variation expected in transiently transfected cells, the average targeting of VAMP-TAg to SVLVs observed in a population of transfected cells can be reduced by saturation of SVLVs.

Internalization of VAMP-TAg to endosomes and SVLVs

VAMP-TAg internalized from the cell surface can be transported either to endosomes or to SVLVs. To observe transport to SVLVs, PC12/VAMP-TAg cells were incubated in ^{125}I-KT3 antibodies. After an hour of internalization at 37°C, the cells were homogenized and a cytoplasmic supernatant was sedimented into a glycerol gradient (Figure 2-9). Internalized ^{125}I-KT3 was identified in a peak co-sedimenting at 80 S with synaptophysin immunoreactivity. To determine if ^{125}I-KT3 was sorted to SVLVs the fraction

Figure 2-9. Transport of VAMP-TAg from the cell surface to SVLVs. PC12/VAMP-TAg cells were incubated in media containing ^{125}I-KT3 for 1 hour at 37°C. The cells were homogenized and a cytoplasmic supernatant was sedimented into a glycerol gradient.

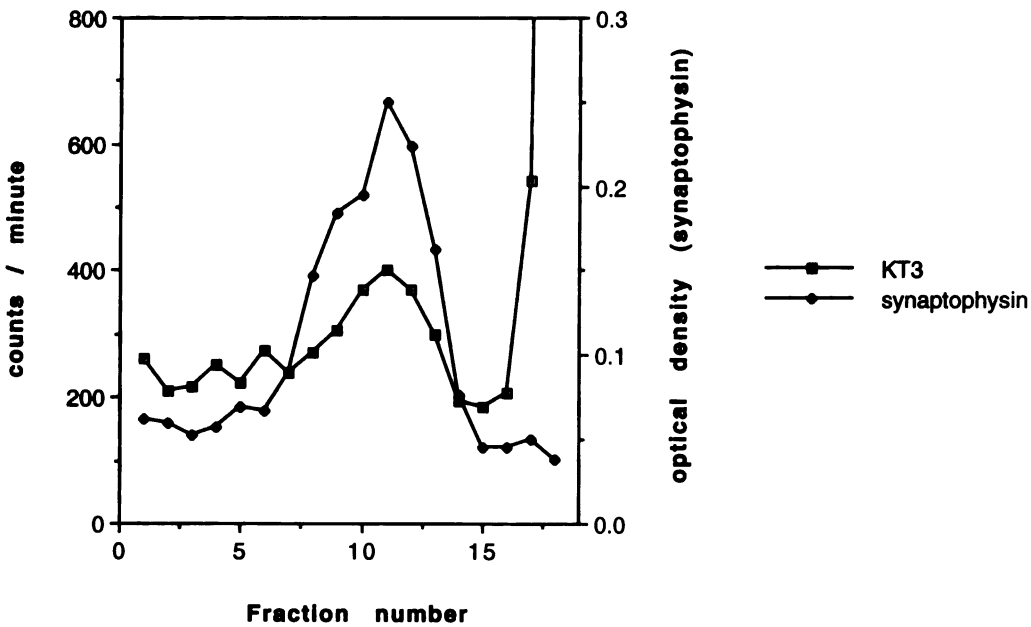
800
600
400
200
0
0.3
0.2
0.1
0.0
0
5
10
15
counts / minute
optical density (synaptophysin)
Fraction number
KT3
synaptophysin

of ^{125}I-KT3 recovered in SVLVs was compared with fraction of an internalized fluid phase marker, horseradish peroxidase, transported to SVLVs in a similar experiment. 4% of the total cell associated ^{125}I-KT3 was recovered in the SVLV peak compared with only 0.3% of the horseradish peroxidase indicating that internalized ^{125}I-KT3 is actively sorted to SVLVs.

The kinetics of transport of ^{125}I-KT3 from the cell surface to SVLVs and endosomes was compared to determine the relationship between the two pathways. For both measurements, ^{125}I-KT3 was bound to VAMP-TAg at the cell surface of transfected PC12 cells at 4°C. The cells were then washed, warmed to 37°C for various times to allow membrane traffic to resume, and then returned to 4°C. To determine the amount of transport to SVLVs, the cells were homogenized and ^{125}I-KT3 sedimenting at 80 S was counted. Total internalized antibody was measured by stripping antibody off the cell surface with a pH 2.4 wash.

The amount of antibody transported to SVLVs reached plateau level of 20% after an hour of internalization (Figure 2-10, A). At early time points, a 6 minute lag was observed before the amount of ^{125}I-KT3 sedimenting at 80 S started to increase (Figure 2-10, B). The existence of this lag indicates that there is an intermediate step in the transport of ^{125}I-KT3 from the cell surface to SVLVs. By contrast, the rate of endocytosis was highest, 3% / minute in the first minutes after warming the cells to 37°C. By 15 minutes, the rate of increase in internalized KT3 declined to a level similar to the rate of accumulation in SVLVs.

Figure 2-10. Kinetics of VAMP-TAg transport from the cell surface to SVLVs and endosomes. (A) Appearance of internalized ^{125}I-KT3 in SVLVs. (B) ^{125}I-KT3 internalization and transport to SVLVs at early time points. PC12/VAMP-TAg cells were incubated in ^{125}I-KT3 at 4°C, washed and warmed to 37°C for various times. ^{125}I-KT3 in SVLVs was measured from fractions sedimenting at 80 S on a glycerol gradient. Total internalized VAMP-TAg was the fraction resistant to stripping from the cell surface with a pH 2.5 wash.

A

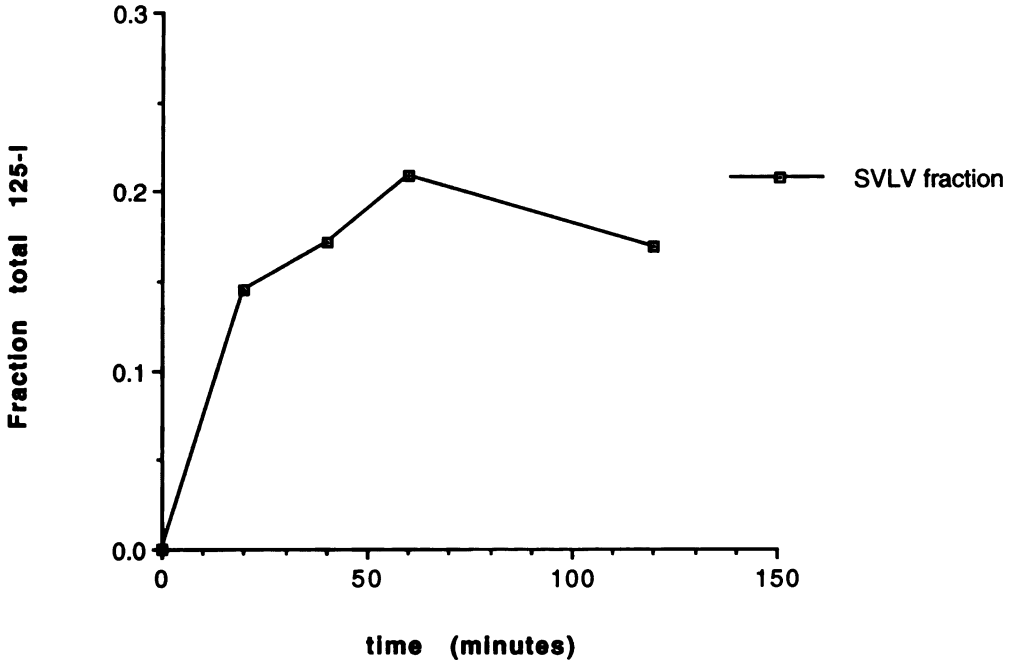
0.3
0.2
0.1
0.0
Fraction total 125-I
0
50
100
150
time (minutes)
SVLV fraction

B

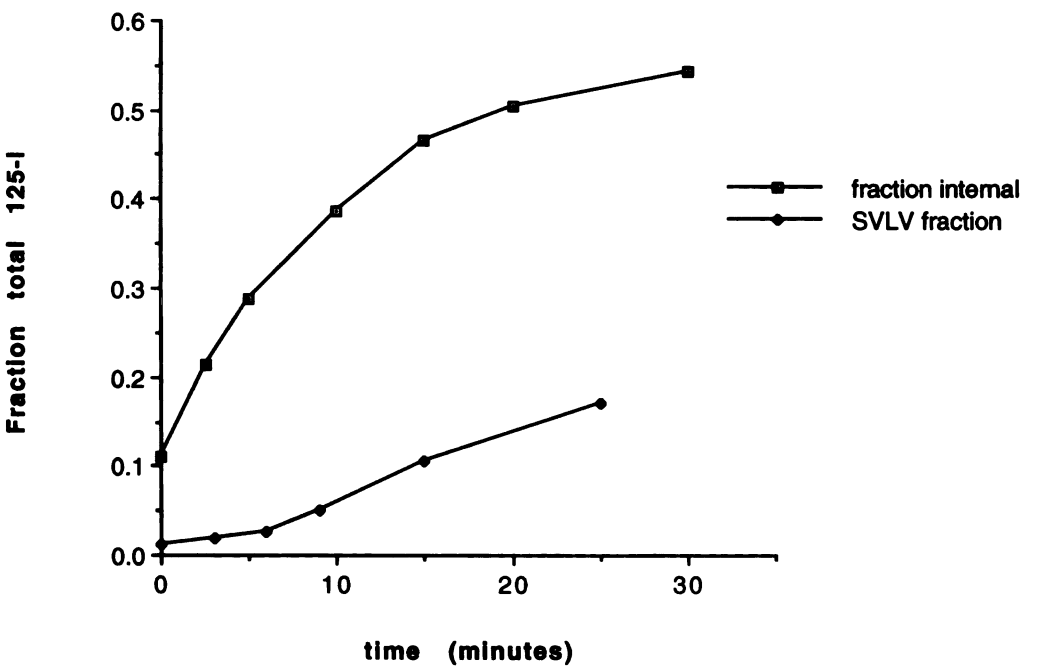
0.6
0.5
0.4
0.3
0.2
0.1
0.0
Fraction total 125-I
0
10
20
30
time (minutes)
fraction internal
SVLV fraction

Discussion

The membrane targeting and transport pathway of an epitope tagged VAMP have been analyzed in transfected PC12 cells. In many respects, VAMP-TAg behaves similarly to synaptophysin. Both proteins are transported through the secretory pathway and are located in SVLVs and endosomes at steady-state. In addition, both VAMP-TAg and synaptophysin cycle between the plasma membrane and endosomes and can also be sorted from the plasma membrane to SVLVs.

The major distinction observed between transfected VAMP-TAg and synaptophysin is that the fraction of VAMP-TAg present in SVLVs is low. This distinction can be explained, at least in part, by saturation of SVLVs with VAMP-TAg as a result of overexpression in a fraction of the transfected cells. Of particular interest in this regard is the observation that overexpression of VAMP-TAg led to a 56% reduction, relative to synaptophysin, in the targeting of endogenous VAMP-2 to SVLVs. This result indicates that VAMP-TAg competes with VAMP-2, but not with synaptophysin, for targeting to SVLVs. The lack of competition between VAMP-TAg and synaptophysin is incompatible with models in which there is a "sortase" which binds to a common feature of synaptic vesicle proteins to target them to SVLVs. As an alternative, VAMPs could be sorted to SVLVs by associating with other synaptic vesicle proteins prior to budding (Bennett et al., 1992).

Synaptic vesicle recycling is a rapid and efficient process (Betz and Bewick 1992) . The site from which synaptic vesicles bud during recycling and *de novo* biogenesis is unknown. Recycling could be extremely rapid if vesicles recycle directly after fusion by resealing a transient fusion pore. This class of recycling, if it occurs in PC12 cells, could not have been detected

by measuring the rate of transport of ^{125}I-KT3 to SVLVs because the assay follows VAMP-TAg originally incorporated in the plasma membrane. The distribution of VAMP-TAg and synaptophysin in PC12 cells suggests that SVLVs could form by budding from endosomes. A 6 minute lag was observed before ^{125}I-KT3 bound to the cell surface accumulates in SVLVs indicating that there is an intermediate between the plasma membrane and SVLVs. Although this intermediate could be a pool of SVLVs which are not released from cells because they are tethered to the cytoskeleton, it is more likely that the lag represents the time required for transport through endosomes. Therefore, we conclude that SVLVs in PC12 cells form by budding from endosomes. In presynaptic nerve terminals, synaptic vesicle proteins are the predominant class of proteins internalized in coated vesicles (Maycox et al., 1992). If these coated vesicles uncoat and fuse with endosomes prior to the formation of recycled synaptic vesicles, sorting of synaptic vesicle proteins within endosomes could occur rapidly and efficiently as a consequence of the scarcity of proteins present which must be excluded from synaptic vesicles.

Materials and methods

cDNA constructions: The rat VAMP-2 (Elferink, et al. 1989) cDNA expression vector pRC/CMV/VAMP-2 was the generous gift of Richard Scheller (Invitrogen, WS Trimble). The VAMP cDNA was modified to create VAMP-TAg by insertion of complementary oligonucleotides between restriction endonuclease cleavage sites at the C-terminus of the coding region. In an initial construction, V-TAg1, the KT3 epitope SPPPEPET from the C-terminus of the SV40 large T antigen (MacArthur and Walter 1984) was inserted between *Afl*II and *Bsu* 36 I. ^{125}I-KT3 bound poorly to cells transfected with V-TAg1 so a spacer region was inserted between the transmembrane domain and the SV40 T antigen sequences to improve the accessibility of the epitope. To provide an insertion site for the spacer, a *Sac* I site was introduced at the transmembrane/extracellular junction of using the oligonucleotide TCGTTTACTTGAGCTCTTCACCTC to prime synthesis from a single stranded m13mp18/V-TAg1 template. 13 amino acids, KGVEPKTYCYYSS, derived from the juxtamembrane region of the extracellular domain of the transferrin receptor were inserted between the *Sac* I and *Afl* II sites. Tyrosine and lysine residues were added to this sequence to provide active sites for biochemical modification by membrane impermeable reagents.

Cell culture and transfections: PC12-KB and CHO-K1 cells were grown in DME-H21/5% FCS/10% HS/1000U/ml penicillin/1000 mcg/ml streptomycin in a 10% CO_2 incubator. PC12 cells were transfected by electroporation at 230 mV, 500 μF. Transient expression was analyzed 1-2 days after electroporation. CHO cells were transfected using DOTAP (Boehringer Mannheim). Clones were

selected by addition of 500 µg/ml G418 (Gibco) two days after transfection and screened for expression by ^{125}I-KT3 surface binding and immunoblotting. Expression of the transgene was routinely induced by addition of 6 mM sodium butyrate 22-24 hours prior to the beginning of an experiment.

Monoclonal antibodies: The KT3 hybridoma (MacArthur and Walter 1984) was from Alexander Kamb (UCSF). The hybridoma was grown in DME-H21 supplemented with 10% fetal calf serum (hyclone) and converted in stages to growth in DME-H21 supplemented with 0.5% fetal calf serum and 2% Ultraser HY (IBF Biotechniques). Finally, the hybridoma was grown for 10 days in serum free DME-H21/2%ultraser and the supernatant was collected and concentrated 10 fold through a YM100 membrane in a pressure cell (Amicon). KT3 was purified from the concentrated supernatant by loading onto a protein G-Sepharose column (Sigma) and eluting at pH 2.7. The purified antibody was concentrated to > 1 mg/ml by ultrafiltration in a centricon 100 and stored at -80 C in 20 mM Hepes, pH 7.4 and 40% glycerol. The antibody was iodinated to a specific activity of 1.5 x 10^6 Ci/mole using iodogen coated tubes (Pierce). The 10.1 monoclonal anti-synaptobrevin (VAMP) antibody (Baumert, et al. 1989) was from Reinhard Jahn (Yale, New Haven , CT). Anti-synaptophysin monoclonal antibodies were purchased from Boehringer Mannheim (SY38) or Sigma (SVP-38).

Immunoprecipitation: Cells were labeled with TRANS ^{35}S-label (ICN) in methionine/cysteine free DME H21/2% dialyzed FCS, chased in growth media, and lysed in NDET (10 mM Tris pH 7.4, 1% NP40, 0.4% deoxycholate, 66 mM EDTA). Samples were clarified by centrifugation (14,000 g, 5 min), and were

then incubated with KT3 for 2 hours at 20°C. Antibody bound proteins were precipitated using protein G-Sepharose (Sigma). When required, washed immunoprecipitates were treated with neuraminidase (Genzyme) for 1 hr at 37°C in 150 mM NaOAc pH 5.5, 150 mM NaCl, 4 mM $CaCl_2$. Neuraminidase was omitted from control reactions. Immunoprecipitates were resolved by SDS-PAGE on 13% gels and detected by fluorography.

Immunoblotting: Samples were resolved by electrophoresis on reducing SDS-15%polyacrilimide gels and transferred to PVDF (Immobilon-P, Millipore) membranes. Blots were probed with monoclonal antibodies diluted into PBS/5% nonfat dry milk/0.05% Tween-20 and developed using the enhanced chemiluminescence (ECL) system (Amersham). A densitometer (Ephortec, Joyce Loebl) was used to quantify band intensities. Multiple films with exposure times ranging from 1 second to 2 hours were scanned and data from saturated or underexposed bands was disregarded. It was established that this densitometry technique can produce linear readings over a 1000 fold range of sample concentrations by quantifying band intensities from an immunoblot of a serially diluted sample.

Immunofluorescent labeling: To observe total VAMP-TAg staining, cells were grown overnight on poly-D-lysine coated glass coverslips, washed in PBS and fixed with 3% paraformaldehyde in PBS. Fixed cells were permeabilized with 0.5% Saponin in PBS/1%BSA for 20 min, incubated with primary antibody in permeabilization buffer for 20 min, and detected with fluorescein conjugated goat anti mouse IgG (Cappel). For the immunofluorescent

endocytosis assay, cells were grown for two days on Matrigel (Collaborative Research) coated chamber slides and incubated at 37°C with KT3 in DME H-21/20 mM Hepes, pH 7.4 for 5 minutes then washed at 4°C with 125mM NaCl/20 mM glycine, pH 2.4. To visualize internalized KT3, the cells were fixed, permeabilized and stained with fluorescein conjugated secondary antibodies as above.

Endocytosis assay with NHS-SS-biotin: The method of Lisanti *et al.* (1990) was followed to label internalized proteins with biotin. Briefly, cell surface proteins were labeled with NHS-SS-Biotin (Pierce), warmed to 37°C for the indicated times (minutes) and then biotin remaining on the cell surface was removed by washing in glutathione. A control sample reflecting the total amount of biotinylated protein was not stripped with glutathione (Lisanti et al., 1990). Cells were lysed in NDET and biotinylated proteins from 1/4 of a 3.5 cm dish were collected with 50 µl streptavidin-agarose beads (Sigma). Biotinylated VAMP-TAg was detected on immunoblots probed with KT3 antibodies. KT3 (8 µg/ml) was present during the washing and incubations steps where indicated.

Isolation of SVLVs: Cells were collected in buffer A (150 mM NaCl, 10 mM Hepes pH 7.4, 1 mM EGTA, 0.1 mM $MgCl_2$, 10 ng/ml pepstatin, 10 ng/ml leupeptin, 10 ng/ml chymostatin, 10 ng/ml aprotinin) at 4°C and homogenized by 7 passes through a ball bearing cell cracker with an 8 µm clearance. Unbroken cells and debris were removed with a 5 minute spin at 2000 g. 200 µl of the postnuclear supernatant was loaded onto a 5-25% glycerol gradient in homogenization buffer with a 0.4 ml, 2.5 M sucrose cushion. For the ^{125}I-KT3

uptake experiments, a cytoplasmic supernatant (S2) was prepared from the postnuclear supernatant by centrifugation for 15 min at 12,000 g and loaded on a glycerol gradient without a sucrose cushion. The gradients were spun at 48 k rpm for 1 hour in a SW55 rotor at 4°C. Fractions were collected from the bottom of the tube with a tube piercer (ISCO). Gradient fractions were precipitated with TCA, washed with acetone, and then resuspended in reducing sample buffer with 7 M urea at 55°C for 20 minutes.

Measurement of variations in VAMP-TAg expression level:
PC12/VAMP-TAg cells were collected in DME H-21/20 mM Hepes, pH 7.4. Live cells at 4°C were incubated with KT3 antibody, washed and stained with FITC-conjugated goat anti-mouse secondary antibody. The intensity of cell surface fluorescence was measured on a benton dixon FACS machine by Paul Dazin (HHMI, UCSF).

Uptake of KT3 into synaptic vesicles: ^{125}I-KT3 was diluted into PBS/5%BSA/1 mg/ml glucose to 2 μg/ml (10^7 cpm/ml) and added to washed cells at 37°C for 45 minutes followed by a 5 minute chase in growth media at 37°C. Cells were washed with ice cold homogenization buffer and fractionated as above on glycerol gradients without a sucrose pad. ^{125}I-KT3 was directly counted in gradient fractions, cell pellets, and the empty ultracentrifuge tube. Counts in each gradient fraction were normalized to the total count of cell associated antibody. The synaptic vesicle peak in the gradient fractions was detected by a well assay (Clift-O'Grady, et al. 1990) modified for enzymatic detection using horseradish peroxidase conjugated goat-anti-mouse secondary antibodies and O-Phenylenediamine tablets (Zymed).

Endocytosis assay using ^{125}I-KT3: PC12/VAMP-TAg cells in 35 mm poly-lysine coated dishes were washed in ice cold PBS/5% BSA and incubated with 10^7 cpm/ml ^{125}I-KT3 in PBS/BSA for 1 hr. Cells were washed 7 times for a total of 30 minutes with ice cold PBS/BSA then transferred to PBS/BSA at 37°C. At various times cells were returned to ice and washed once to remove antibody released at 37°C. KT3 remaining bound to the cell surface was removed by washing 2 x 15 min with 20 mM glycine, 125 mM NaCl, 1mM Ca, 1mM Mg, 5% BSA, pH 2.4. Cell-associated KT3 was collected by lysing the cells with NDET. The pH 2.4 washes and NDET lysates were counted in a gamma counter (Beckman) and the fraction internalized was calculated as (NDET - bg(t=0)) / (NDET + pH2.4 - bg(t=0)). Control experiments established that 10% of the ^{125}I KT3 bound to paraformaldehyde-fixed PC12/VAMP-TAg cells after 10 min at 37°C was resistant to stripping at pH 2.4.

Postscript

During the course of these experiments, Bauerfiend *et al* (1993) also concluded that SVLVs are formed by budding from an endosomal intermediate. They found that horseradish peroxidase (HRP) internalized for 7 minutes could be recovered in early endosomes, but not in SVLVs. HRP was chased predominantly to late endosomes, but a small HRP signal was detected in SVLVs after an additional 53 minute incubation in HRP free media. One distinction between the experiments reported in this chapter and those of Bauerfiend *et al*, is that the low density synaptophysin containing organelles studied by Bauerfiend *et al* were isolated on isopycnic sucrose gradients rather than by sedimentation velocity so they may not be identical to SVLVs. In particular, the vesicles studied by Bauerfiend *et al* equilibrate between 0.7 M and 0.8 M sucrose, while SVLVs reach equilibrium at 0.9 M sucrose (Clift-O'Grady, et al. 1990) . In addition, Bauerfiend *et al* found that all synaptophysin containing organelles in their PC12 homogenates sedimented as a single population of 154 S whereas others find synaptophysin in at least two populations by sedimentation through glycerol gradients (Cameron, et al. 1991). Bauerfiend et al suggest that endosomes in their PC12 cells are fragmented during homogenization.

Chapter Three

An amphipathic helix regulates endocytosis of the synaptic vesicle protein VAMP in neuroendocrine cells

VAMP (synaptobrevin), an 18 kD membrane protein of synaptic vesicles, is believed to participate in the fusion of synaptic vesicles with the presynaptic plasma membrane (Elferink, et al. 1989) (Sollner, et al. 1993a) (Schiavo, et al. 1992). After exocytosis, synaptic vesicle membrane proteins are recovered by endocytosis to form new vesicles. As a first step in understanding how synaptic vesicle proteins are correctly targeted, a systematic *in vitro* mutagenesis approach was taken to identify an endocytosis signal in VAMP. Mutation of methionine 46 to alanine inhibited endocytosis by 80% in neuroendocrine PC12 cells. The methionine 46 signal has three features which distinguish it from previously identified endocytosis signals: methionine 46 is located on the hydrophobic face of a predicted amphipathic alpha helix; mutation of methionine 46 does not inhibit endocytosis in CHO cells; and, a large deletion including the methionine 46 signal does not block endocytosis. These results suggest that VAMP is retained on the plasma membrane by an interaction with a component involved in the synaptic vesicle cycle and that the function of the methionine 46 signal is to promote release of VAMP from this complex to allow access to coated pits.

An SV40 T-antigen epitope tag(MacArthur and Walter 1984) was appended via a spacer sequence to the hydrophobic C-terminal transmembrane domain of rat VAMP-2 to create VAMP-TAg (Figure 3-1).

Figure 3-1. Construction of epitope-tagged VAMP-2 (VAMP-TAg) and its derivatives. VAMP-2 is attached to the cytoplasmic surface of synaptic vesicles via a C-terminal membrane anchor. The cytoplasmic domain can be demarcated into a 31 amino acid proline-rich sequence that is variable between members of the VAMP/synaptobrevin family and a highly conserved region predicted to contain two amphipathic helices. The SV40 large T-antigen C-terminal epitope for the KT3 monoclonal antibody(MacArthur and Walter 1984) was appended to the C-terminus of VAMP. To improve antibody binding, a spacer was inserted between the transmembrane domain and the epitope Tag. The spacer was derived from the corresponding juxtamembrane domain of the transferrin receptor, but modified to contain sites for biotinylation. (A) Diagrammatic representation of the deletions and chimera. (B) Sequence of the conserved domain of rat VAMP-2. The amino acids that form the hydrophobic face of the predicted amphipathic helices are indicated in bold face.

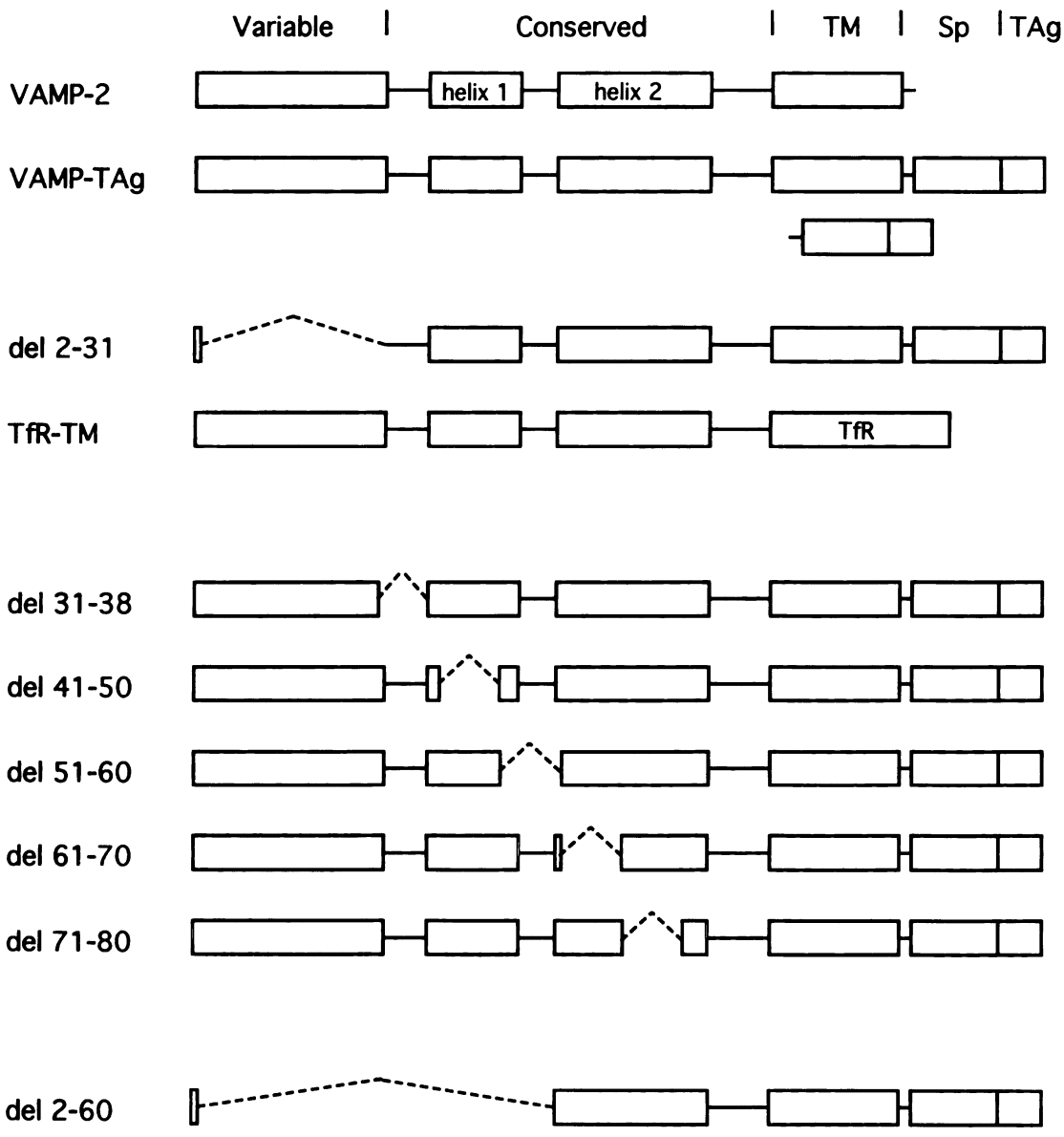
Variable
Conserved
TM
Sp
TAg
VAMP-2
helix 1
helix 2
VAMP-TAg
del 2-31
TfR-TM
TfR
del 31-38
del 41-50
del 51-60
del 61-70
del 71-80
del 2-60

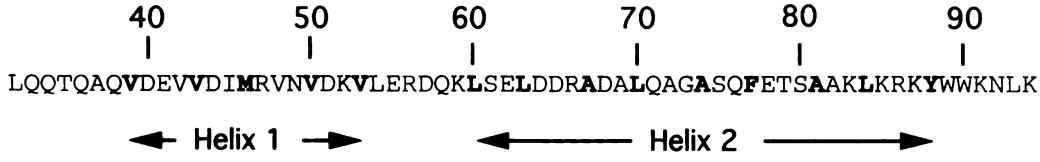
40
50
60
70
80
90
LQQTQAQVDEVVDIMRVNVDKVLERDQKLSELDDRADALQAGASQFETSAAKLKRKYWWKNLK
Helix 1
Helix 2

When expressed in undifferentiated PC12 cells, VAMP-TAg is targeted to synaptic vesicle-like vesicles (Chapter 2). In addition, sufficient VAMP-TAg is on the plasma membrane at steady-state to allow binding of ^{125}I-labeled monoclonal antibody against the T-antigen epitope to the cell surface. Endocytosis of VAMP-TAg was measured by determining the fraction of ^{125}I-labeled antibody which was resistant to acid stripping from the cell surface after various periods of chase at 37°C.

To determine which domains of VAMP-TAg are required for endocytosis, mutants were constructed with a deletion of the proline rich amino terminal domain (del 2-31) or a replacement of the transmembrane domain with the transmembrane domain of the transferrin receptor (TfR-TM) (Figure 3-2,A). In both cases, the internalization rate in PC12 cells was not diminished implying that the juxtamembrane region of the cytoplasmic domain, conserved between members of the VAMP family, is sufficient for endocytosis. A series of internal deletions within the conserved domain were constructed and assayed for endocytosis in transiently transfected PC12 cells (Figure 3-2, B). Deletion of amino acids 41 to 50 (del 41-50) inhibited endocytosis by 70%. This inhibition of endocytosis was accompanied by an enhanced cell surface localization detected by immunofluorescent staining of del 41-50 transfected PC12 cells compared with cells transfected with full length VAMP-TAg (Figure 3-3). Since del 41-50 had the most severely reduced rate of endocytosis a third series of mutations were constructed in which amino acids 41 through 50 were each changed, individually, to alanine. An 80% inhibition of endocytosis was measured for a substitution of methionine 46 (Figure 3-2, C).

Figure 3-2. Endocytosis in PC12 cells of VAMP-TAg compared with (A) the variable domain deletion and transmembrane domain replacement; (B) internal deletions within the conserved domain; (C) alanine scan mutations within helix 1; and (D) a large deletion including the variable domain and helix 1. Poor expression of del 2-60 was overcome by increasing the amount of DNA used for transfections from 40 to 300 ug. A zero time control (about 10% of total counts) is subtracted. Values are the mean; standard deviations (n=3) are indicated. Background binding to nontransfected cells was less than 10%.

A

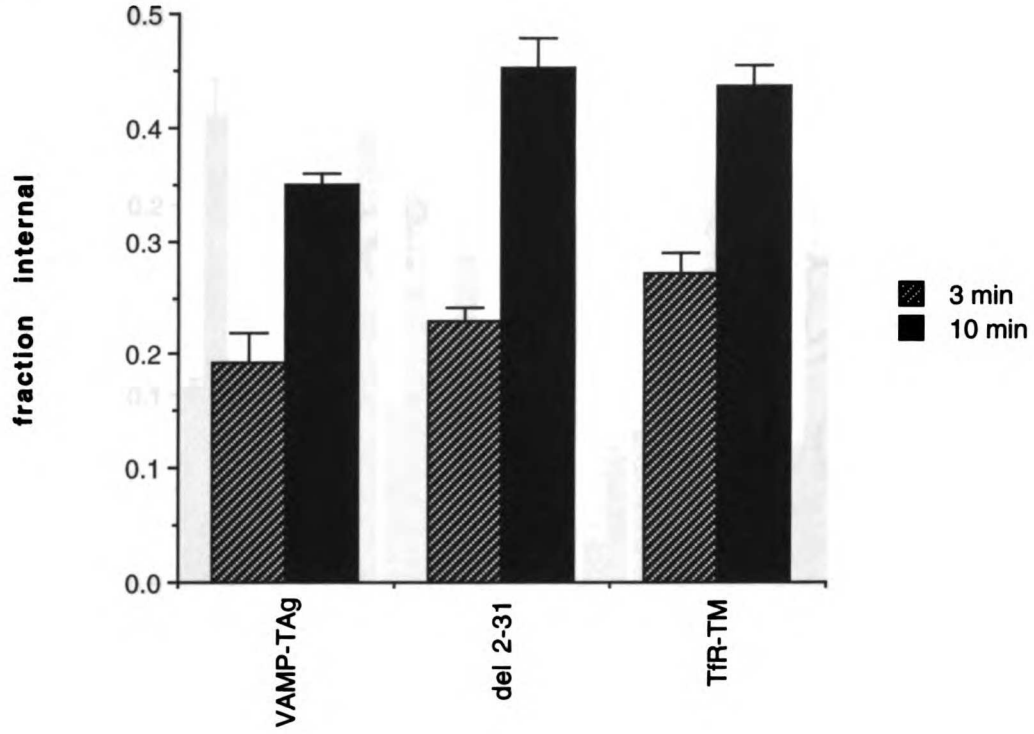
fraction internal
0.5
0.4
0.3
0.2
0.1
0.0
VAMP-TAg
del 2-31
TfR-TM
3 min
10 min

B

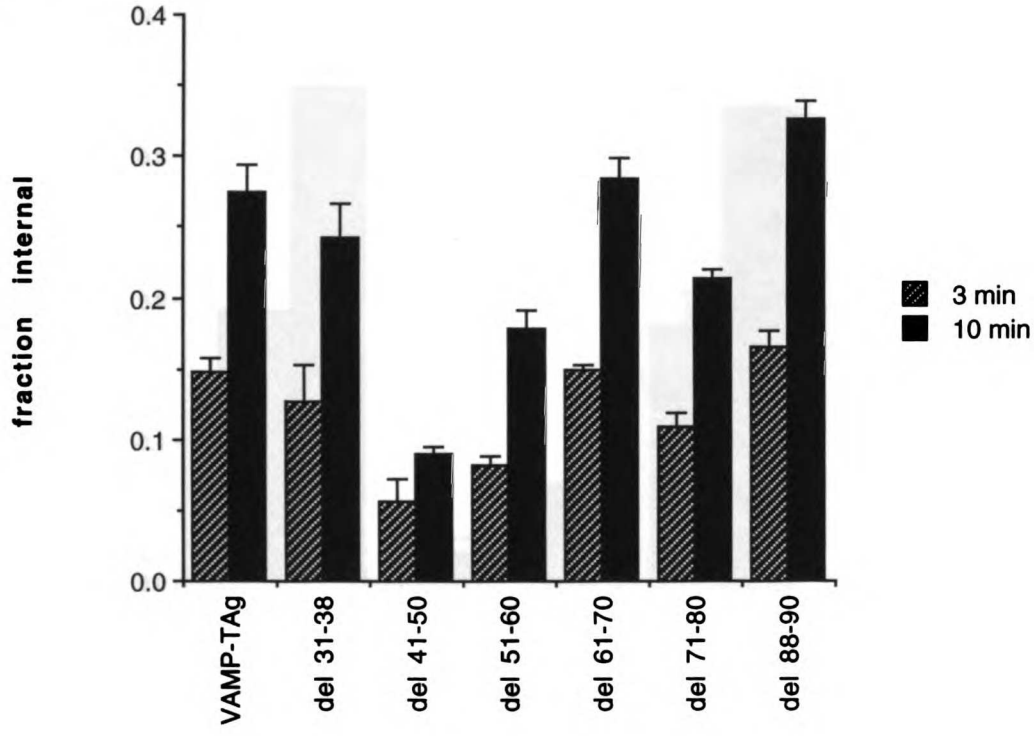
fraction internal
0.4
0.3
0.2
0.1
0.0
VAMP-TAg
del 31-38
del 41-50
del 51-60
del 61-70
del 71-80
del 88-90
3 min
10 min

C

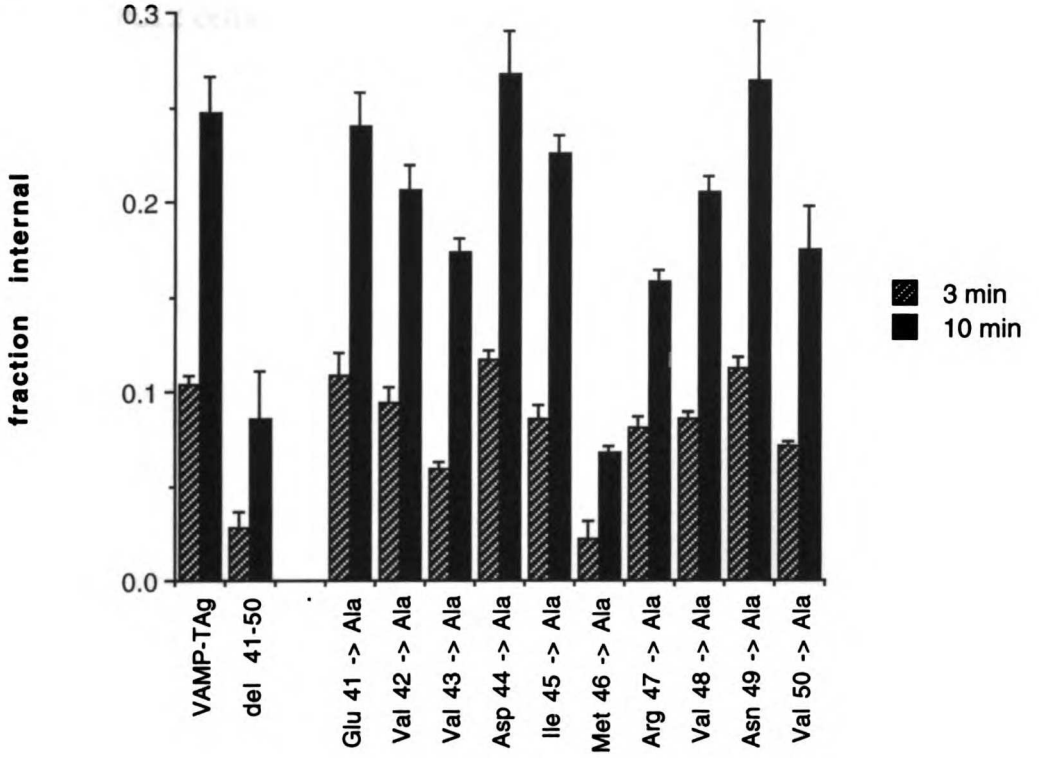
fraction internal
0.3
0.2
0.1
0.0
3 min
10 min
VAMP-TAg
del 41-50
Glu 41 -> Ala
Val 42 -> Ala
Val 43 -> Ala
Asp 44 -> Ala
Ile 45 -> Ala
Met 46 -> Ala
Arg 47 -> Ala
Val 48 -> Ala
Asn 49 -> Ala
Val 50 -> Ala

D

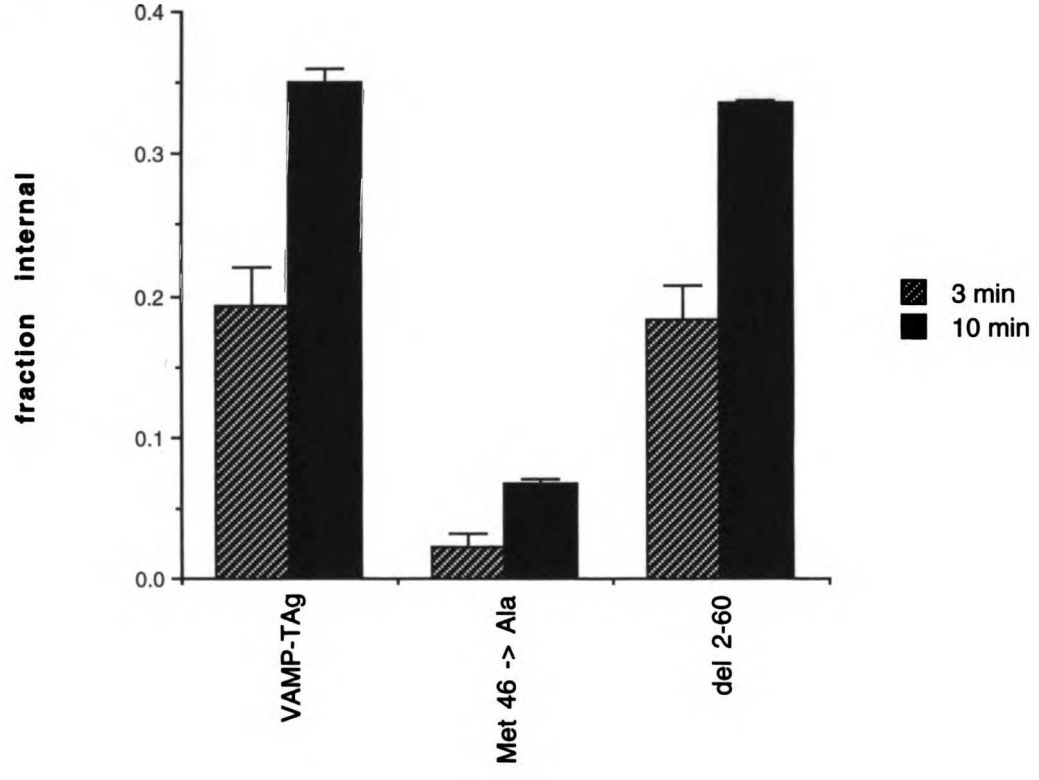
fraction internal
0.4
0.3
0.2
0.1
0.0
3 min
10 min
VAMP-TAg
Met 46 -> Ala
del 2-60

Figure 3-3. Immunofluorescent staining of VAMP-TAg and del 41-50 in transfected PC12 cells.

VAMP-TAg

del 41-50

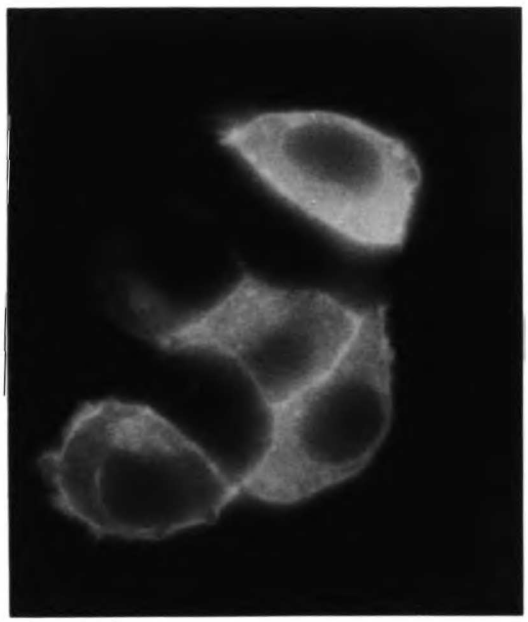

Endocytosis of many recycling receptors requires a signal containing tyrosine (Trowbridge et al., 1993) . These signals share a tight turn conformation(Bansal and Gierasch 1991, Collawn et al., 1990) and promote internalization by interacting with the adapter proteins of clathrin coated pits (Pearse 1988) . The sequence of the methionine 46 signal of VAMP does not fit the tyrosine endocytosis signal motif nor the more recently identified signal with a dileucine motif (Letourneur and Klausner 1992) . Rather, methionine 46 is centrally located in a predicted amphipathic helix of 15 amino acids (Dascher, et al. 1991) . Supporting this prediction, mutations in other amino acids on the hydrophobic face of this helix (Valine 43 and Valine 50) also inhibited endocytosis.

This novel signal could be required for entry into a neural specific endocytic pathway specialized for recycling of synaptic vesicle proteins. CHO cells would be unlikely to have this putative neural specific pathway because they do not express synaptic vesicle proteins or contain synaptic vesicle sized organelles (Clift-O'Grady, et al. 1990) . To see if PC12 and CHO cells have a different pathway for endocytosis, internalization of the polymeric immunoglobulin receptor (pIgR) was compared between the two cell types. (Figure 3-4, A) The pIgR utilizes two tyrosine containing signals for endocytosis (Okamoto et al., 1992). Endocytosis of pIgR was inhibited 37% by a Tyr 734 mutation and 58% by a double Tyr 734 / Tyr 668 mutation in both cell types. The identical response of the two cell types to mutations in the endocytosis signal of pIgR implies that they share a common mechanism for endocytosis.

VAMP-TAg was expressed in CHO cells to determine if it can utilize the endocytosis pathway shared between PC12 and CHO cells. Internalization of

VAMP-TAg in CHO cells was rapid indicating that no components specific to PC12 cells are required for endocytosis. Therefore, VAMP-TAg is probably not internalized by a neural specific pathway in PC12 cells since it can be rapidly internalized by the common pathway. However, when the mutant forms of VAMP-TAg were expressed, it was found that mutation of methionine 46 to alanine reduced endocytosis by only 14% in CHO cells (Figure 3-4, B). Since CHO cells internalize VAMP-TAg rapidly, yet the methionine 46 mutation is relatively benign, the most plausible explanation for the strong reduction of VAMP-TAg internalization by the mutation in PC12 cells is that a PC12 specific interaction inhibits entry into a common endocytotic pathway.

One way in which endocytosis can be inhibited is by binding to a component that cannot be concentrated in coated pits. For example, immobilization on the cell surface via an interaction with actin filaments has been reported to inhibit endocytosis of the B1 isoform of the Fc receptor in macrophages by preventing access to clathrin coated pits (Miettinen et al., 1992) . The possibility that VAMP-TAg is retained on the cell surface in PC12 cells is supported by the observation that VAMP-TAg internalization was more extensive in CHO cells than in PC12 cells. This difference is not simply a reflection of the more rapid growth rates of CHO cells because the extent of pIgR endocytosis after 10 minutes at 37°C is similar in the two cell types (Figure 3-4, C). Thus, the methionine 46 signal may be required to counteract PC12 specific surface retention of VAMP-TAg.

If retention of VAMP-TAg on the cell surface prevents endocytosis in PC12 cells, it should be possible to identify a mutation which is not retained. Such a mutant should have an increased internalization rate in PC12 cells but not in CHO cells. Perhaps because the presence of the methionine 46 signal

Figure 3-4. Comparison of endocytosis in PC12 and CHO cells. (A) Endocytosis of pIgR internalization signal mutants in PC12 and CHO cells. (B) Endocytosis of the methionine 46 to alanine mutation in CHO cells. (C) Endocytosis of VAMP-TAg and pIgR in PC12 and CHO cells.

A

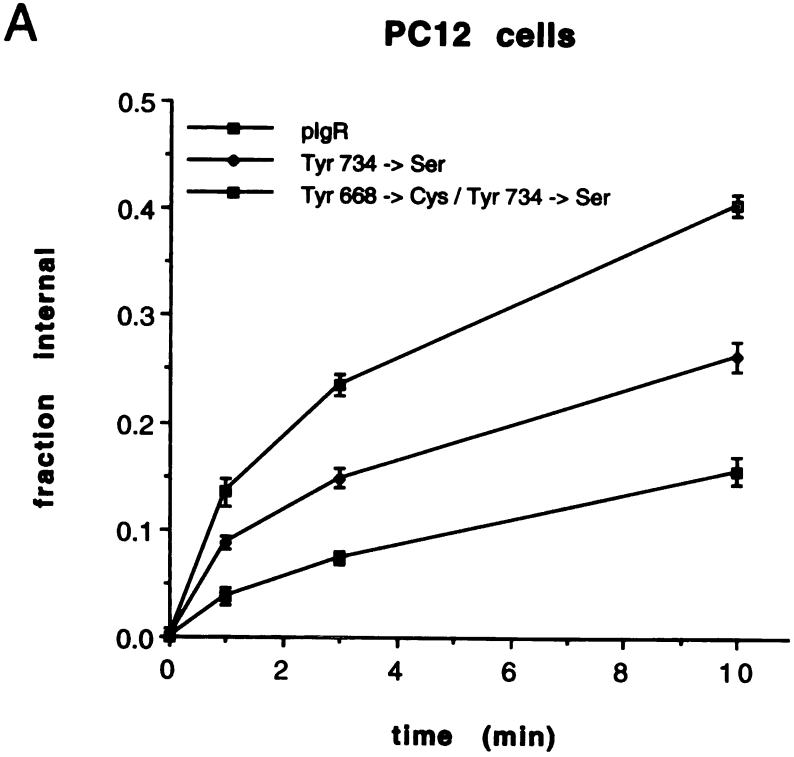
PC12 cells
pIgR
Tyr 734 -> Ser
Tyr 668 -> Cys / Tyr 734 -> Ser
fraction internal
0.5
0.4
0.3
0.2
0.1
0.0
0
2
4
6
8
10
time (min)

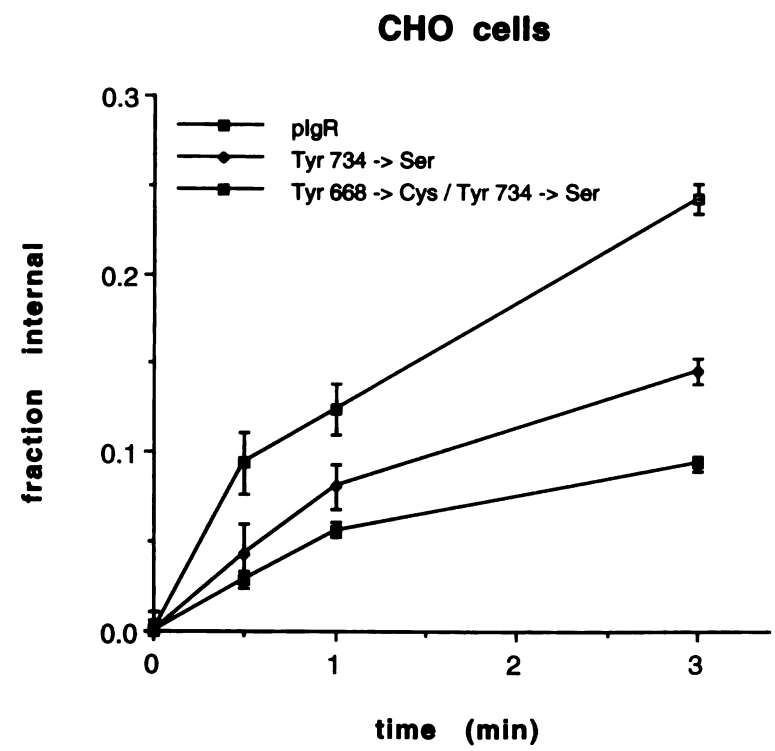
CHO cells
pIgR
Tyr 734 -> Ser
Tyr 668 -> Cys / Tyr 734 -> Ser
fraction internal
0.3
0.2
0.1
0.0
0
1
2
3
time (min)

B

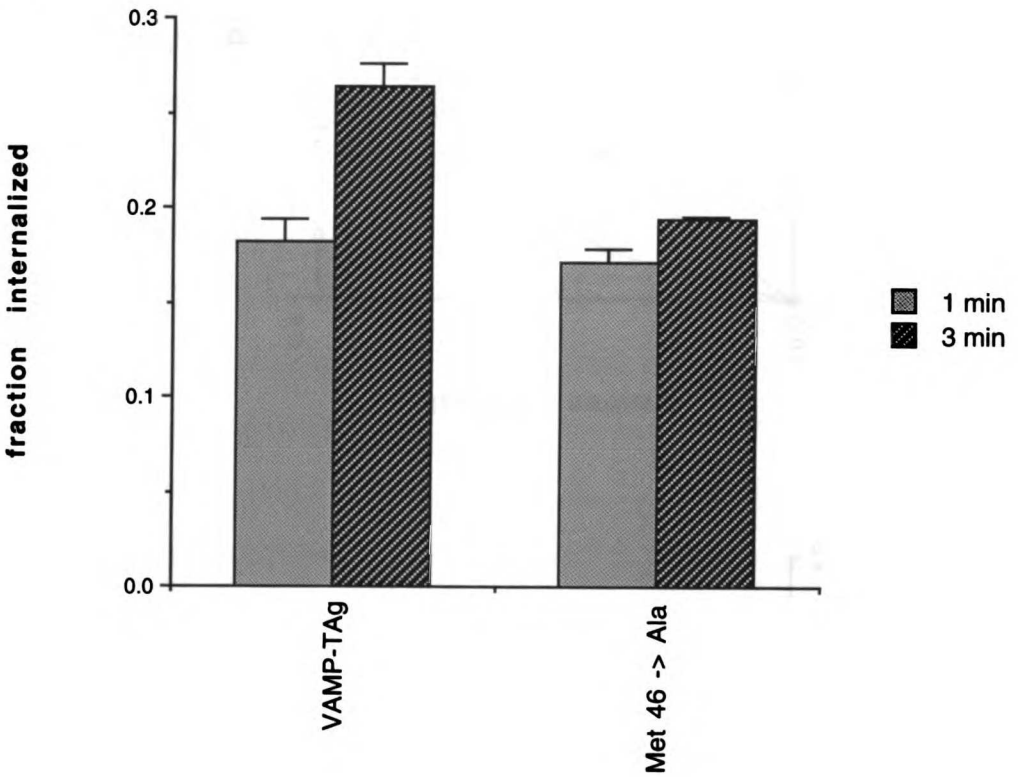
fraction internalized
0.3
0.2
0.1
0.0
VAMP-TAg
Met 46 -> Ala
1 min
3 min

C

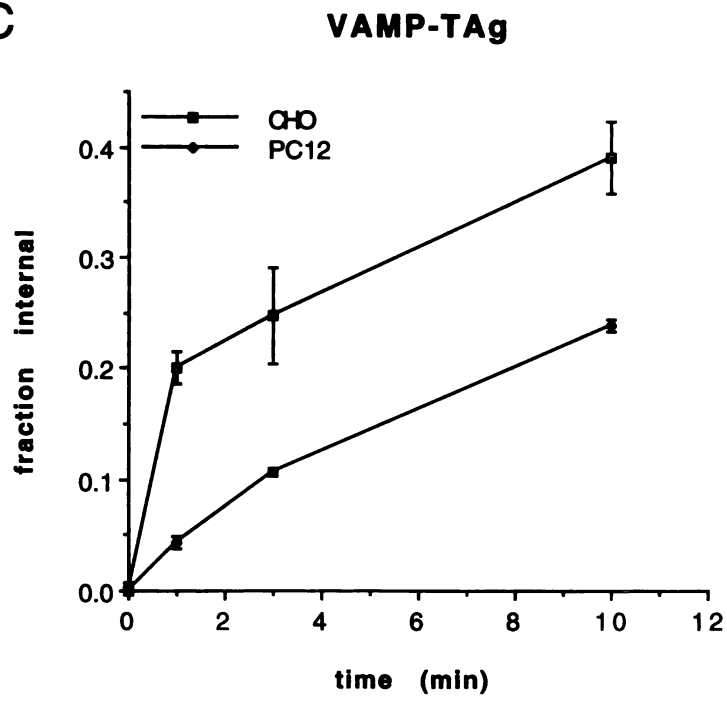
VAMP-TAg
CHO
PC12
fraction internal
0.0
0.1
0.2
0.3
0.4
0
2
4
6
8
10
12
time (min)

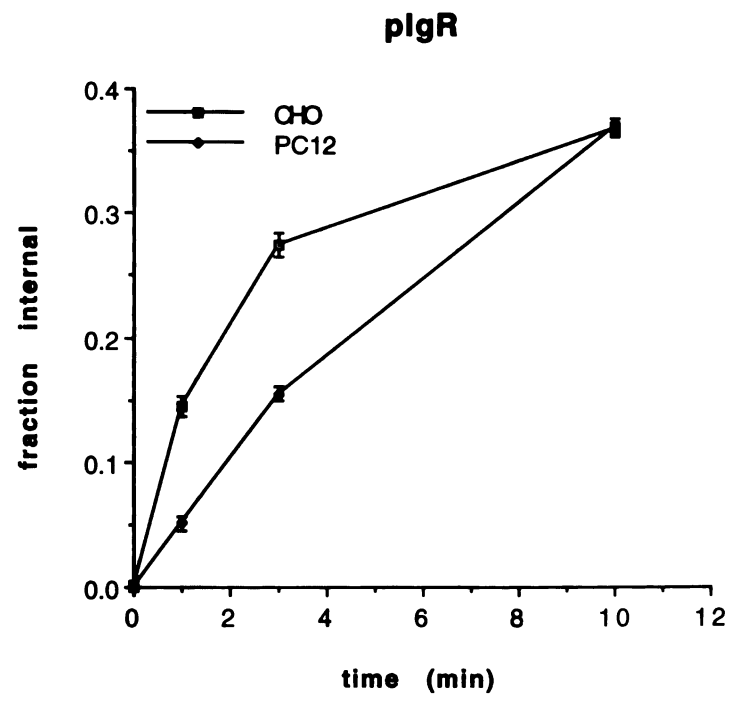
pIgR
CHO
PC12
fraction internal
0.0
0.1
0.2
0.3
0.4
0
2
4
6
8
10
12
time (min)

opposes effective retention, none of the VAMP-TAg mutants had this property (data not shown). However, a VAMP-TAg mutant (del 2-60) with a large deletion including the proline rich variable domain and the entire helix containing methionine 46 was rapidly internalized in PC12 cells (Figure 3-2, D). We suggest that because del 2-60 lacks signals for both retention and release of retention that the sum of these effects is to allow it to be internalized, without impediment, by the common mechanism of endocytosis shared by PC12 and CHO cells.

PC12 cells express synaptic vesicle proteins and target them to synaptic vesicle-like vesicles (Clift-O'Grady, et al. 1990) . It is possible that binding to a synaptic vesicle fusion complex absent from CHO cells is responsible for the unusual internalization of VAMP-TAg. VAMP interacts with syntaxin and SNAP-25 in a SNARE particle proposed to nucleate assembly of a synaptic vesicle fusion complex (Sollner, et al. 1993b) . If components of this complex are retained on the plasma membrane, VAMP must dissociate from the complex prior to endocytosis. Perhaps the methionine 46 signal is required for dissociation from the fusion complex. The identification of proteins whose interaction with VAMP is altered by the methionine 46 mutation may aid in understanding synaptic vesicle fusion as well as endocytosis.

Methods

cDNA constructions: A rat VAMP-2 (Elferink, et al. 1989) cDNA expression vector, pRC/CMV/VAMP-2, was the generous gift of Richard Scheller (Stanford). The epitope tag was created by inserting complementary oligonucleotides between AflII and Bsu3-61 restriction sites. To generate the spacer, complementary oligonucleotides were inserted between AflII site and a SacI site created by oligonucleotide-directed mutagenesis at the lumenal boundary of the transmembrane domain. The sequence of the C-terminus of VAMP-TAg is S_{116}SKGVEPKETYCYKSSSPPPEPET. In the TfR-FM chimera, the transmembrane domain of VAMP-TAg was replaced with the transmembrane domain of the transferrin receptor (McClelland et al., 1984), by inserting complementary oligonucleotides between BclI and SacI sites. Deletions and alanine scanning mutations were constructed by oligonucleotide directed mutagenesis in m13mp18.

Endocytosis assays: VAMP-TAg cDNAs in the pRC/CMV expression vector were transfected into PC12 and CHO cells by electroporation (Chapter 2). The DNA concentration was adjusted to equalize levels of surface expression. Cells were replated on polyD lysine coated dishes and VAMP-TAg expression was induced by incubation for 22-24 hrs with 6mM sodium butyrate. Antibody was purified on a protein G column from KT3 hybridoma supernatant and iodinated in iodogen coated tubes to 80 μCi/mg. Monovalent F_{ab} fragments of a polyclonal antibody against pIgR were iodinated to 20 μ Ci/mg using the ICl method (Breitfeld et al., 1989). Cells were incubated with 10^7 cpm/ml. ^{125}I-KT3 in PBS/5% BSA for 45 min at 4°C. Unbound antibody was removed by

extensive washing at 4°C and the cells were incubated in PBS/BSA at 37°C for various times. Antibody remaining at the cell surface was removed by two 15 minute washes at 4°C in labeling media supplemented with 30mM glycine and adjusted to pH 2.4. Acid resistant antibody was collected by lysing the cells with detergent then scraping them from the dish. Radioactivity remaining with the cells divided by the sum of internalized and surface label gave the fraction internal. F_{ab} fragments of antibodies to the pIgR and expression vectors for the wild type pIgR and mutant forms were the generous gift of Dr. Keith Mostov (UCSF).

Immunofluorescence microscopy: PC12/VAMP-TAg and PC12/del 41-50 cells were plated on poly-D-lysine coated coverslips, washed in PBS and fixed with 3% paraformaldehyde in PBS. Fixed cells were permeabilized with 0.5% Saponin in PBS/1%BSA for 20 min, incubated with KT3 antibody in permeabilization buffer for 20 min, and detected with fluorescein conjugated goat anti mouse IgG (Cappel).

Chapter Four

Signals in VAMP-TAg which affect targeting to SVLVs

Abstract

Signals in VAMP-TAg were identified which affect targeting to SVLVs in PC12 cells. A 60 amino acid region of the cytoplasmic domain of VAMP-TAg conserved between VAMP family members is sufficient for SVLV targeting. Mutations within this domain can either increase or decrease the fraction of VAMP-TAg recovered in SVLVs. Mutations which inhibit VAMP-TAg targeting to SVLVs overlap with the signal for VAMP-TAg endocytosis in PC12 cells centered on methionine 46. However, mutations within this region have more potent effects on SVLV targeting than on endocytosis. Three mutations were identified in which the fraction recovered in SVLVs increased by more than 5 times. A PC12-derived cell line was generated expressing one of these mutations, del 61-70. The extent of endocytosis of the fluid phase marker horseradish peroxidase into SVLVs in PC12/del 61-70 cells was normal, but more del 61-70 was transported from the cell surface to SVLVs. These results suggest that del 61-70 is sorted to SVLVs more efficiently than VAMP-TAg. The SVLVs of PC12/del 61-70 cells are saturated with mutant VAMP-TAg. Since SVLVs recycle in PC12/del 61-70 cells, and VAMP-2 is excluded from SVLVs by competition with the del 61-70 mutant VAMP-TAg, the del 61-70 mutation does not block the functions of VAMP-TAg required for SVLV exocytosis.

Introduction

In recent years, many synaptic vesicle membrane proteins have been cloned and characterized (Jahn and Sudhof 1994). Since most attention has been focused on dissecting the process of membrane fusion, little is known about how these proteins are targeted to synaptic vesicles. No primary sequence similarities which might act as signals for targeting to vesicles have been noted among the identified synaptic vesicle membrane proteins. In addition, it is not known whether there is an intracellular machinery which selects synaptic vesicle membrane proteins and promotes their budding into a small organelle or if synaptic vesicles self-assemble under appropriate conditions of protein concentration, pH and membrane potential.

Proteins are recycled to SVLVs by transport through an endosomal intermediate (Chapter 2). Therefore, synaptic vesicle proteins must be internalized to endosomes prior to entering SVLVs. This suggests that at least two signals may be required for targeting to SVLVs: an endocytosis signal and an SVLV targeting signal. An additional signal may be required for targeting to axons (de Hoop and Dotti 1993).

We chose to identify targeting signals in VAMP (synaptobrevin) because it is the synaptic vesicle protein with the lowest molecular weight and highest concentration. VAMP is an 18 kDa protein attached to the cytoplasmic face of synaptic vesicles by a C-terminal anchor (Trimble 1993). Two VAMP isoforms have been cloned from a variety of species. These isoforms have a highly conserved region in their cytoplasmic domain adjacent to the transmembrane anchor which might be predicted to contain signals for targeting to synaptic vesicles. However, this domain is also shared by a

variety of structurally and antigenically related proteins targeted to other organelles.

One complexity involved in the study of targeting signals in VAMP is that mutations in VAMP might affect not only targeting to synaptic vesicles, but also the dynamic cycle of synaptic vesicles themselves. Cleavage of VAMP by the tetanus toxin light chain endoprotease strongly inhibits neurotransmission implying that active VAMP is required by synaptic vesicles(Schiavo, et al. 1992). VAMP sediments in a 7S complex with two neural specific plasma membrane proteins, syntaxin and SNAP-25, in detergent extracts from rat brain (Sollner, et al. 1993b). This complex serves as a binding site for NSF and alpha-SNAP, proteins identified both genetically and biochemically as participants in a variety of intracellular membrane fusion processes. Therefore, it seems plausible to predict that mutations in VAMP defective in formation of the 7S complex or mutants which form a 7S complex to which NSF cannot bind are defective for synaptic vesicle fusion. These defects could block the SVLV recycling pathway in PC12 cells if they are dominant to VAMP-2 , the isoform endogenously expressed by PC12 cells.

Results

The conserved domain of VAMP is sufficient for targeting to SVLVs

Since VAMP is a relatively small protein, it was possible to construct a comprehensive set of mutants to identify signals (Figure 4-1). First, it was determined which domain of VAMP-TAg is required for SVLV targeting. Three mutants were constructed to determine if the targeting information in VAMP-TAg could be localized to the proline rich N-terminal domain, the conserved

Figure 4-1. Derivitives of VAMP-TAg used to identify SVLV targeting signals. (A) Rat VAMP-2 has a cytoplasmic domain subdivided into a proline-rich variable domain and a conserved domain containing two predicted amphipathic helicies. VAMP-TAg was constructed by linking an SV40 T antigen epitope tag to the C-terminus of the transmembrane domain of VAMP-2 via a short spacer. (B) Large deletions from the N-terminus of VAMP-TAg and a chimera in which the transmembrane domain of VAMP-TAg is replaced by the transmembrane domain of the transferrin receptor. (C) Proteins containing only the conserved domain of VAMP-TAg. Cellubrevin is a VAMP homologue found in recycling endosomes in many cell types. (D) Internal deletions within the conserved domain of VAMP-TAg. (E) Sequence of the VAMP-TAg conserved domain. Amino acids found on the hydrophobic faces of two predicted amphipathic helicies are highlighted.

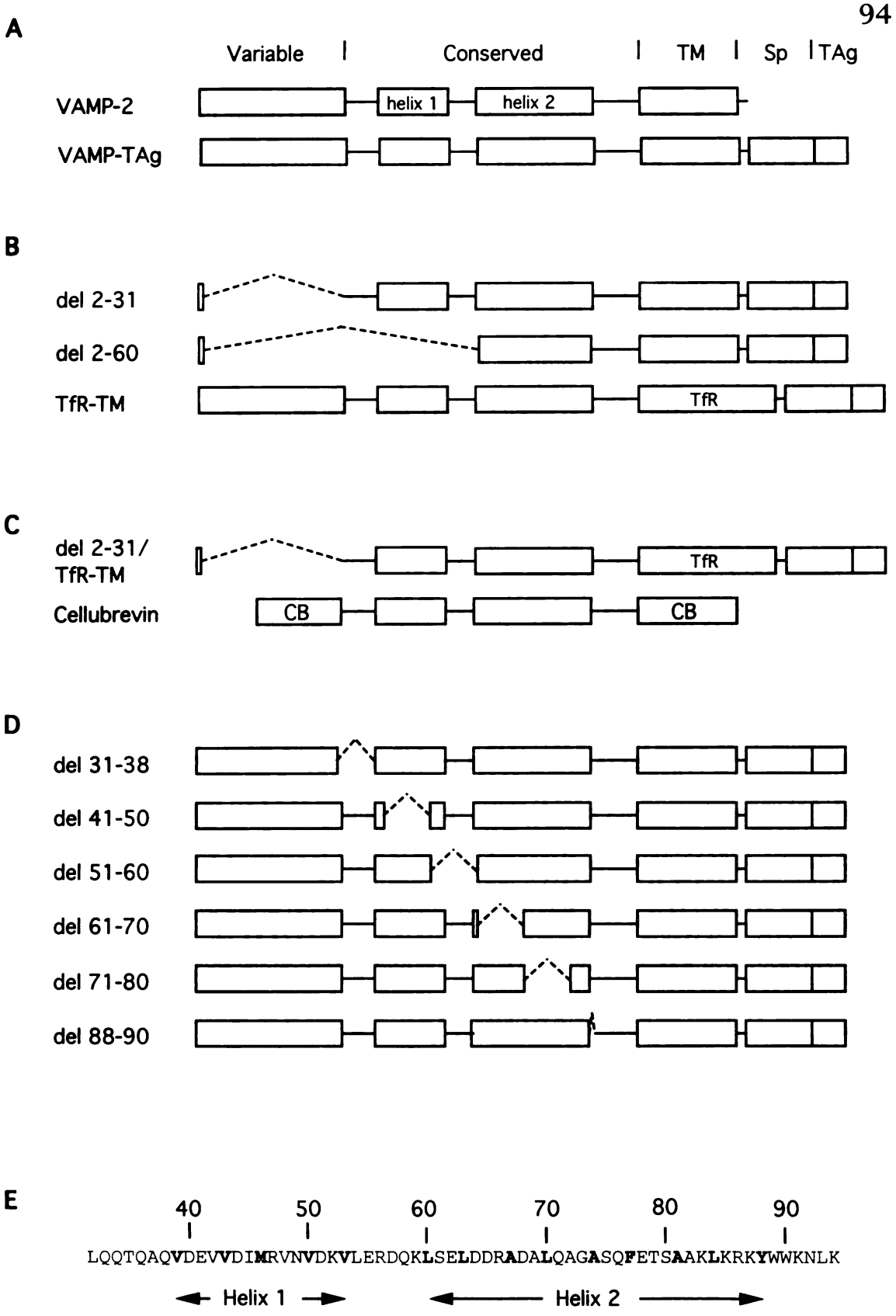
A
Variable
Conserved
TM
Sp
TAg
VAMP-2
helix 1
helix 2
VAMP-TAg
B
del 2-31
del 2-60
TfR-TM
TfR
C
del 2-31/
TfR-TM
TfR
Cellubrevin
CB
CB
D
del 31-38
del 41-50
del 51-60
del 61-70
del 71-80
del 88-90
E
40
50
60
70
80
90
LQQTQAQVDEVVDIMRVNVDKVLERDQKLSELDDRADALQAGASQFETSAAKLKRKYWWKNLK
Helix 1
Helix 2

helical domain, or the transmembrane domain (Figure 4-1, B). Del 2-31 is a deletion of the N terminal domain; del 2-60 is a larger deletion which also includes part of the conserved domain; and TfR-TM is a chimera in which the transmembrane domain of VAMP-TAg is replaced by the transmembrane domain of the transferrin receptor. These mutants were transiently transfected into PC12 cells and their extent of targeting to SVLVs was analyzed by immunoblotting of fractions from velocity sedimentation gradients (Figure 4-2, A). Like VAMP-TAg, del 2-31 and TfR-TM were both targeted to the SVLV peak implying that the region they share, the conserved helical domain, contains signals for targeting to SVLVs. Del 2-60 was not targeted to SVLVs suggesting that amino acids 32 to 60 are required for targeting.

To determine if the conserved domain of VAMP is sufficient for targeting to SVLVs, a double mutation was constructed combining both the variable domain deletion and the transmembrane domain substitution (Figure 4-1, C). Del 2-31 / TfR-TM is also targeted to SVLVs (Figure 4-2, B). The fraction of del 2-31 / TfR-TM which sediments with SVLVs has a lower molecular weight than the majority of the transiently expressed protein suggesting that a post-translational modification inhibits targeting to SVLVs.

The conserved domain of VAMP-TAg is 97% identical to a homologous domain in cellubrevin. Cellubrevin was overexpressed in PC12 cells by transient transfection to determine if the conserved domain will target cellubrevin to SVLVs (Figure 4-2, B). A small peak of cellubrevin was observed co-sedimenting with SVLVs. Therefore, the conserved domain of VAMP is sufficient for targeting to SVLVs.

Figure 4-2. Identification of a domain of VAMP-TAg required for SVLV targeting. (A) Velocity sedimentation analysis of PC12 cells transfected with VAMP-TAg and mutations presented in figure 1B. (B) Sedimentation analysis of proteins which share only the conserved domain of VAMP-TAg. S=Synaptophysin, V=VAMP-TAg derivative, C=cellubrevin.

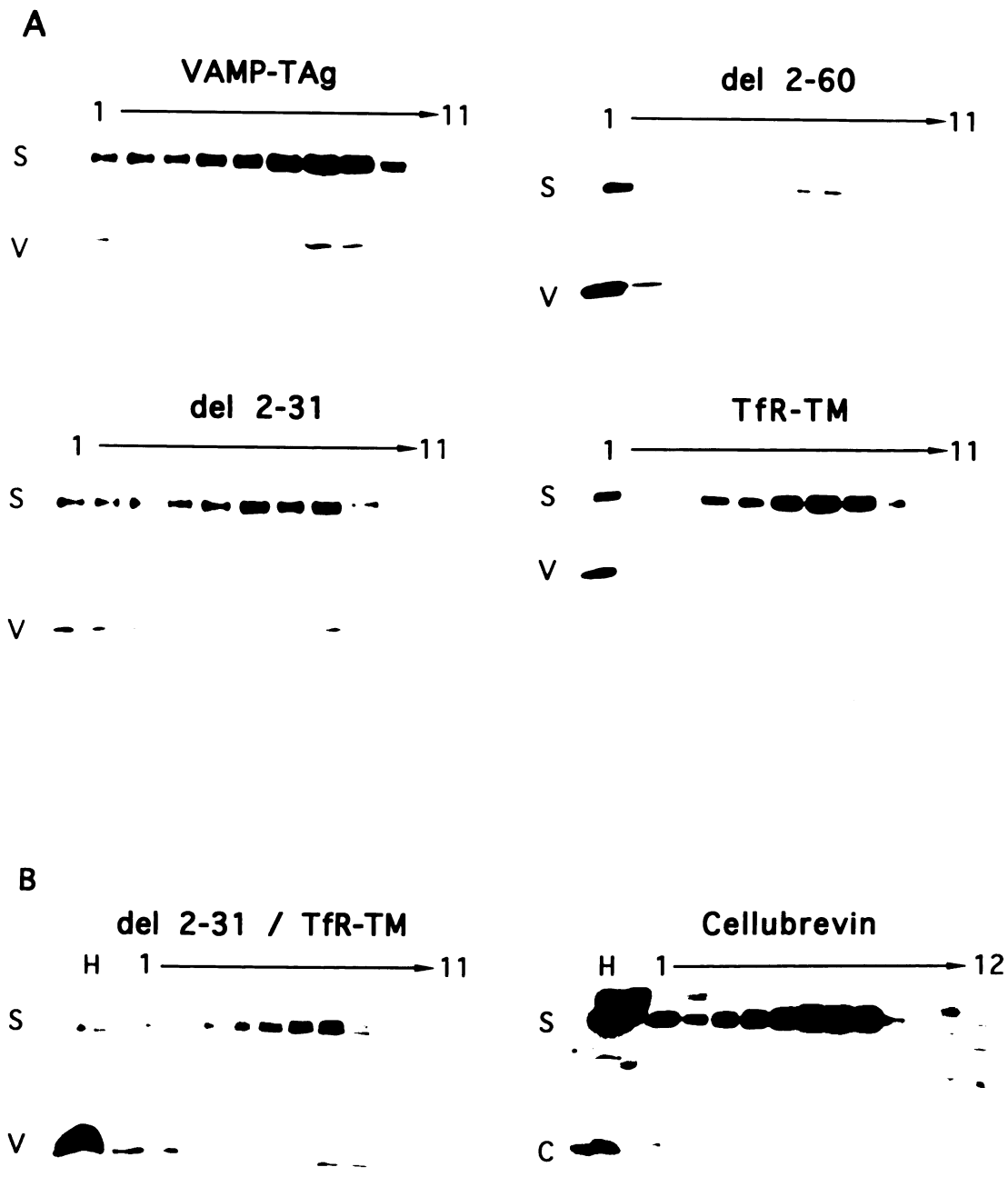
A
VAMP-TAg
1
11
S
V
del 2-60
1
11
S
V
del 2-31
1
11
S
V
TfR-TM
1
11
S
V
B
del 2-31 / TfR-TM
H
1
11
S
V
Cellubrevin
H
1
12
S
C

Mutations can increase or decrease the fraction of VAMP-TAg recovered in SVLVs

To identify more precisely signals within the conserved domain involved in targeting to SVLVs a series of internal deletions were constructed (Figure 4-1, D). Transport of each mutant through the secretory pathway of transfected PC12 cells was verified by binding ^{125}I-KT3 to the cell surface. Therefore, the internal deletions did not have grossly deletorious effects on protein folding which might have resulted in retention in the endoplasmic reticulum and premature degradation. Binding of ^{125}I-KT3 to the surface of transfected PC12 cells was measured to verify that the internal deletions did not cause retention in the endoplasmic reticulum due to misfolding. Targeting of the internal deletion mutants to SVLVs was measured by immunoblotting of gradient fractions from transiently transfected cells as above (Figure 4-3, A). Deletions of amino acids 31-38, 41-50 and 51-60 each blocked targeting to SVLVs. By contrast, deletions of 61-70, 71-80 and 88-90 were recovered in SVLVs. These results are consistant with the absence of SVLV targeting observed for del 2-60 and suggest that SVLV targeting requires sequences throughout the amino terminal portion of the conserved domain.

The amount of a transiently expressed protein recovered in the SVLV peak from a glycerol gradient depends not only on the fraction of the protein which is targeted to SVLVs, but also on the yield of SVLVs and the total expression level of the protein. Therefore, a procedure was developed to quantitatively compare the targeting to SVLVs of VAMP-TAg and the internal deletions. A homogenate was prepared from PC12 cells transfected with each mutant. Membrane proteins extracted with TX-114 from an aliquot of each homogenate were immunoblotted to determine the expression level of each

Figure 4-3. SVLV targeting of VAMP-TAg mutants with internal deletions within the conserved domain. (A) Sedimentation analysis on glycerol gradients. An aliquot of postnuclear supernatant (S1) was run on each gel to demonstrate expression of the VAMP-TAg mutants. S=Synaptophysin, V=VAMP-TAg derivative. (B) To directly compare SVLV targeting of the internal deletions, pooled SVLV peaks and membrane protein fractions from the homogenate were immunoblotted in parallel. (C) A relative SVLV targeting index was calculated to quantitatively compare the fraction of each mutant targeted to SVLVs.

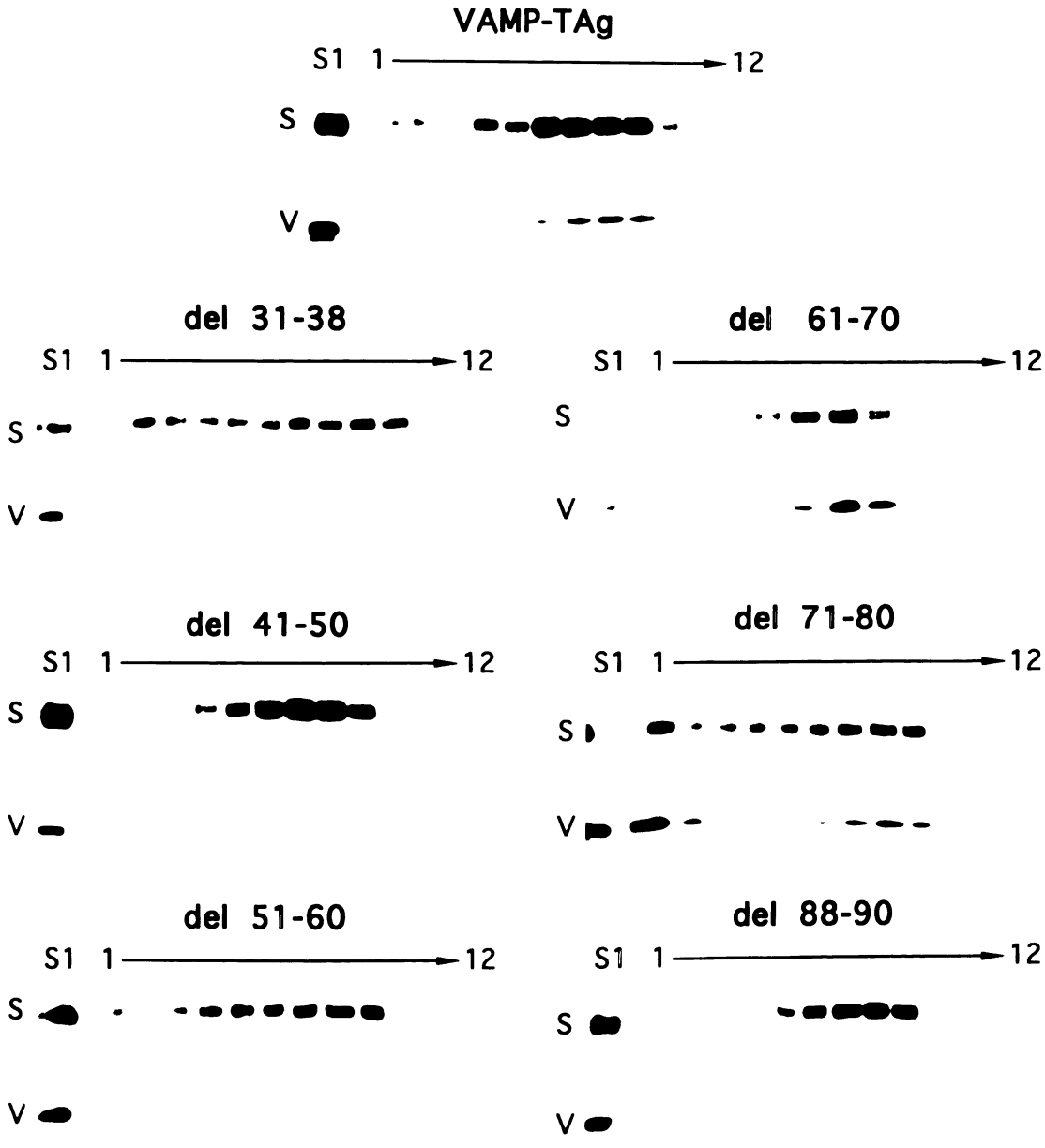
VAMP-TAg
S1 1 12
S
V
del 31-38
S1 1 12
S
V
del 61-70
S1 1 12
S
V
del 41-50
S1 1 12
S
V
del 71-80
S1 1 12
S
V
del 51-60
S1 1 12
S
V
del 88-90
S1 1 12
S
V

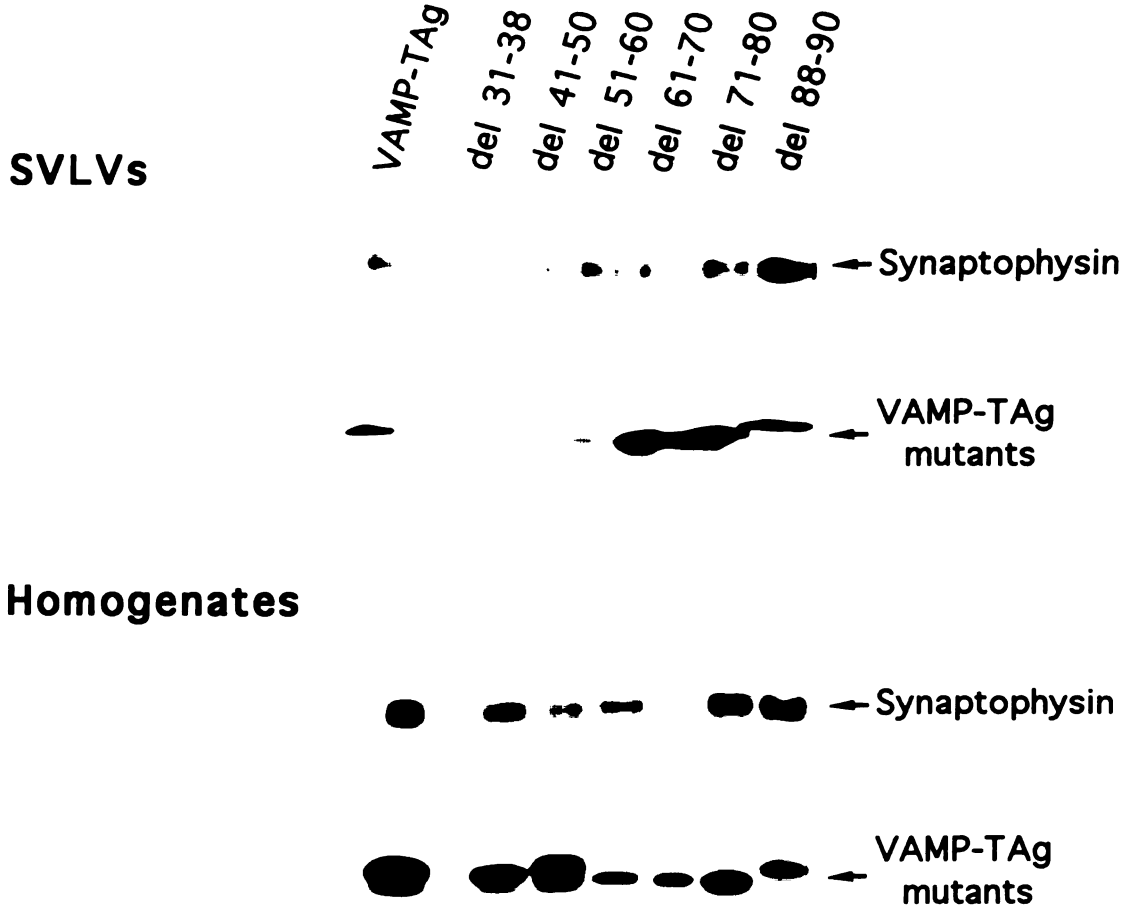
SVLVs
VAMP-TAg
del 31-38
del 41-50
del 51-60
del 61-70
del 71-80
del 88-90
Synaptophysin
VAMP-TAg mutants
Homogenates
Synaptophysin
VAMP-TAg mutants

C

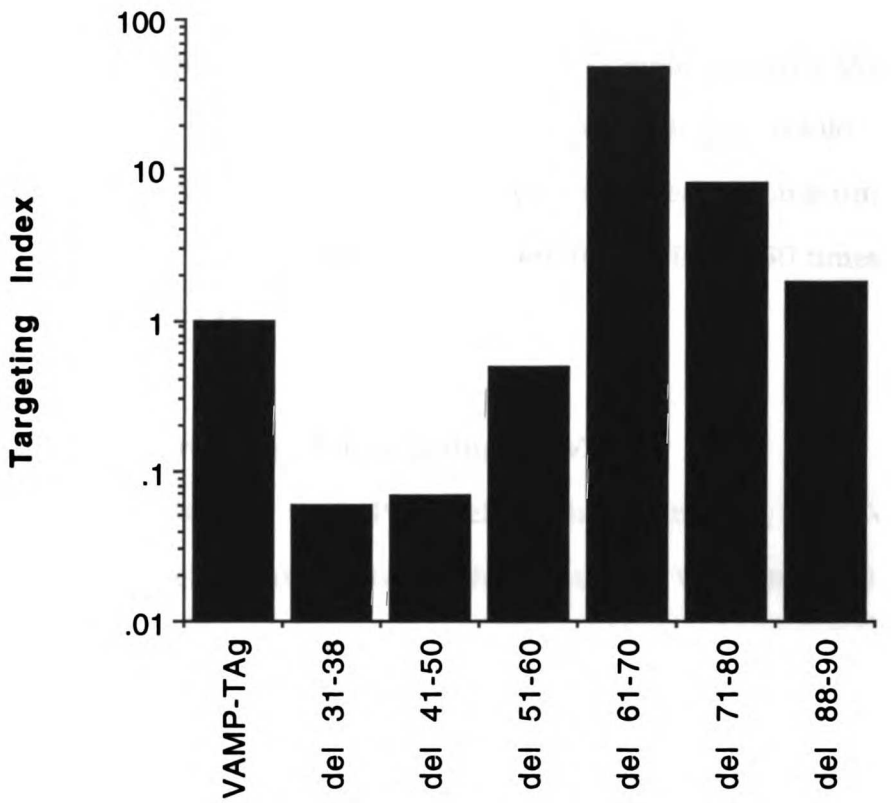
Targeting Index
100
10
1
.1
.01
VAMP-TAg
del 31-38
del 41-50
del 51-60
del 61-70
del 71-80
del 88-90

mutant relative to synaptophysin. Then, the SVLV peaks of sedimentation gradients for each mutant were analyzed on adjacent lanes of a second immunoblot (Figure 4-3, B). The amount of synaptophysin within each peak indicates the yield of SVLVs. An SVLV targeting index was then calculated for each mutant (see methods) using relative measurements of immunoblot signal intensities quantified by densitometry (Figure 4-3, C). Compared with VAMP-TAg, the fraction of del 31-38 and del 41-50 in SVLVs was reduced 20 fold indicating that these deletions have defects in a signal required for targeting to SVLVs. By contrast, the fraction of del 61-70 present in SVLVs is 50 times greater than that of VAMP-TAg.

An endocytosis signal is required for targeting to SVLVs

Because del 41-50 is defective in PC12 cells both for targeting to SVLVs and for endocytosis, the relationship between the two signals was compared by analyzing a series of mutations in which each amino acid from 41 to 50 was changed, individually, to alanine. Targeting to SVLVs was assayed by immunoblotting of velocity sedimentation gradient fractions and a targeting index was calculated for each alanine substitution mutant (Figure 4-4). Substitution of bulky hydrophobic amino acids with alanine strongly inhibited SVLV targeting whereas mutations of charged amino acids either had minor effects or, in the case of Asn49Ala, increased targeting to SVLVs. The Met46Ala mutant which had the strongest inhibition of endocytosis, had an SVLV targeting index of 0.1. However, Val43Ala, Val48Ala, and Val50Ala, which reduced endocytosis by less than 30%, inhibited SVLV targeting by greater than 85%.

Figure 4-4. SVLV targeting of alanine scanning mutations surrounding the methionine 46 endocytosis signal of VAMP-TAg. (A) Sedimentation analysis on glycerol gradients. Membrane proteins extracted with TX-114 from an aliquot of homogenate (H) were run on each gel to demonstrate expression of the VAMP-TAg mutants. (B) Pooled SVLV peaks and membrae protein fractions from the homogenate were immunoblotted in parallel. (C) A relative SVLV targeting index was calculated to quantitatively compare the fraction of each mutant targeted to SVLVs.

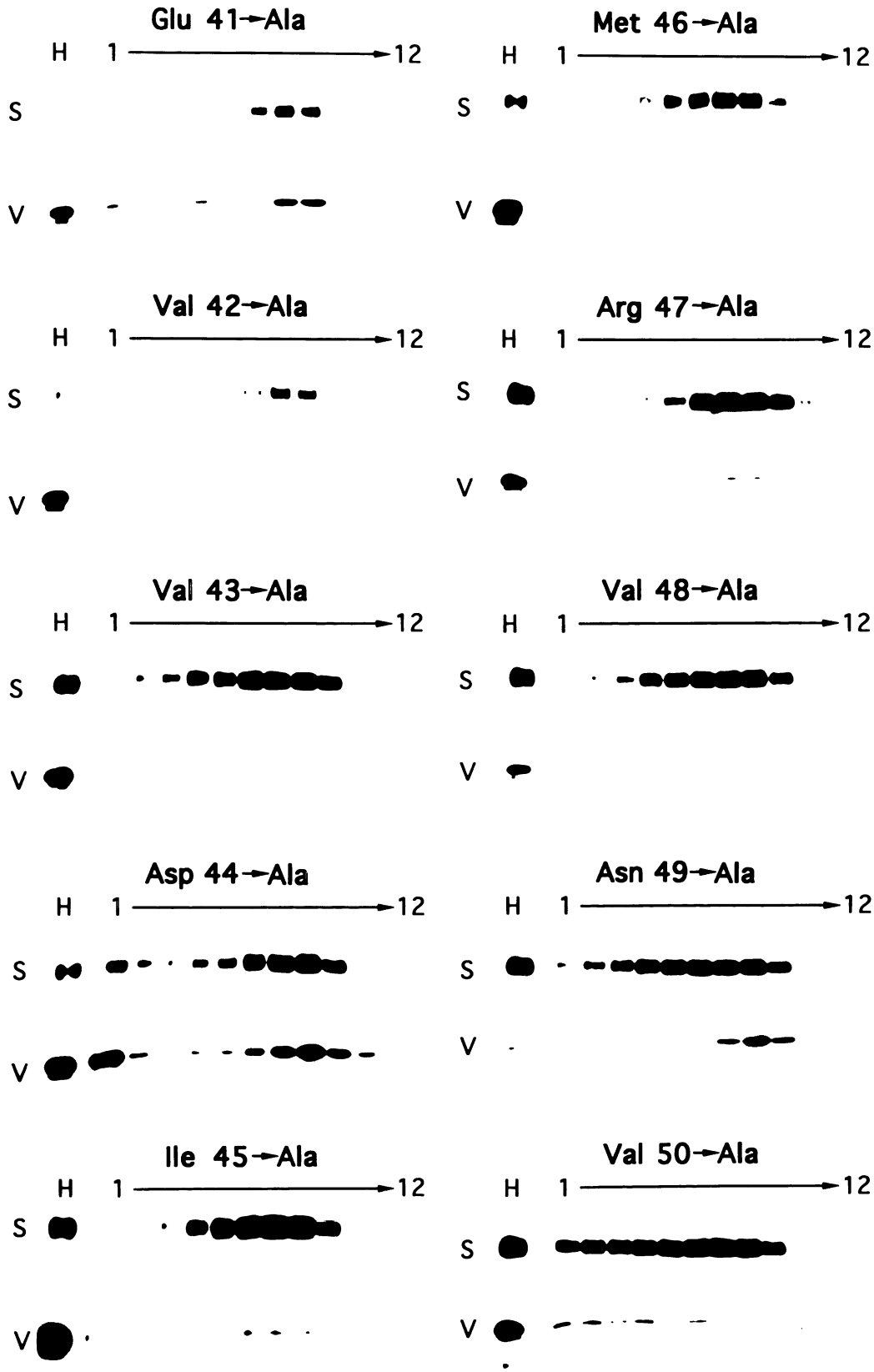
Glu 41→Ala
Met 46→Ala
Val 42→Ala
Arg 47→Ala
Val 43→Ala
Val 48→Ala
Asp 44→Ala
Asn 49→Ala
Ile 45→Ala
Val 50→Ala
H
1
12
S
V

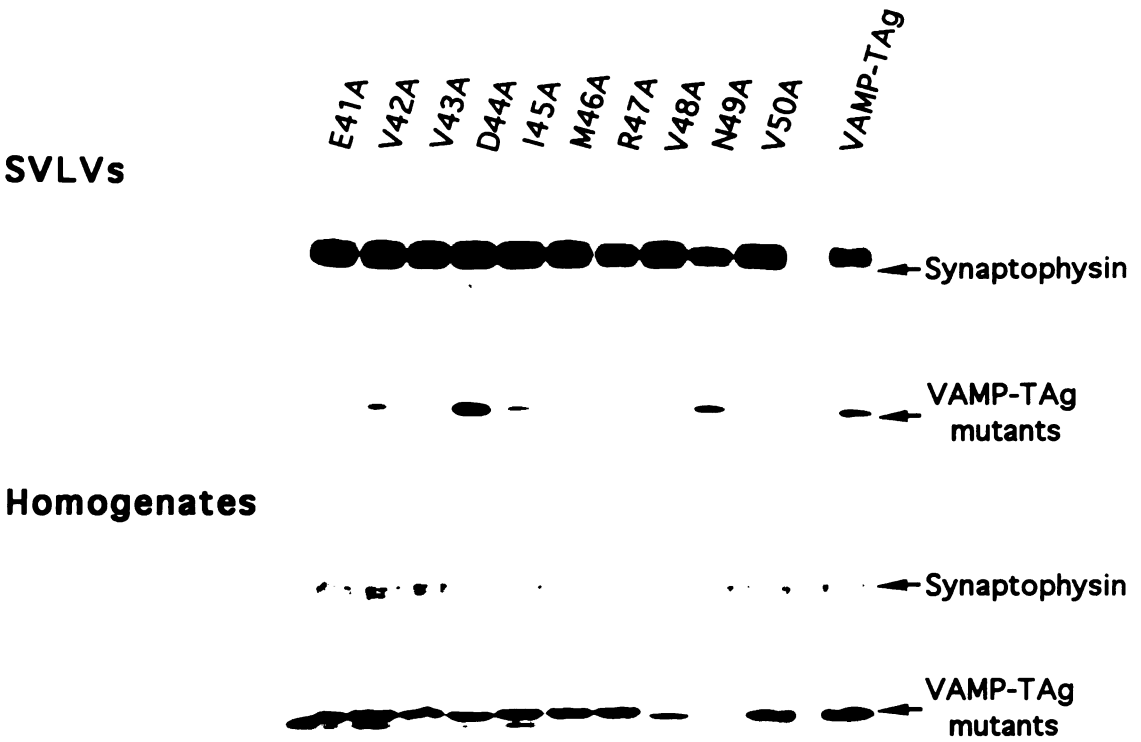
E41A
V42A
V43A
D44A
I45A
M46A
R47A
V48A
N49A
V50A
VAMP-TAg
SVLVs
Synaptophysin
VAMP-TAg mutants
Homogenates
Synaptophysin
VAMP-TAg mutants

C

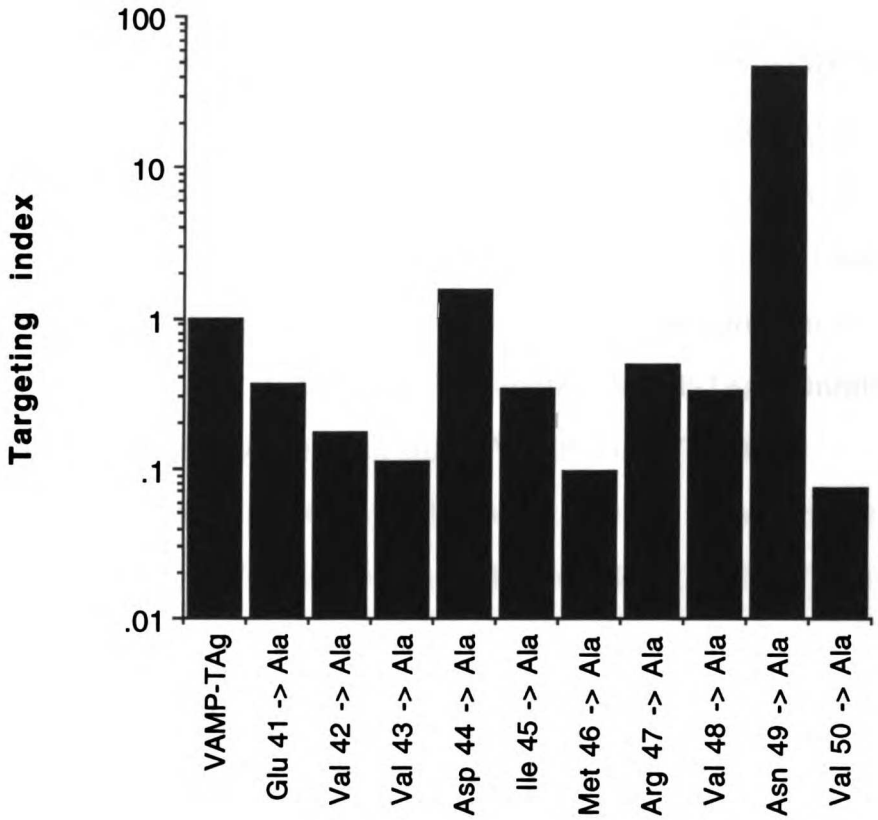
Targeting index
100
10
1
.1
.01
VAMP-TAg
Glu 41 -> Ala
Val 42 -> Ala
Val 43 -> Ala
Asp 44 -> Ala
Ile 45 -> Ala
Met 46 -> Ala
Arg 47 -> Ala
Val 48 -> Ala
Asn 49 -> Ala
Val 50 -> Ala

Mutations can increase sorting to SVLVs

Three VAMP-TAg mutants, del 61-70, del 71-80, and Asn49Ala, had a targeting index greater than 5. Increased recovery of a mutant in SVLVs could result from either an increase in the rate of sorting to SVLVs or a decline in the exocytosis rate of SVLVs containing the mutant. To distinguish between these possibilities, stable PC12 cell lines expressing VAMP-TAg and del 61-70 were compared. The increased recovery of del 61-70 in SVLVs observed in transiently transfected cells was reproduced in the cell lines (Figure 4-5, A, B).

For a mutant VAMP-TAg to block exocytosis of SVLVs, the mutant must be not only nonfunctional for exocytosis, it must also block the function of the endogenously expressed VAMP-2. One way for a mutant VAMP-TAg to inhibit VAMP-2 function would be to prevent sorting of VAMP-2 to SVLVs by saturation of the SVLV targeting pathway (Chapter 2). To test for saturation, the recovery of VAMP-2 in SVLVs was compared between PC12/VAMP-TAg and PC12/del 61-70 cells by probing immunoblots of the SVLV peaks with anti-VAMP antibody (Figure 4-5, C). VAMP-2 was partially excluded from the SVLVs of PC12/del 61-70 cells. Therefore, the SVLVs of PC12/del 61-70 cells must depend primarily on the del 61-70 mutant for VAMP activity.

Uptake of the fluid phase tracer horseradish peroxidase (HRP) to SVLVs was measured to determine if recycling of SVLVs was affected by the del 61-70 mutation. It was necessary to conduct this experiment on clonal cell lines because less than 10% of the cells in a population of transiently transfected PC12 cells express foreign protein (data not shown). Consequently, mainly nonexpressing cells would be observed if HRP uptake was measured in transiently transfected cells. PC12/del 61-70 and PC12/VAMP-TAg control cells were incubated with HRP at 37°C for 1 hour. The amount of HRP recovered in

Figure 4-5. Saturation of SVLVs with del 61-70 in a stable PC12-derived cell line. (A) Velocity sedimentation analysis. (B) Comparison of pooled SVLVs and homogenates from the cell lines with transiently transfected PC12 cells. (C) Immunoblot analysis of pooled SVLV fractions with anti-VAMP antibody indicates that the endogenous VAMP is partially excluded from SVLVs in PC12/del 61-70 cells.

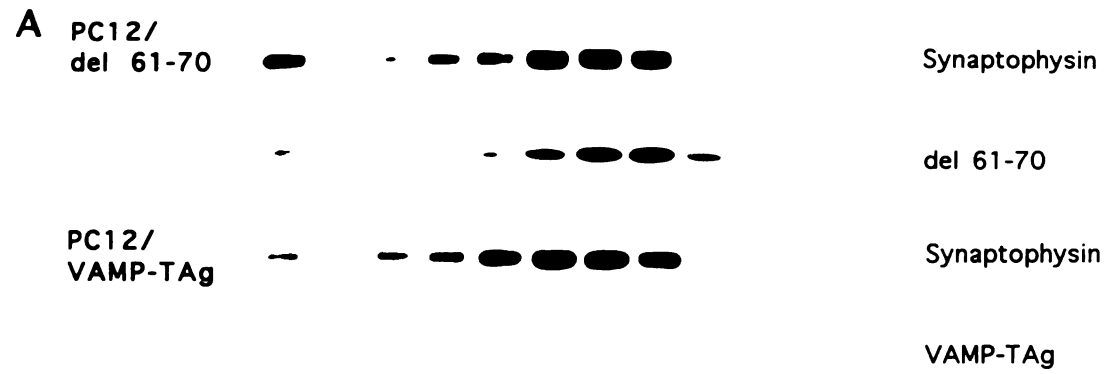
A
PC12/
del 61-70
Synaptophysin
del 61-70
PC12/
VAMP-TAg
Synaptophysin
VAMP-TAg

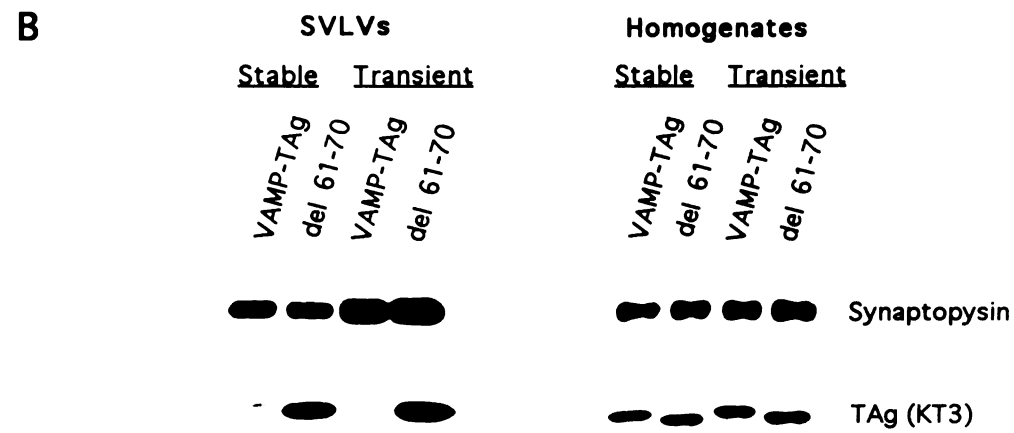
B
SVLVs
Homogenates
Stable
Transient
Stable
Transient
VAMP-TAg
del 61-70
VAMP-TAg
del 61-70
VAMP-TAg
del 61-70
VAMP-TAg
del 61-70
Synaptopysin
TAg (KT3)

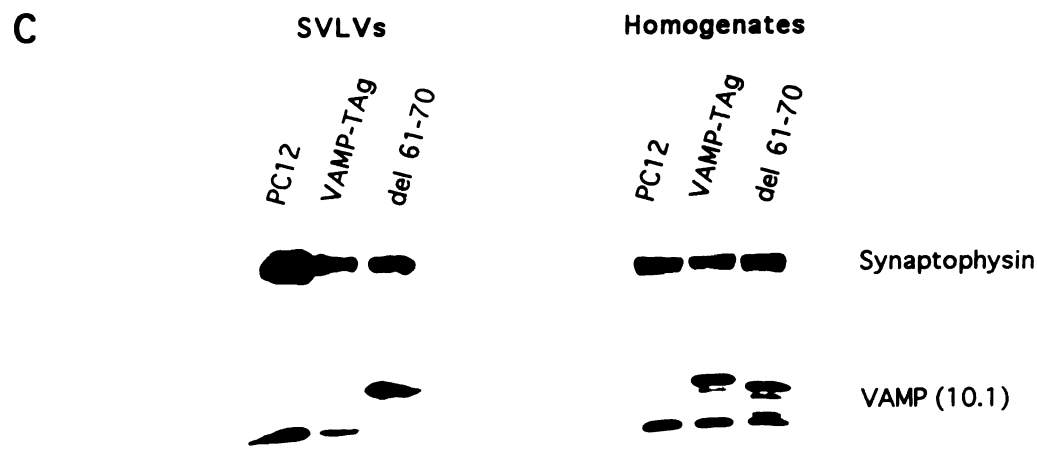
C
SVLVs
Homogenates
PC12
VAMP-TAg
del 61-70
PC12
VAMP-TAg
del 61-70
Synaptophysin
VAMP (10.1)

SVLVs for the two cell types was similar indicating that SVLV recycling is not blocked by the del 61-70 mutation (Figure 4-6, A). Since the rates of SVLV exocytosis and recycling must balance to maintain a constant number of SVLVs, basal SVLV exocytosis must also be unaffected by the del 61-70 mutation.

An alternate explanation for the increased recovery of del 61-70 in SVLVs is that it is sorted there more efficiently. To compare sorting, PC12/del 61-70 and PC12/VAMP-TAg cells were incubated with ^{125}I-KT3 at 37°C for 1 hour. The fraction of total cell associated antibody recovered in SVLVs was three times greater for PC12/del 61-70 cells than for PC12/VAMP-TAg cells (Figure 4-6, B). This suggests that increased sorting to SVLVs from the cell surface is involved in targeting a greater fraction of the total del 61-70 mutant to SVLVs.

Figure 4-6. Membrane traffic in PC12/del 61-70 cells. Uptake of HRP (A) or ^{125}I-KT3 (B) to SVLVs was compared between PC12-derived cell lines expressing del 61-70 and VAMP-TAg.

A

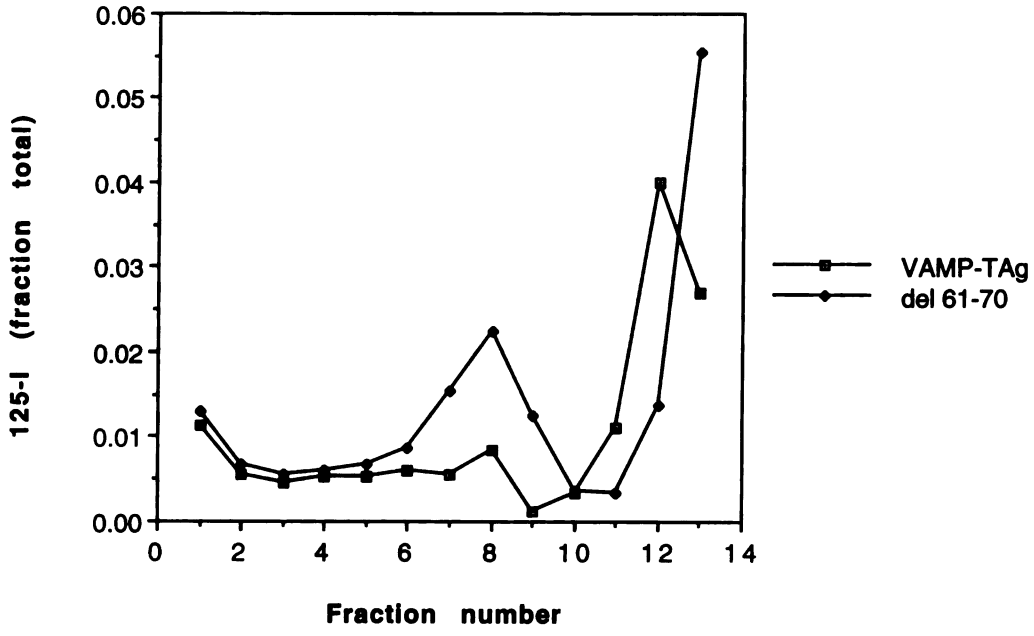
0.06
0.05
0.04
0.03
0.02
0.01
0.00
125-I (fraction total)
0
2
4
6
8
10
12
14
Fraction number
VAMP-TAg
del 61-70

B

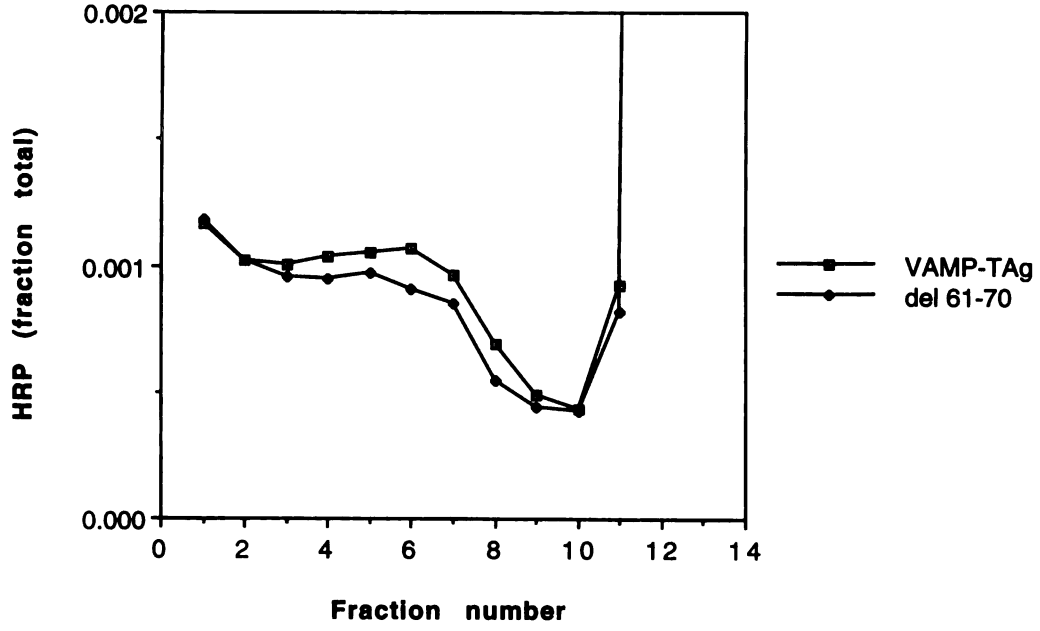
0.002
0.001
0.000
HRP (fraction total)
0
2
4
6
8
10
12
14
Fraction number
VAMP-TAg
del 61-70

Discussion

The conserved domain of VAMP-TAg is sufficient for targeting to SVLVs. Mutations within this domain can either increase or decrease the fraction of VAMP-TAg recovered in SVLVs. It has been proposed that an interaction between VAMP, as a component of synaptic vesicles, and syntaxin, on the presynaptic plasma membrane, targets synaptic vesicles to their appropriate fusion site. An appealing extension of this idea is that specific interactions between distinct members of the VAMP and syntaxin gene families located on other transport vesicles and their fusion targets provide a general mechanism for targeting intracellular fusion events (Sollner, et al. 1993b). A prediction of this model is that the members of the VAMP family must be targeted to distinct transport vesicles to prevent aberant fusions. This prediction is contradicted by the observation that VAMP-TAg and cellubrevin have overlapping distributions in PC12 cells.

Cellubrevin is a homolog of VAMP expressed at low levels in many cell types including non-neuronal cells (McMahon, et al. 1993) . Cleavage of cellubrevin by tetanus toxin inhibits the recycling of ^{125}I-transferrin from endosomes to the cell surface implying that cellubrevin functions in recycling endosomes (Galli et al., 1994). However, when cellubrevin is overexpressed in PC12 cells, it can be detected in SVLVs. Likewise, VAMP-TAg must be present in recycling endosomes since it is primarily located in endosomes and only a fraction of the VAMP-TAg in endosomes is sorted to SVLVs (Chapter 2). Perhaps it is only the high expression of VAMPs in neurons, relative to cellubrevin, that is responsible for its apparently selective targeting to synaptic vesicles (McMahon, et al. 1993). The overlapping distribution of these members of the VAMP family in transfected

PC12 cells suggests that VAMP isoforms do not serve as an address system for vesicle fusions.

Role of the Methionine 46 helix in SVLV targeting and endocytosis

SVLVs are generated primarily by budding from endosomes. Therefore, mutations which prevent delivery of VAMP-TAg to endosomes should also inhibit targeting to synaptic veisles. The Met46Ala mutation inhibits endocytosis in PC12 cells by 80% (Chapter 3). Conforming to expectations, the Met46Ala mutant is also not targetd to SVLVs. Additional mutations were identified, including Val43Ala, Val48Ala and Val50Ala, which are not targeted to SVLVs but have only modest effects on endocytosis. Mutations which inhibit sorting to SVLVs from endosomes would have this phenotype. However, the overlap between mutations affecting mainly SVLV targeting and those affecting both endocytosis and SVLV targeting is unlikely to be coincidental. All of the mutations in the alanine scanning mutagenesis series which inhibited SVLV targeting had a statistically significant, if small, inhibitory effect on the rates of endocytosis. This suggests that there is a common interaction involving this region of VAMP-TAg which is required for both endocytosis and SVLV targeting.

The interaction involving methionine 46 which is required for endocytosis is not thought to be a direct interaction with coated pits. Rather, it is required for release from a PC12 specific inhibition of VAMP-TAg endocytosis (Chapter 3). A partially defective interaction with a component required for SVLV targeting might be sufficient to release VAMP-TAg from retention at the cell surface. The predicted helix surrounding the methionine 46 targeting signal has been proposed to act as a fusion peptide (Jahn and

Sudhof 1994). An interaction with another synaptic vesicle protein which masks the hydrophobic fusion activity could promote endocytosis and synaptic vesicle targeting.

Implications of increased targeting to SVLVs

The del 61-70 mutant had increased targeting to synaptic vesicles. Generation of a stable PC12 cell line expressing del 61-70 made it possible to determine that expression of this mutant VAMP did not block the basal recycling of SVLVs by measuring HRP internalization. Since the del 61-70 mutation increased the amount of ^{125}I-KT3 transported to SVLVs but not the rate of ^{125}I-KT3 internalization, the increased targeting to SVLVs is probably the result of more efficient sorting from endosomes to SVLVs There are two possible reasons why the fraction of del 61-70 in endosomes transported to SVLVs would increase relative to the proportion returned to the plasma membrane. Either sorting to SVLVs has become more efficient or return to the plasma membrane is less efficient. Extensive mutagenesis has been carried out on the cytoplasmic tail of the transferrin receptor without effects being observed on the recycling rate from endosomes to the cell surface suggesting that this pathway is not signal mediated (McGraw and Maxfield 1990) . Therefore, deletion of amino acids 61-70 probably removes an inhibition of sorting to SVLVs.

A dominant negative mutant of VAMP would be useful for future studies of synaptic vesicle biogenesis and function. Mutations which increase targeting of VAMP-TAg to SVLVs have the potential to be dominant inhibitors of function by saturating the SVLV targeting pathway and excluding functional VAMP. A dominant negative mutant would have to have both

increased targeting to SVLVs and impaired function. There is no evidence from trafficking studies that del 61-70 it is functionally impaired.

It has been predicted that the amphipathic helix surrounding methionine 46 is the active domain of VAMP for promoting fusion (Jahn and Sudhof 1994). Many mutations within this domain block targeting to SVLVs indicating that the SVLV targeting and functional domains are linked. Since most endosomal proteins are excluded from SVLVs, mutations which block SVLV targeting are likely to be epistatic to mutations which increase recovery in SVLVs. There is, however, a mutation within the methionine 46 helix with increased recovery in SVLVs. This mutation, Asn49Ala, is currently the best candidate for a dominant negative inhibitor of VAMP function.

Methods

Plasmids and antibodies: pRC/CMV/VAMP-2 was the generous gift of Richard Scheller (Elferink, et al. 1989). The VAMP-TAg mutants were constructed as described in chapters 2 and 3. The pCMV5/cellubrevin expression vector was a gift of T. C. Sudhof (Dallas) (McMahon, et al. 1993). Antibodies used included SVP-38 (anti-synaptophysin, Boehringer Manneheim), KT3 (anti-T antigen) (MacArthur and Walter 1984), 10.1 (anti-synaptobrevin/VAMP) (Baumert, et al. 1989), and anti-cellubrevin (McMahon, et al. 1993).

Cell culture and transfection: PC12 (KB) and CHO-K1 cells were grown in DME H-21 media supplemented with 10% horse serum, 5% fetal calf serum, 1000 U/ml penicillin and 1000 mcg / ml streptomycin in a humidified 37°C incubator with 10% CO2. Electroporation was found to be the most efficient method for transfection of PC12 cells (Muller et al., 1990). Cells were collected from a confluent 15 cm dish in electroporation buffer (137 mM NaCl, 5 mM KCl, 0.7 mM Na_2HPO_4, 6 mM dextrose, 20 mM Hepes, pH 7.05) pelleted, and resuspended in 650 µl electroporation buffer. Plasmid DNA was added to the resuspended cells. The amount of DNA was varied between 40 and 300 µg to equalize expression of the VAMP-TAg proteins. After a 10 minute incubation at 25°C the PC12 cells were pulsed in a BTX-300 electroporator set to 500 µF and 230 mV. The cells were transferred to 20 ml growth media supplemented with 3 mM EGTA for 30 minutes at 37°C to recover from the shock of electroporation and then spun down and plated on a 15 cm dish. For transient expression, the day after transfection, the cells were re-fed with growth media supplemented

with 6 mM sodium butyrate. Experiments were carried out on cells 22-24 hours after butyrate addition.

To generate stable PC12 cell lines, three days after transfection the cells were diluted onto 10 cm dishes and subjected to selection in 500 μg/ml (active) G418 (Gibco) for approximately 1 month until resistant colonies appeared. Cell lines were screened by ^{125}I-KT3 surface binding and immunoblotting.

SVLV isolation: SVLVs were isolated by a variation of the method of Clift-O'Grady *et al* (Clift-O'Grady, et al. 1990). Cells from a confluent 15 cm dish were washed, collected, pelleted, and resuspended in 500 ul buffer A (150 mM NaCl, 0.1 mM $MgCl_2$, 1 mM EGTA, 10 mM Hepes, pH 7.4) at 4°C, then homogenized by 9 passes through a ball bearing cell cracker with a nominal clearance of 8 μm. The homogenate was divided into 400 μg aliquots which were brought up to 150 to 200 μl in buffer A (approximately a 1:2 dilution). Post-nuclear supernatants were prepared by a 5 minute centrifugation at 1000 x g and either used immediately or rapidly frozen in liquid nitrogen for storage at -80°C. To isolate SVLVs, the supernatant from a 15 minute centrifugation at 10,000 x g was loaded above a 5 ml 5-25% glycerol gradient in buffer A. SVLVs were sedimented into the gradient during a 46 minute centrifugation at 55 kRPM (287,000 x g) in an SW55 rotor and collected in 7 drop (350 μl) fractions from the bottom of the tube. Where indicated, the pooled SVLV peak included drops 40 to 58.

Immunoblotting: Samples were prepared for electrophoresis by precipitation of gradient fractions in 10% tricholoracetic acid, 0.1 mg/ml deoxycholate, washed in acetone, and resuspended in reducing sample buffer

with 7 M urea for 15-30 minutes at 55°C. Homogenates were processed in parallel after concentration of membrane proteins by a TX-114 phase partition. After resolution on SDS-13%PAGE gels, samples were transferred to PVDF (immobilon-P, Millipore) membranes and probed with SVP-38 and KT3 (or 10.1 as described) monoclonal antibodies using the ECL (Amersham) detection system. Cellubrevin was detected with a rabbit polyclonal antibody (McMahon, et al. 1993).

Quantification of SVLV targeting: Immunoblot band intensities were quantified by densitometry (Ephortec, Joyce Loebl). By quantifying band intensities from an immunoblot of a serially diluted sample, it was established that this densitometry technique can produce linear readings over a 1000 fold range of sample concentrations. Multiple films with exposure times from 1 second to 2 hours were scanned and data from saturated or underexposed bands was disregarded. A quantitative measurement of the comparative efficiency of targeting the VAMP-TAg mutants to SVLVs was made by calculating a targeting index, S:

$$S = \frac{\dfrac{(\text{Mut/p38})\ \text{SVLVs}}{(\text{Mut/p38})\ \text{Homog}}}{\dfrac{(\text{VAMP-TAg/p38})\ \text{SVLVs}}{(\text{VAMP-TAg/p38})\ \text{Homog}}}$$

Internalization assays: KT3 monoclonal antibody against the T antigen epitope tag was purified from serum free hybridoma supernatant by protein G affinity chromatography and iodinated in 100 ug aliquots with 1 mCi Na ^{125}I

by the iodogen method (Pierce). To demonstrate transport of VAMP-TAg from the plasma membrane to SVLVs, PC12/VAMP-TAg cells were incubated with 10^7 cpm/ml ^{125}I-KT3 for 1 hour at 37°C in PBS/5%BSA, then washed 7 times at 4°C in PBS/BSA prior to isolation of SVLVs as described above. The ^{125}I-KT3 peak in SVLVs was measured by counting gradient fractions, without further processing, on a gamma counter.

For uptake of HRP, cells were incubated in growth media supplemented with 10mg/ml HRP (Sigma, typeII) for 1 hour at 37°C prior to isolation of SVLVs as above. Peroxidase activity in gradient fraction was measured using the substrate 0-dianisidine (Sigma).

Bibliography

Alvarez de Toledo, G., Fernandez-Chacon, R., and Fernandez, J. M. (1993). Release of secretory products during transient vesicle fusion. Nature *363,* 554-8.

Annaert, W. G., Llona, I., Backer, A. C., Jacob, W. A., and De Potter, W. P. (1993). Catecholamines are present in a synaptic-like microvesicle-enriched fraction from bovine adrenal medulla. Journal of Neurochemistry *60,* 1746-54.

Bansal, A., and Gierasch, L. M. (1991). The NPXY internalization signal of the LDL receptor adopts a reverse-turn conformation. Cell *67,* 1195-201.

Bauerfeind, R., Regnier-Vigouroux, A., Flatmark, T., and Huttner, W. B. (1993). Selective storage of acetylcholine, but not catecholamines, in neuroendocrine synaptic-like microvesicles of early endosomal origin. Neuron *11,* 105-21.

Baumert, M., Maycox, P. R., Navone, F., De Camilli, P., and Jahn, R. (1989). Synaptobrevin: an integral membrane protein of 18,000 daltons present in small synaptic vesicles of rat brain. Embo Journal *8,* 379-84.

Bennett, M. K., Calakos, N., Kreiner, T., and Scheller, R. H. (1992). Synaptic vesicle membrane proteins interact to form a multimeric complex. Journal of Cell Biology *116,* 761-75.

Betz, W. J., and Bewick, G. S. (1992). Optical analysis of synaptic vesicle recycling at the frog neuromuscular junction. Science *255,* 200-3.

Braun, J. E., Fritz, B. A., Wong, S. M., and Lowe, A. W. (1994). Identification of a vesicle-associated membrane protein (VAMP)-like membrane protein in zymogen granules of the rat exocrine pancreas. Journal of Biological Chemistry *269,* 5328-35.

Breitfeld, P. P., Casanova, J. E., Harris, J. M., Simister, N. E., and Mostov, K. E. (1989). Expression and analysis of the polymeric immunoglobulin receptor in Madin-Darby canine kidney cells using retroviral vectors. Methods in Cell Biology *32,* 329-37.

Cain, C. C., Trimble, W. S., and Lienhard, G. E. (1992). Members of the VAMP family of synaptic vesicle proteins are components of glucose transporter-containing vesicles from rat adipocytes. Journal of Biological Chemistry *267,* 11681-4.

Cameron, P. L., Sudhof, T. C., Jahn, R., and De Camilli, P. (1991). Colocalization of synaptophysin with transferrin receptors: implications for synaptic vesicle biogenesis. Journal of Cell Biology *115,* 151-64.

Clift-O'Grady, L., Linstedt, A. D., Lowe, A. W., Grote, E., and Kelly, R. B. (1990). Biogenesis of synaptic vesicle-like structures in a pheochromocytoma cell line PC-12. Journal of Cell Biology *110,* 1693-703.

Collawn, J. F., Stangel, M., Kuhn, L. A., Esekogwu, V., Jing, S. Q., Trowbridge, I. S., and Tainer, J. A. (1990). Transferrin receptor internalization sequence YXRF implicates a tight turn as the structural recognition motif for endocytosis. Cell *63,* 1061-72.

Courtoy, P. J., Quintart, J., and Baudhuin, P. (1984). Shift of equilibrium density induced by 3,3'-diaminobenzidine cytochemistry: a new procedure for the analysis and purification of peroxidase-containing organelles. Journal of Cell Biology *98,* :870-6.

Dascher, C., Ossig, R., Gallwitz, D., and Schmitt, H. D. (1991). Identification and structure of four yeast genes (SLY) that are able to suppress the functional loss of YPT1, a member of the RAS superfamily. Molecular and Cellular Biology *11,* 872-85.

de Hoop, M. J., and Dotti, C. G. (1993). Membrane traffic in polarized neurons in culture. Journal of Cell Science *17,* 85-92.

Elferink, L. A., Trimble, W. S., and Scheller, R. H. (1989). Two vesicle-associated membrane protein genes are differentially expressed in the rat central nervous system. Journal of Biological Chemistry *264,* 11061-4.

Galli, T., Chilcote, T., Mundigl, O., Binz, T., Niemann, H., and De Camilli, P. (1994). Tetanus toxin-mediated cleavage of cellubrevin impairs exocytosis of transferrin receptor-containing vesicles in CHO cells. Journal of Cell Biology *125,* 1015-24.

Grote, E., Bennett, M. K., and Kelly, R. B. (1994). unpublished observation.

Harding, C., Heuser, J., and Stahl, P. (1983). Receptor-mediated endocytosis of transferrin and recycling of the transferrin receptor in rat reticulocytes. Journal of Cell Biology *97,* 329-39.

Heuser, J. (1989). The role of coated vesicles in recycling of synaptic vesicle membrane. Cell Biology International Reports *13,* 1063-76.

Holtzman, E., Freeman, A. R., and Kashner, L. A. (1971). Stimulation-dependent alterations in peroxidase uptake at lobster neuromuscular junctions. Science *173,* 733-6.

Hopkins, C. R., and Trowbridge, I. S. (1983). Internalization and processing of transferrin and the transferrin receptor in human carcinoma A431 cells. Journal of Cell Biology *97,* 508-21.

Hunt, J. M., Bommert, K., Charlton, M. P., Kistner, A., Habermann, E., Augustine, G. J., and Betz, H. (1994). A post-docking role for synaptobrevin in synaptic vesicle fusion. Neuron *12,* 1269-79.

Jahn, R., and Sudhof, T. C. (1993). Synaptic vesicle traffic: rush hour in the nerve terminal. Journal of Neurochemistry *61,* 12-21.

Jahn, R., and Sudhof, T. C. (1994). Synaptic vesicles and exocytosis. Annual Review of Neuroscience *17,* 219-46.

Johnston, P. A., Cameron, P. L., Stukenbrok, H., Jahn, R., De Camilli, P., and Sudhof, T. C. (1989). Synaptophysin is targeted to similar microvesicles in CHO and PC12 cells. Embo Journal *8,* 2863-72.

Kelly, R. B. (1991). Secretory granule and synaptic vesicle formation. Current Opinion in Cell Biology *3,* 654-60.

Kiene, M. L., and Stadler, H. (1987). Synaptic vesicles in electromotoneurones. I. Axonal transport, site of transmitter uptake and processing of a core proteoglycan during maturation. Embo Journal *6,* 2209-15.

Letourneur, F., and Klausner, R. D. (1992). A novel di-leucine motif and a tyrosine-based motif independently mediate lysosomal targeting and endocytosis of CD3 chains. Cell *69,* 1143-57.

Linstedt, A. D., and Kelly, R. B. (1991). Synaptophysin is sorted from endocytotic markers in neuroendocrine PC12 cells but not transfected fibroblasts. Neuron *7,* 309-17.

Lisanti, M. P., Caras, I. W., Gilbert, T., Hanzel, D., and Rodriguez-Boulan, E. (1990). Vectorial apical delivery and slow endocytosis of a glycolipid-anchored fusion protein in transfected MDCK cells. Proceedings of the National Academy of Sciences of the United States of America *87,* 7419-23.

Lupas, A., Van Dyke, M., and Stock, J. (1991). Predicting coiled coils from protein sequences. Science *252,* 1162-4.

MacArthur, H., and Walter, G. (1984). Monoclonal antibodies specific for the carboxy terminus of simian virus 40 large T antigen. Journal of Virology *52,* 483-91.

Matteoli, M., Takei, K., Perin, M. S., Sudhof, T. C., and De Camilli, P. (1992). Exo-endocytotic recycling of synaptic vesicles in developing processes of cultured hippocampal neurons. Journal of Cell Biology *117,* :849-61.

Maycox, P. R., Link, E., Reetz, A., Morris, S. A., and Jahn, R. (1992). Clathrin-coated vesicles in nervous tissue are involved primarily in synaptic vesicle recycling. Journal of Cell Biology *118,* 1379-88.

McClelland, A., Kuhn, L. C., and Ruddle, F. H. (1984). The human transferrin receptor gene: genomic organization, and the complete primary structure of the receptor deduced from a cDNA sequence. Cell *39,* 267-74.

McGraw, T. E., and Maxfield, F. R. (1990). Human transferrin receptor internalization is partially dependent upon an aromatic amino acid on the cytoplasmic domain. Cell Regulation *1,* 369-77.

McMahon, H. T., Ushkaryov, Y. A., Edelmann, L., Link, E., Binz, T., Niemann, H., Jahn, R., and Sudhof, T. C. (1993). Cellubrevin is a ubiquitous tetanus-toxin

substrate homologous to a putative synaptic vesicle fusion protein. Nature *364,* 346-9.

Meldolesi, J., Madeddu, L., Torda, M., Gatti, G., and Niutta, E. (1983). The effect of alpha-latrotoxin on the neurosecretory PC12 cell line: studies on toxin binding and stimulation of transmitter release. Neuroscience *10,* 997-1009.

Miettinen, H. M., Matter, K., Hunziker, W., Rose, J. K., and Mellman, I. (1992). Fc receptor endocytosis is controlled by a cytoplasmic domain determinant that actively prevents coated pit localization. J. Cell Biol. *116,* 875-888.

Muller, S. R., Sullivan, P. D., Clegg, D. O., and Feinstein, S. C. (1990). Efficient transfection and expression of heterologous genes in PC12 cells. Dna and Cell Biology *9,* 221-9.

Okamoto, C. T., Shia, S. P., Bird, C., Mostov, K. E., and Roth, M. G. (1992). The cytoplasmic domain of the polymeric immunoglobulin receptor contains two internalization signals that are distinct from its basolateral sorting signal. Journal of Biological Chemistry *267,* 9925-32.

Osen-Sand, A., Catsicas, M., Staple, J. K., Jones, K. A., Ayala, G., Knowles, J., Grenningloh, G., and Catsicas, S. (1993). Inhibition of axonal growth by SNAP-25 antisense oligonucleotides in vitro and in vivo. Nature *364,* 445-8.

Pashkov, V., N., G., Tsurupa, G., Storchak, L., Shatursky, O., Himmerlreich, N., and Grishin, E. (1993). Monoclonal antibodies can uncouple the main alpha-

latrotoxin effects: toxin-induced Ca2+ influx and stimulated neurotransmitter release. Neuroscience *56,* 695-701.

Pearse, B. M. (1988). Receptors compete for adaptors found in plasma membrane coated pits. Embo Journal *7,* 3331-6.

Perez-Vilar, J., Hidalgo, J., and Velasco, A. (1991). Presence of terminal N-acetylgalactosamine residues in subregions of the endoplasmic reticulum is influenced by cell differentiation in culture. Journal of Biological Chemistry *266,* 23967-76.

Protopopov, V., Govindan, B., Novick, P., and Gerst, J. E. (1993). Homologs of the synaptobrevin/VAMP family of synaptic vesicle proteins function on the late secretory pathway in S. cerevisiae. Cell *74,* 855-61.

Regnier-Vigouroux, A., Tooze, S. A., and Huttner, W. B. (1991). Newly synthesized synaptophysin is transported to synaptic-like microvesicles via constitutive secretory vesicles and the plasma membrane. Embo Journal *10,* 3589-601.

Schiavo, G., Benfenati, F., Poulain, B., Rossetto, O., Polverino de Laureto, P., DasGupta, B. R., and Montecucco, C. (1992). Tetanus and botulinum-B neurotoxins block neurotransmitter release by proteolytic cleavage of synaptobrevin. Nature *359,* 832-5.

Schubert, D., and Klier, F. G. (1977). Storage and release of acetylcholine by a clonal cell line. Proceedings of the National Academy of Sciences of the United States of America *74,* 5184-8.

Sollner, T., Bennett, M. K., Whiteheart, S. W., Scheller, R. H., and Rothman, J. E. (1993a). A protein assembly-disassembly pathway in vitro that may correspond to sequential steps of synaptic vesicle docking, activation, and fusion. Cell *75,* 409-18.

Sollner, T., Whiteheart, S. W., Brunner, M., Erdjument-Bromage, H., Geromanos, S., Tempst, P., and Rothman, J. E. (1993b). SNAP receptors implicated in vesicle targeting and fusion. Nature *362,* 318-24.

Steinman, R. M., Silver, J. M., and Cohn, Z. A. (1974). Pinocytosis in fibroblasts. Quantitative studies in vitro. Journal of Cell Biology *63,* 949-69.

Sudhof, T. C., Baumert, M., Perin, M. S., and Jahn, R. (1989). A synaptic vesicle membrane protein is conserved from mammals to Drosophila. Neuron *2,* 1475-81.

Sudhof, T. C., and Jahn, R. (1991). Proteins of synaptic vesicles involved in exocytosis and membrane recycling. Neuron *6,* 665-77.

Thomas-Reetz, A. C., and De Camilli, P. (1994). A role for synaptic vesicles in non-neuronal cells: clues from pancreatic beta cells and from chromaffin cells. Faseb Journal *8,* 209-16.

Torri-Tarelli, F., Haimann, C., and Ceccarelli, B. (1987). Coated vesicles and pits during enhanced quantal release of acetylcholine at the neuromuscular junction. Journal of Neurocytology *16,* 205-14.

Trimble, W. S. (1993). Analysis of the structure and expression of the VAMP family of synaptic vesicle proteins. Journal de Physiologie *87,* 107-15.

Trimble, W. S., Cowan, D. M., and Scheller, R. H. (1988). VAMP-1: a synaptic vesicle-associated integral membrane protein. Proceedings of the National Academy of Sciences of the United States of America *85,* 4538-42.

Trowbridge, I. S., Collawn, J. F., and Hopkins, C. R. (1993). Signal-dependent membrane protein trafficking in the endocytic pathway. Annual Review of Cell Biology *9,* 129-61.

Valtorta, F., Fesce, R., Grohovaz, F., Haimann, C., Hurlbut, W. P., Iezzi, N., Torri-Tarelli, F., Villa, A., and Ceccarelli, B. (1990). Neurotransmitter release and synaptic vesicle recycling. Neuroscience *35,* 477-89.

Wiedenmann, B., Rehm, H., Knierim, M., and Becker, C. M. (1988). Fractionation of synaptophysin-containing vesicles from rat brain and cultured PC12 pheochromocytoma cells. Febs Letters *240,* 71-7.

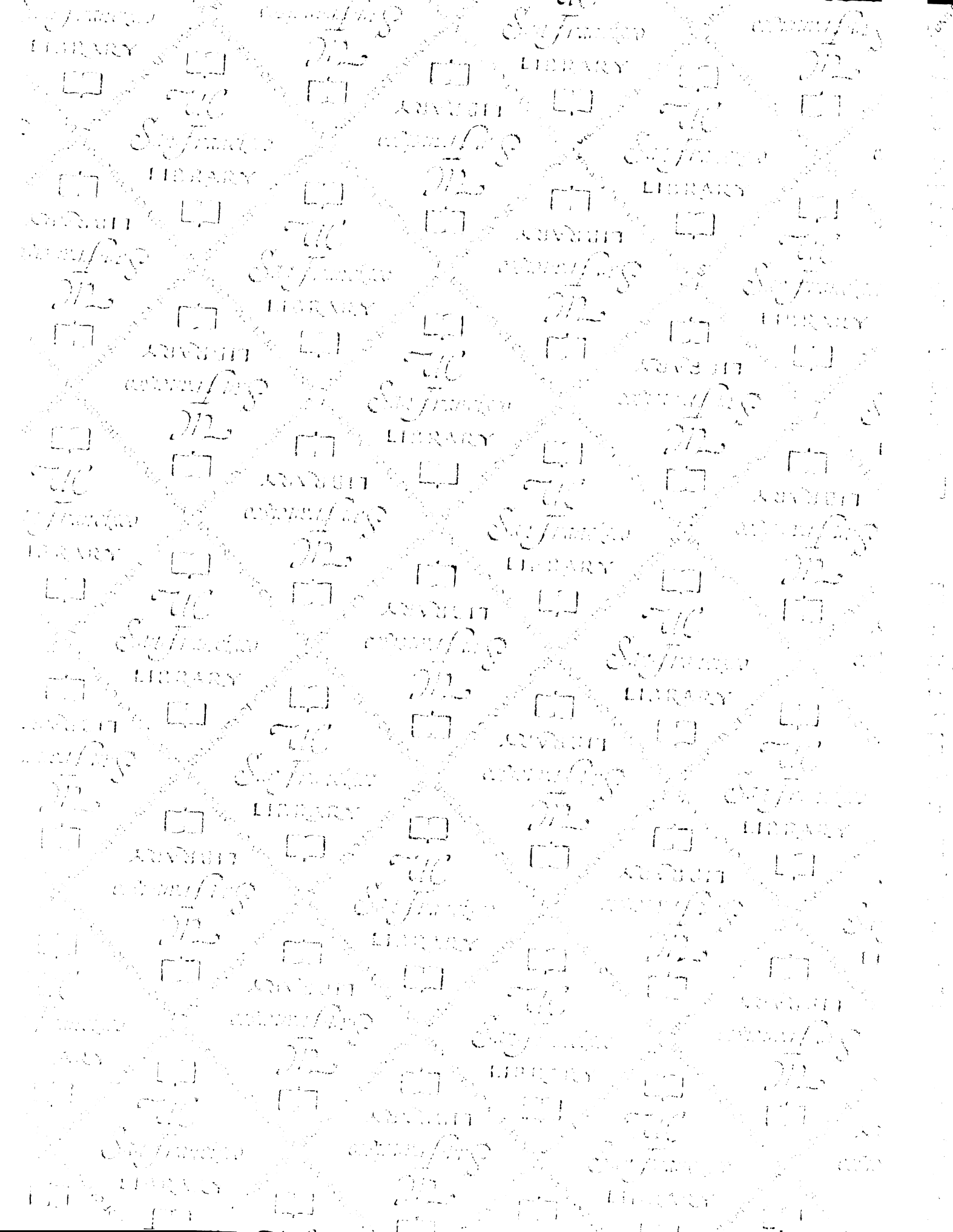
LIBRARY